



**NTNU – Trondheim**  
Norwegian University of  
Science and Technology

# Effects of Mastic Ingredients and Composition on Asphalt Mixture Properties

**Ingvild Ødegård**

Civil and Environmental Engineering

Submission date: June 2015

Supervisor: Helge Mork, BAT

Co-supervisor: Nils Uthus, Statens vegvesen

Norwegian University of Science and Technology  
Department of Civil and Transport Engineering





Report Title: Effects of Mastic Ingredients and Composition on Asphalt Mixture Properties	Date: June 8, 2015		
	Number of pages (incl. appendices): 108		
	Master Thesis	X	Project Work
Name: Ingvild Ødegård			
Professor in charge/supervisor: Helge Mork			
Other external professional contacts/supervisors: Nils Uthus			

**Abstract:** This master thesis purports to address the effects of different filler types in asphalt mastics and relate the differences to asphalt mixture properties and volumetric composition. Due to variations in properties for different filler types, e.g. particle size, density, mineral composition, Rigden voids, specific surface area and binder interaction, the same filler amount by weight yields variations in occupied volume and bind different amounts of bitumen. Uncontrolled variations of the filler fraction can cause binder drainage as a result of insufficient reinforcement or a dry mixture with unsatisfactory coating of the aggregates. The literature review focused on outlining characteristics and effects of different fillers and mastic composition and to relate variations in mixture performance to filler types and the ratio of filler to binder. An experimental laboratory research has been conducted to evaluate the effects of using different filler types. Mixtures with limestone and hydrated lime have been compared to mixtures with natural sieved dust from Vassfjell and Steinkjer aggregates on the 0.063 mm sieve. The results showed that the Rigden void content in the filler has an effect on the compacted asphalt mixture. Higher Rigden void content yields higher indirect tensile strength and a tendency to lower the abrasion resistance. The outcome from cyclic compression test was scattered, and there were too few data point to give any adequate conclusion. The tests showed that the F/A-ratio by mass or volume had less influence on the mixture performance. The air void content and the degree of compaction of the specimen greatly influenced the outcome, which coincide with results in the literature. The air void content was related to the Rigden void content, and in the literature it was found that higher Rigden void content in the filler gave higher air void content in the compacted specimens. Furthermore, increasing Rigden void content tended to increase the effective volumetric filler particle concentration in the mastics.

**Keywords:**

- |                        |
|------------------------|
| 1. Asphalt mastic      |
| 2. Filler              |
| 3. Mixture performance |
| 4. Rigden void content |



## **PREFACE**

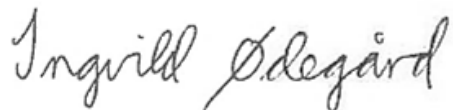
This report has been carried out during spring 2015, and it concludes the master thesis in the course TBA4940 Highway Engineering given by Department of Civil and Transportation Engineering at Norwegian University of Science and Technology, Faculty of Engineering Science and Technology.

The completion of this thesis would not have been possible without the valuable help of my supervisors. For that reason, I want to express my sincere gratitude to Professor Helge Mork at Norwegian University of Science and Technology and Nils Uthus from the Directorate of Public Roads for advices and inputs throughout this study.

Furthermore, I wish to gratefully acknowledge Andreas Kjosavik for guidance and assistance in the preliminary process and during the preparation of the laboratory research. Special thanks to Lisbeth Johansen, Bent Lervik and Sara Anastasio for appreciated help in the laboratory. I am also grateful to Norwegian University of Science and Technology for providing materials and test equipment and to Norwegian Public Roads Administration for financial support.

Lastly, I want to say thanks to Filip. Way to go, buddy.

Trondheim, June 8, 2015

A handwritten signature in black ink, reading "Ingvild Ødegård". The signature is written in a cursive style with a large initial 'I'.

Ingvild Ødegård



## ABSTRACT

This master thesis purports to address the effects of different filler types in asphalt mastics and relate the differences to asphalt mixture properties and volumetric composition. Due to variations in filler properties, e.g. particle size, Rigden voids, specific surface area and binder interaction, the same filler amount by weight yields variations in occupied volume and adheres different amount of bitumen. The Norwegian mixture design does not specify requirements for the fillers beyond the maximum and minimum filler percentages by mass and general controls of the quality. Uncontrolled variations of the filler fraction can cause binder drainage as a result of insufficient reinforcement or a dry mixture with poor aggregate coating, and the ratio of filler to binder by mass is not a satisfying parameter that takes the complexity of volumetric differences of the different filler types into account.

The first part in this report is a literature review which has been undertaken to assemble relevant test methods and requirements that can contribute to further testing. The focus has been directed towards outlining characteristics of different fillers and mastic compositions and to relate variations in mixture performance to filler types and F/A- ratio by mass and volume. The second part is an experimental research with the aim of evaluating the effects of different filler types on asphalt mixture performance. Mixtures with limestone and hydrated lime have been compared to mixtures with fillers from Vassfjell and Steinkjer aggregates passing the 0.063 mm sieve. Due to the complexity of the mastic properties, the sieving curve and the binder content have been kept constant to reduce the number of parameters.

The outcome from the laboratory research showed, in accordance to the literature, that Rigden void content in the filler has an effect on the compacted asphalt mixture. Higher Rigden void content yields higher indirect tensile strength and higher abrasion resistance. The result from cyclic compression test was scattered, and there were too few data points to give any adequate conclusions. The F/A- ratio by mass and volume had less influence on the mixture performance. The air void content in the specimens greatly influenced the outcome, where the densest specimens had the highest indirect tensile strength and the lowest Cantabro loss. The air void content was related to the Rigden void content. Results in the literature showed that as the Rigden void content increases, the air void content in compacted specimen increases. Data from the outcome in this study had a narrow range of air voids for the specimens tested and the trend mentioned was not that evident. The effective volumetric particle concentration for the natural fillers in the mastics increased as the Rigden void content increased, while there was no impact on the F/A-ratio by volume with increasing the Rigden void content.

Based on the results, the main conclusion is that Rigden void content is a critical parameter for mixture properties. Rigden void content affects the particle concentration in the mastic, which is related to mastic viscosity and the ability to coat the coarser aggregates. Additional requirements for the Rigden void content and particle concentration should be specified to ensure adequate performance between filler and binder. The National Cooperative Highway Research Program in the US suggests a range of filler to binder ratio of 0.6 to 1.2 by mass and proposed to introduce requirements for the mastic viscosity in the revised Superpave standard.





## SAMMENDRAG

Hensikten med denne masteroppgaven er å evaluere ulike typer filler brukt i asfalmørtel og relatere forskjellene til egenskaper og volumetriske forhold i asfaltblandinger. På grunn av variasjoner i filleregenskaper, som kornstørrelse, Rigden-hulrom, overflateareal og samspill med bindemiddel, så vil samme mengde filler målt i vekt gi variasjoner i okkupert volum og binde ulike mengder bindemiddel. Norske standarder spesifiserer ikke krav til filleren utenom grenser for vekt av fillerinnhold og generell kvalitetskontroll. Ukontrollerte variasjoner av filler kan forårsake alt fra utvasking av bindemiddelet som et resultat av utilstrekkelig forsterkning i mørtelen til en tørr asfaltblending der tilslaget får dårlig innpakning av bindemiddelet, og masseforholdet mellom filler og bindemiddel er ikke en tilfredsstillende parameter som tar hensyn til kompleksiteten av volumetriske forskjeller blant fillertyper.

Den første delen av denne rapporten er en litteraturstudie som har blitt gjennomført for å finne relevante testmetoder og krav som kan bidra til ytterligere testing. Fokuset har blitt rettet mot å redegjøre for karakteristikker av ulike fillertyper og mørtelkomposisjoner og å relatere variasjoner i asfaltegenskaper og anvendt fillertype til forholdet mellom bindemiddel og filler i vekt og volum. Den andre delen av studien er en laboratorieanalyse som har blitt utført for å eksegere effekten av å bruke ulike typer filler. Asfaltblandinger med kalkstein og hydratkalk har blitt sammenliknet med asfaltblandinger med egenfiller mindre enn 0,063 mm siktet fra tilslag fra Steinkjer og Vassfjell. På grunn av kompleksiteten av mørtelparametere, har siktekurven og bindemiddelinholdet blitt holdt konstant for å redusere antall variabler.

Utfallet fra laboratorieforsøket viste, i samsvar med funn i litteraturen, at Rigden-hulrommet i filleren har en effekt på de komprimerte asfaltprøvene. Høyere Rigden-hulrom gir høyere indirekte strekkstyrke og en tendens til å øke motstanden mot abrasjon. Det var spredte resultater fra syklisk kryp og for få datapunkter til å gi en klar konklusjon. Mengdeforholdet mellom filler og bindemiddel hadde i mindre grad påvirkning på blandingens egenskaper. Prøvenes hulrom hadde stor påvirkning på resultatene, og de mest kompakte prøvene hadde høyest indirekte strekkstyrke og lavest partikkeltap. Hulrom i asfaltprøvene er relatert til Rigden-hulrom i filleren. Resultater fra litteraturstudien viste at når Rigden-hulrommet øker, så øker også asfaltprøvenes hulrom. Data fra laboratorieforsøket hadde liten variasjon i hulrom og trenden var ikke like tydelig. Den effektive volumetriske partikkelkonsentrasjonen for egenfilleren i mørtelen ble høyere med økende Rigden-hulrom, mens det ikke gjorde noe utslag i volumforholdet mellom filler og bindemiddel med økende Rigden-hulrom.

Basert på resultatene fra studien, så er konklusjonen at Rigden-hulrom er en viktig faktor for asfaltblandingens egenskaper. Rigden-hulrom påvirker den effektive partikkelkonsentrasjonen av filler i mørtelen, som igjen er relatert til mørtelens viskositet og dens evne til å drapere og dekke det grovere tilslaget. Ytterligere krav til Rigden-hulrom og partikkelkonsentrasjon i mørtelen bør bli satt for å sikre tilstrekkelig samspill mellom filler og bindemiddel. En studie av amerikanske National Cooperative Highway Research Program foreslår at masseforholdet mellom filler og bindemiddel bør ligge mellom 0,6 til 1,2, og det er ønsket at det blir innført krav til mørtelviskositet i standardene under reviderte utgaver av Superpave.



# TABLE OF CONTENTS

PREFACE .....	V
ABSTRACT .....	VII
SAMMENDRAG .....	IX
TABLE OF CONTENTS .....	XI
LIST OF TABLES .....	XIII
LIST OF FIGURES.....	XIV
CHAPTER 1: INTRODUCTION .....	1
1.1 Background.....	1
1.2 Scope of work.....	2
1.3 Method.....	2
CHAPTER 2: LITERATURE REVIEW .....	3
2.1 General.....	3
2.2 Properties of the mastic constituents .....	4
2.2.1 Physical properties of the filler .....	4
2.2.2 Chemical properties of the filler.....	8
2.2.3 Binder properties .....	10
2.3 Asphalt mastics.....	12
2.4 Asphalt mixtures.....	19
CHAPTER 3: METHODOLOGICAL DESIGN .....	28
3.1 General.....	28
3.2 Type of asphalt .....	28
3.2.1 Aggregates and filler .....	28
3.2.2 Bitumen .....	29
3.3 Sample preparation .....	30
3.4 Asphalt mixture .....	32
3.4.1 Rice density .....	32
3.4.2 Air void content.....	32
3.5 Testing procedures for the compacted specimens .....	33
3.5.1 Indirect tensile strength test.....	33

3.5.2	Cantabro test.....	33
3.5.3	Cyclic compression test.....	33
3.5.4	Statistical analysis .....	34
CHAPTER 4: RESULTS .....		35
4.1	Filler and mixture properties .....	35
4.2	Indirect tensile strength test.....	36
4.3	Cantabro test .....	37
4.4	Cyclic compression test .....	37
4.5	Two-tailed t-test.....	42
CHAPTER 5: DATA ANALYSIS.....		44
5.1	Indirect tensile strength test .....	44
5.2	Cantabro test .....	46
5.3	Cyclic compression test .....	47
5.4	Additional evaluations.....	49
5.4.1	Coating .....	49
5.4.2	Rigden void content .....	51
CHAPTER 6: DISCUSSION OF FINDINGS .....		53
6.1	Effects of mixture properties .....	53
6.1.1	F/A-ratio .....	53
6.1.2	Air void content.....	54
6.2	Effects of filler properties.....	55
CHAPTER 7: CONCLUSION AND FURTHER INVESTIGATIONS.....		58
7.1	Conclusion and recommendations.....	58
7.2	Further investigations .....	60
REFERENCES.....		61
APPENDIX		

## LIST OF TABLES

Table 2.1: Filler mass for similar effective volume concentration (Lerfald, 2000) .....	17
Table 2.2: Mastic properties for best mixture performance (Faheem and Bahia, 2009).....	19
Table 2.3: Specifications for cyclic creep .....	24
Table 3.1: Applied binder content in the asphalt mixture .....	30
Table 3.2: Ratios of the aggregate fractions in the different mixture series .....	31
Table 4.1: Filler density, Rigden void content and Rice density .....	35
Table 4.2: Volumetric filler particle concentrations in the mastics .....	35
Table 4.3: F/A-ratio by mass and volume for the three batches in the four different series ...	36
Table 4.4: t-test indirect tensile strength .....	43
Table 4.5: t-test Cantabro loss.....	43
Table 4.6: t-test cumulative axial strain at 3600 load cycles.....	43
Table 4.7: t-test creep rate in stage 2 of the creep curve .....	43

## LIST OF FIGURES

Figure 1: Schematic diagram of a drum mix plant.....	1
Figure 2: Specific gravity for different filler types (NCHRP Project 9-45, 2010).....	6
Figure 3: Rigden voids for different filler types (NCHRP Project 9-45, 2010).....	7
Figure 4: The fixed binder coating filler particles.....	8
Figure 5: Schematic of fractional voids in asphalt mastics .....	16
Figure 6: Mastic viscosity with respect to F/A-ratio (Kavussi and Hicks, 1997) .....	18
Figure 7: Creep curve with different stages (NS-EN 12697-25:2005) .....	24
Figure 8: Packing of filler in mastics (Tunncliff, 1962) .....	27
Figure 9: Sieving curve for Ab 11 .....	28
Figure 10: Desiccator and Rigden apparatus.....	29
Figure 11: Loose asphalt mixture and vacuum desiccator for determining Rice density .....	32
Figure 12: Los Angeles machine and specimens before and after the Cantabro test.....	33
Figure 13: Setup for cyclic compression test in the NAT machine .....	34
Figure 14: Indirect tensile strength test .....	36
Figure 15: Range of indirect tensile strength values, including average values .....	37
Figure 16: Range of Cantabro loss values, including average values .....	37
Figure 17: Variations in the applied load pulse due to noise in the system .....	38
Figure 18: Displacement measurements from the LVDTs.....	38
Figure 19: Final surface displacement for specimen c.3.2 with limestone .....	39
Figure 20: Displacement at 3600 load cycles.....	39
Figure 21: Creep curves for series A with Steinkjer filler .....	40
Figure 22: Creep curves for series B with Vassfjell filler.....	40
Figure 23: Creep curves for series C with limestone .....	41
Figure 24: Creep curves for series D with hydrated lime .....	41
Figure 25: Cumulative axial strain at 3600 load cycles .....	42
Figure 26: Indirect tensile strength vs F/A-ratio by mass .....	44
Figure 27: Indirect tensile strength vs F/A-ratio by volume .....	44
Figure 28: Indirect tensile strength vs Rigden void content.....	45
Figure 29: Indirect tensile strength vs air void content .....	45
Figure 30: Cantabro loss vs F/A-ratio by mass .....	46
Figure 31: Cantabro loss vs F/A-ratio by volume .....	46
Figure 32: Cantabro loss vs Rigden void content .....	47

Figure 33: Cantabro loss vs air void content.....	47
Figure 34: Cumulative axial strain at 3600 load cycles vs F/A-ratio by mass.....	48
Figure 35: Cumulative axial strain at 3600 load cycles vs F/A-ratio by volume.....	48
Figure 36: Cumulative axial strain at 3600 load cycles vs Rigden void content .....	49
Figure 37: Cumulative axial strain at 3600 load cycles vs air void content.....	49
Figure 38: Aggregate coating .....	50
Figure 39: Saw kerf surface for evaluation of the aggregate coating.....	50
Figure 40: Air void content vs Rigden void content .....	52
Figure 41: F/A-ratio by mass and volume vs Rigden void content.....	52
Figure 42: Effective volumetric particle concentration in mastic vs Rigden void content .....	52





# CHAPTER 1: INTRODUCTION

## 1.1 Background

Asphalt is a well-known and broadly used construction material for roads, highways and large open spaces, such as airports, schoolyards and parking lots. Hot mix asphalt (HMA) consists of asphalt binder and a blend of coarse and fine aggregates, filler and air voids. In addition, there could be added constituents like polymer modifiers or agents to improve binder properties and the bond between the binder and the aggregates. Mastic is the term used for the combination of filler material and asphalt binder. Most of the asphalt mixtures contain added filler in addition to the natural occurring dust in the aggregates. Furthermore, the filler material serves as reinforcement in the mastic to prevent binder drainage and as an extension of the binder for coating the aggregates.

Today, HMA used in the field is produced at HMA mixing plants or in mobile HMA facilities. Figure 1 depicts a flow chart of the mixing procedure at a stationary drum mix plant. As the figure shows, filler dust is collected when the different stockpile fractions are blended. The collected filler dust is recycled in the blending process, and additional filler is added if there is not sufficient amount of sieved and natural filler. The asphalt mixture design determines the weight relationship of aggregate fractions and binder that fulfills desired criteria. An automatic weighing system controls the amount of added filler and binder, before all the constituents are mixed and conveyed to the truck loading station<sup>1</sup>.

Due to variations in properties for different filler types, e.g. particle size, gradation, density, mineral composition, filler fractional voids, specific surface area and binder interaction, the same filler amount by weight yields variations in occupied volume and bind different amounts of bitumen. Uncontrolled variations of the filler fraction can cause binder drainage due to insufficient reinforcement of the mastic or a dry mixture with unsatisfactory coating of the aggregates, which will be discussed in details later.

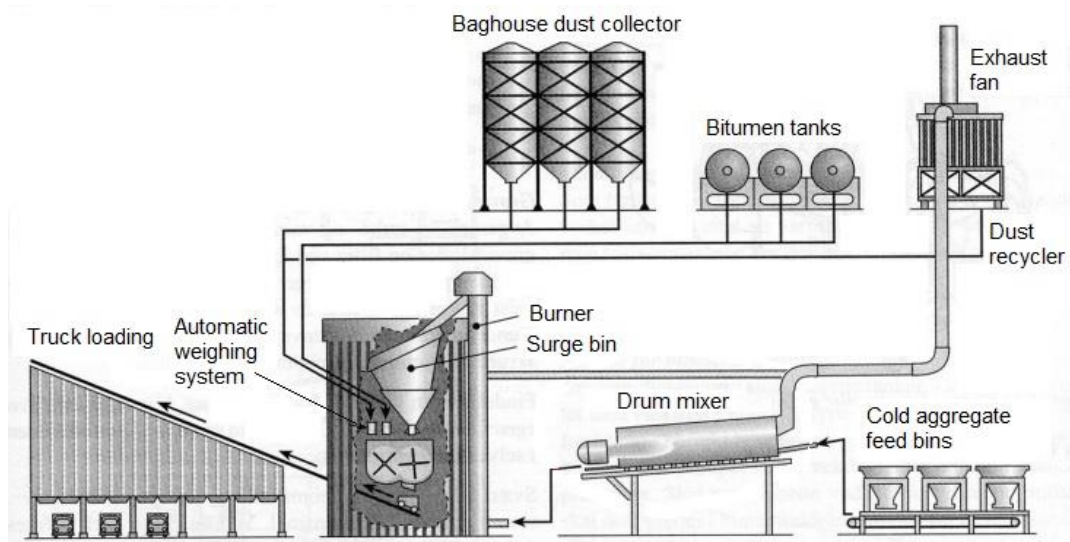


Figure 1: Schematic diagram of a drum mix plant

<sup>1</sup> Personal communication, Dr. Steve Perkins, April 23, 2014

There is no lack of studies in the literature showing that mineral fillers have significant effects on asphalt mastic behavior and asphalt mixture properties. However; the current mixture design in Norwegian standards does not specify filler requirements beyond the guidelines for maximum and minimum filler percentages by mass and general controls of the filler quality. The surface interaction between binder and filler in the mastic can be critical for the mixture performance, and the filler concentration by mass is not a satisfying parameter that takes the complexity of volumetric variations of the different fillers into account.

## **1.2 Scope of work**

In this report, the scope of work has been to outline characteristics and effects of different mastic ingredients and compositions. The objective of this research work has been to evaluate variations in mixture performance and filler types and relate them to mixture properties and ratios of mastic constituents. Effects of limestone and hydrated lime in mastics have been compared to the effects of natural aggregate dusts.

The main questions raised have been: What are the impacts of different filler types on the asphalt mixture performance, and how could these effects be related to filler properties, filler to binder ratios and volumetric composition? Should additional factors for the filler fraction be implemented in future mixture designs to guarantee essential asphalt mixture capability, in addition to requirements for the filler and the weight relationship between filler and binder?

## **1.3 Method**

This study has been divided into two main parts. The first part is a literature review with the aim of assembling national and international descriptions of appropriate test methods and mixture design requirements that are relevant in this context and can contribute to further testing. The literature review does also include an analysis of aspects of different filler types in relation to mastic properties, as well as evaluations of mastic constituents and what factors that have the most effect on asphalt mixture performance.

The second part of this study is an experimental laboratory research which has been undertaken to evaluate the effects of using different filler types, both natural fillers and manufactured fillers. The approach in this thesis has been limited to evaluate a selection of four filler types mixed with a commonly used binder type in Norwegian asphalt. The sieving curve has been kept constant for all series for reducing the number of variables, since mastic properties are results of several parameters, e.g. filler type, binder type, surface interaction and filler to binder ratio. Fundamental properties indicating the pavement life of asphalt mixtures have been studied in detrimental tests to investigate the degree of impact for the different types of filler.

## CHAPTER 2: LITERATURE REVIEW

### 2.1 General

Mastic is the term used for the combination of filler and bituminous binder in asphalt mixtures, and the behavior of mastics has long been known to influence the performance and many of the properties of final asphalt mixtures, such as stiffening, workability, fatigue cracking and moisture susceptibility (Mogawer and Stuart, 1996; Buttlar et al, 1999). The properties of asphalt mastics are dependent on several factors, especially binder properties, filler properties and the ratio of filler to binder. Furthermore, there are great varieties in filler materials and binders. A given binder type reacts differently with different fillers, hence the mastic properties are depending on the combination of the particular filler and binder.

Norwegian standards specify filler as fine material where 100 % pass the 2 mm sieve, 95 % pass the 0.125 mm sieve and 83 % pass the 0.063 mm sieve (NS-EN 13043, 2002). Filler occurs naturally in aggregates as dust derived from crushing the aggregates in different fractions. If the amount of natural fillers is not sufficient, additional fillers will be added. Sieved natural dust from crushed aggregates collected by baghouse dust collectors are used, while the most common type of added mineral fillers in mixtures is limestone (NCHRP Project 9-45, 2010). Filler materials are also manufactured in the industry, such as hydrated lime, fly ash or slag. Imported filler like Portland cement and biomass ashes have also been used as materials to fill up the finest fractions of asphalt mixtures (Melotti et al, 2013).

There are two main views on the role of the filler in asphalt mixtures, and it is believed that both roles are played simultaneously. The first theory presumes that the filler serves as a volume-filling material in the voids of the coarser aggregates in the asphalt mixture. This phenomenon will provide higher specimen density and strength of the asphalt mixture. Secondly, due to the physical and chemical nature, the filler is assumed to act as an extender of the binder by being an active material that adsorbs components in the binder (Tunnicliff, 1962; Al-Suhaibani et al, 1992).

In the following sections, the influence of the constituents will be discussed and test methods will be reviewed. The properties of the different filler types will be studied in relation to asphalt mastic and mixture performance. Articles, literature and scientific papers have been found in the databases Engineering Village, Scopus and Google Scholar, the libraries at Norwegian University of Science and Technology and the Directorate of Public Roads, as well as handbooks and manuals regarding road technology. The following search terms have been used: Asphalt mastic, binder, mineral filler, filler property, mixture performance, binder interaction, characteristics, hot mix asphalt, ratio and test methods.

## 2.2 Properties of the mastic constituents

### 2.2.1 Physical properties of the filler

Filler fractional voids, or Rigden voids, are the void content in the filler material when compacted to maximum density, and the void content is primarily affected by the geometrical characteristics of the filler, i.e. particle size and shape, gradation, surface texture and angularity (Rigden, 1947; Tayebali et al, 1998). When asphalt binder is mixed with dry filler, the binder that fills the Rigden voids in the filler material is labeled fixed binder (Liao et al, 2012). The excess binder that remains outside the filler fractional void structure is called free binder, and it is free to lubricate the mastic and provide fluidity to the mixture. As higher the Rigden void content, as lower the amount of free binder (Mogawer and Stuart, 1996).

Rigden voids are found by Method 14.4282 in Handbook R210 by Norwegian Public Road Administration (NPRA). The filler sample with known specific density is dried at  $110 \pm 5$  °C until constant mass is obtained, before it is cooled in a desiccator for 90 minutes. Filter paper is put in a metal cylinder and weighed with 0.01 grams accuracy, and the thickness of the paper and the height of a stamp are measured. Thereafter, approximately 10 grams of filler is put in the cylinder, and the filter paper and the stamp are placed on top and put in the Rigden apparatus. In the Rigden apparatus, the cylinder and the stamp are lifted along the metal bars to a height of  $100 \pm 25$  mm and released with a free fall 100 times. The height of the compacted filler with the filter paper and stamp is found, and the weight of the cylinder, filler and filter paper is measured. The Rigden void content is calculated by equation (1):

$$V_R = \left( 1 - \frac{1000m}{(h_1 - h_2)A\rho_f} \right) * 100 \quad (1)$$

where  $V_R$  = Rigden void content (%),  $m$  = mass of the compacted filler (g),  $h_1$  = height of compacted filler, stamp and filter paper (mm),  $h_2$  = height of stamp and filter paper (mm),  $A$  = inside cross section area of cylinder ( $\text{mm}^2$ ),  $\rho_f$  = density of the filler material ( $\text{g/cm}^3$ ).

Norwegian standards specify a range of Rigden void content of 28 % and 55 % for added filler in asphalt mixtures (NPRA N200). Furthermore, the filler should be sufficiently dry, free of lumps and not contain organic contaminants. Three parallel tests shall be conducted, and the all of the calculated Rigden void values need to be within  $\pm 1$  % of the average value of the three calculated values.

Kavussi and Hicks (1997) mention a problem with the sensitivity of the Rigden void content test. Under the same test conditions for one filler type, there could be variations in the calculated void content due to different surfaces at the base of the apparatus. Having a countertop surface of steel gave the tested limestone filler Rigden void content of 36.2 %, while the same filler got 34.9 % when the surface was a wood table. By placing and clamping the Rigden apparatus on a wooden stand fastened on the countertop, the discrepancy in the outcome was drastically reduced for all surfaces, and the range of the values for the mentioned surfaces were reduced to 35.3 % and 35.7 %.

The German filler test is a method for measuring the amount of filler that is needed to absorb 15 grams of hydraulic oil. The oil is put in a bowl, and a small amount of filler is added. The filler and the oil are mixed and attempts are made to form the mixture to a ball. If the ball sticks together, more mineral filler is added and the procedure is repeated until the mixture loses cohesion and is unable to hold the ball form. The total amount of filler added is noted as the test value. The German filler test correlates with Rigden voids. High Rigden void content in a filler material equals low value in the German filler test, because the hydraulic oil is fixed in the voids and less filler is needed to make the mixture loose cohesion (Kandhal et al, 1998).

Another main property of filler materials is the density. The general term *density* is defined as the amount of mass a specific volume of a specific material has at a given temperature (NPRA R210). In American literature, the term specific gravity is broadly used as a replacement for the term density (Ødegård, 2014). The relationship between specific gravity and density is seen in equation (2) below:

$$\rho_f = G_m \rho_w \quad (2)$$

where  $\rho_f$  = density of filler ( $\text{g}/\text{cm}^3$ ),  $G_m$  = specific gravity,  $\rho_w$  = water density at actual temperature ( $\text{g}/\text{cm}^3$ ).

The specific density of the filler can be found by Method 14.427 (NPRA R210) utilizing a pycnometer. The weight of the pycnometer with a glass stopper is found, and then filled with distilled water at temperature 25 °C. A funnel is used to fill a sample of dry filler material in the pycnometer, before it is weighed utilizing a balance with 0.001 grams accuracy. Distilled water is added until the filler material is submerged and the weight is measured. The pycnometer is placed in a vacuum desiccator where vacuum is applied to remove the entrapped air in the filler. Thereafter, the pycnometer is removed from the apparatus and placed in a water bath at 25 °C for at least one hour. The pycnometer is then weighed. The filler density is found using equation (3):

$$\rho_f = \frac{(m_4 - m_1)\rho_w}{m_2 - m_1 - m_5 + m_4} \quad (3)$$

where  $\rho_f$  = density of filler ( $\text{g}/\text{cm}^3$ ),  $\rho_w$  = density of water ( $\text{g}/\text{cm}^3$ ),  $m_1$  = mass of pycnometer and glass stopper (g),  $m_2$  = mass of pycnometer and glass stopper with distilled water (g),  $m_4$  = mass of pycnometer and glass stopper with filler (g),  $m_5$  = mass of pycnometer and glass stopper with filler and water (g).

The water temperature has to be stable, because the density of water varies with the temperature. Water expands with increasing temperature, and if the temperature of the water is higher than specified, less water can fill the voids, resulting in a higher filler density. In Handbook of Chemistry and Physics 95<sup>th</sup> Edition by Haynes et al (2014), the relationship between water density and water temperature is listed, as seen in table B.1 in Appendix B.

In asphalt mixtures, the amount of filler used is based on a mass ratio of the constituents. When the density and specific gravity vary between different fillers, the volume fraction of filler added in asphalt mastics varies similarly. The effect of filler-binder ratios in mastics will be discussed in detail later. Results from NCHRP Project 9-45 (2010) showed that manufactured fillers, in this case fly ash and furnace slag, had the lowest and the highest specific gravity values, respectively. The specific gravities for the fillers tested can be seen in figure 2. As the figure shows, two similar filler types can have varied specific gravity depending on the source, e.g. soft granite fillers from different sources have a range of specific gravity values of 2.40 and 2.58. The specific gravity might also vary within the same stockpile of aggregates.

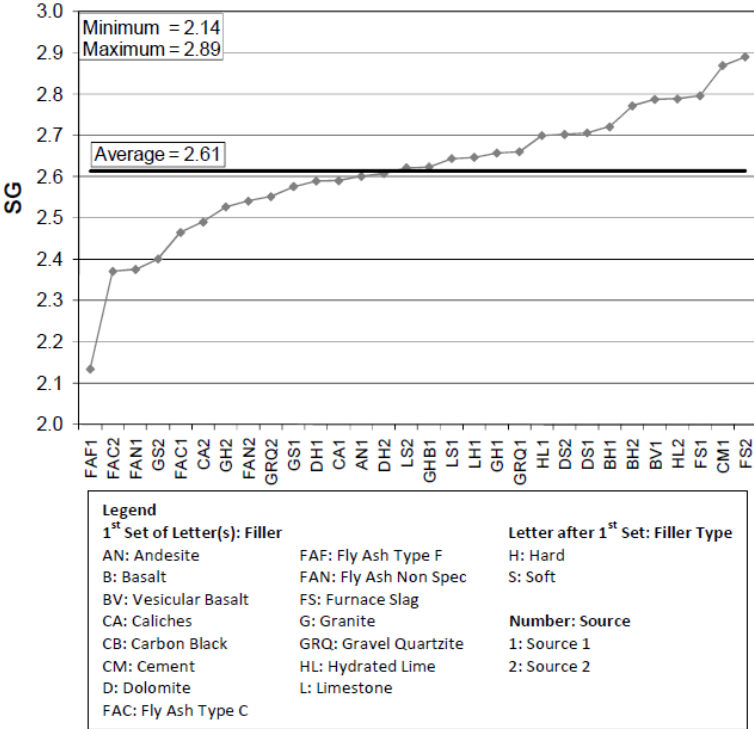


Figure 2: Specific gravity for different filler types (NCHRP Project 9-45, 2010)

The filler density is a function of several physical factors. The particle geometry, particle size distribution and morphology are crucial. Particle shape, angularity, morphology and texture can be found by microscopy and image analysis software (NCHRP Project 9-45, 2010). In the study by Lerfald (2000) it was found that the shape of hydrated lime varied significantly from baghouse dusts and limestone. While limestone had spherical shape and the baghouse dusts were slightly elongated, the hydrated lime had porous particles with irregular shape, and the surface area was considerably high. The shape of manufactured fillers is dependent on the production process, and hydrated lime is the result of calcination of calcium carbonate to calcium oxide stabilized by added water (Lerfald, 2000). Buttler et al (1999) utilized a nitrogen adsorption analyzer for evaluating surface area of the filler particles, where the layers of adsorption of nitrogen gas isotherms on the filler surface area are measured. The procedure is known as the Brunauer-Emmett-Teller (BET) method and was developed in the 1930s (Sing, 1998). Geber and G6mse (2010) found that the presence of feldspar will increase the surface area. Hence, andesite filler has high surface area while limestone has low.

Buttlar et al (1999) found the particle size distribution in the filler materials by the principle of liquid phase photosedimentation. This method uses a suspending liquid with surfactants as a dispersing agent, and the outcome is the size distribution and median particle size of the filler tested (Buttlar et al, 1999). Other methods for evaluating the size distribution in filler materials are sieving or laser diffraction. Harris and Stuart (1995) concluded in their study that the latter gave the most precise results. In this method, filler particles in a wet dispersion scatter light beams from a laser in all directions. The detected scattered light pattern is dependent on the size of the filler particles, and the pattern is analyzed for producing size distribution of the filler material (NCHRP Project 9-45, 2010). Further discussion of the technical aspects of these methods can be found elsewhere in the literature (Harris and Stuart, 1995; Sing, 1998; Tayebali et al, 1998).

The particle geometry has great variations depending on the type and origin of the filler material. Rigden voids are affected by shape, size, angularity and texture of the fillers, and are therefore used as an indication of the particle geometry (Anderson, 1979). The joint study NCHRP Project 9-45 revealed a wide range of Rigden voids. The extreme values in the upper and lower range occurred for manufactured fillers, where fly ash had Rigden void content as low as 26.2 % and furnace slag had 49.1 %. Limestone filler had values around 30 %. There were no link between the Rigden void content, mineralogy and source of the filler (NCHRP Project 9-45, 2010). Graphical illustration of the test results from the study is enclosed in figure 3. The minimum and maximum values of the Rigden void content found in the joint study correspond with the Norwegian requirements of 28 % and 55 % found in NPRA N200.

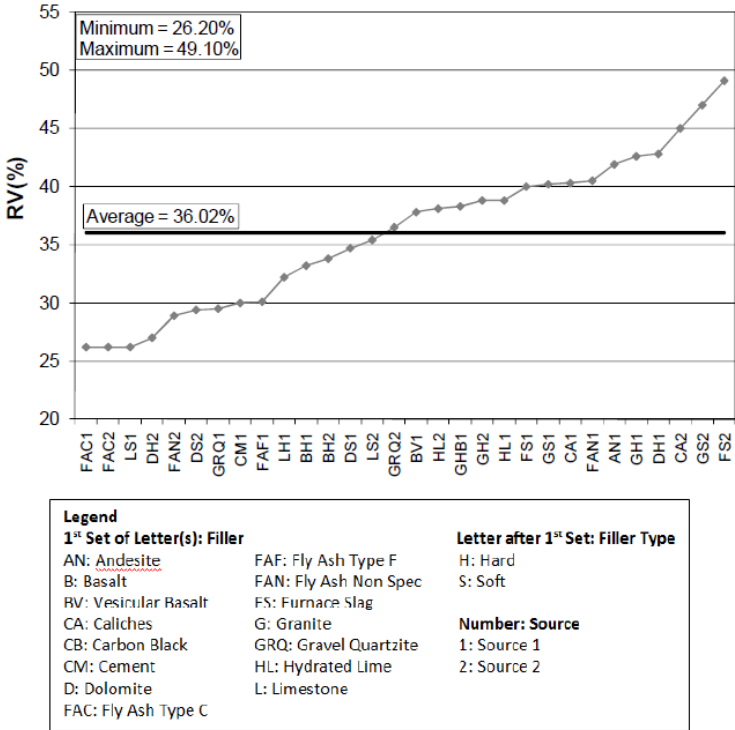


Figure 3: Rigden voids for different filler types (NCHRP Project 9-45, 2010)

Another property used to characterize filler is the fineness modulus (FM), which is an empirical factor calculated by equation (4), rounded to the nearest 0.01. Wang et al (2011)

conducted FM tests on filler materials where the sieves used had mesh sizes of 75, 50, 30, 20, 10, 5, 3 and 1  $\mu\text{m}$ . The procedure is described in ASTM C 125, and finer material yields lower FM values. The FM value is used as an indicator of shape and texture of filler, and the value is considered an important factor of the filler which completes the overall picture of the geometric properties of the filler along with the Rigden void content, which indicates the size distribution and surface area (NCHRP Project 9-45, 2010). The equation is outlined below:

$$FM = \frac{\sum \text{Cumulative percentages retained on the specified sieves}}{100} \quad (4)$$

where FM = fineness modulus.

### 2.2.2 Chemical properties of the filler

As mentioned previously, the binder in asphalt mastics is either free or fixed. The fixed binder can be divided into two parts, which can be seen in figure 4. The first part is adhered in the filler material and acts as a part of the particle, while the second part is not adsorbed, but affected by the adsorption of the inner part (Faheem and Bahia, 2010). The fixed binder and the filler interact and form chemical bonds. The strength of the chemical bonds is dependent on the surface activity and mineralogy of the filler. Ishai and Craus (1996) found that higher geometric irregularity of the filler yields higher adsorption intensity. This effect will result in a strengthening of the binder-filler bonds and a relative increase in the fixed binder amount, while the mastic will get higher consistency and strength (Ishai and Craus, 1996).

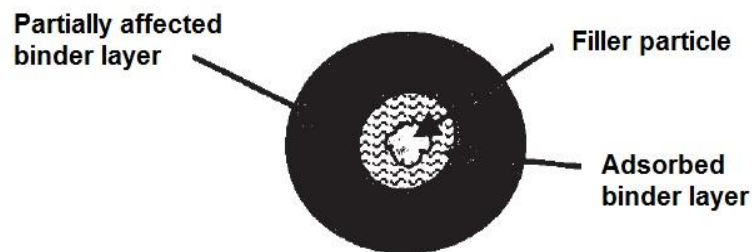


**Figure 4: The fixed binder coating filler particles**

Tunnicliff (1962) postulated that the filler stiffening effect is at its peak at the filler surface and decreases with the distance from the surface, and the gradient is depending on the surface chemistry of the filler. This explains why fillers of similar shape, gradation, Rigden void content and surface texture have various stiffening effect, when they have different mineralogy and surface chemistry.

The clay content in filler materials is critical. Woodward et al (2002) mention several aspects of clay in asphalt mixtures that are of importance. The first aspect is the relatively large surface area of clay minerals, which require more bitumen for coating. Another aspect is that clay minerals can become plastic when exposed to water. Furthermore, active clays from the smectite and montmorillonite group are considered harmful due to the tendency to retain



moisture, which is undesirable in freezing-thawing cycles (Woodward et al, 2002). High moisture content in the filler reduces the filler-binder bonds in mastics caused by the surface charge of the water, and the water absorption affects the frost resistance of the asphalt mixture. In addition, clays and friable particles tend to form lumps that can break down during loads or stresses. Small amounts of expansive and swelling clay in concentrated areas yield uneven strength and have considerable effects on mastic properties (Wang et al, 2011).

The methylene blue value (MBV) test is a technique used to determine the clay content. In liquid state, methylene blue is a cationic dye that gets adsorbed on negatively charged clay surface areas. The method utilizes titration, and 2 grams of dry filler is mixed with 200 mL distilled and deionized water. Methylene blue solution is added and the mixture is shaken for 2 hours, before it is put to rest until adsorption equilibrium is reached. Thereafter, 5 mL of the mixture is centrifuged and a spectrophotometer is used to determine the amount of methylene blue remaining in the mixture and the amount adsorbed by the mineral fillers (Santamarina et al, 2002). The results from NCHRP Project 9-45 study showed that manufactured filler, i.e. fly ash and furnace slag, had low MBV. Low MBV for limestone and hydrated lime as well, while basalt and andesite fillers had high values (NCHRP Project 9-45, 2010).

Another method for evaluating clay content is by examining the plasticity. The plasticity of fine materials is defined as the difference between the plastic limit and the liquid limit of materials finer than 0.4 mm (NPRA R210). The procedure of finding the plastic limit is described in Method 14.442 in NPRA R210 and is determined by rolling out a thread of 20 grams of moisturized filler. The plastic limit is the water content where the thread breaks apart at 3.2 mm diameter. The liquid limit is the water content in the filler sample at which the groove of a cone becomes 10 mm when the cone is released from the surface of the filler. The process is further described in Method 14.441 in NPRA R210. The two measures mentioned are used to find the plasticity index, as seen in equation (5):

$$PI = LL - PL \quad (5)$$

where PI = plasticity index, PL = plastic limit, LL = liquid limit.

Materials with PI values above 30 are defined as highly plastic, while non-plastic materials have values between 0 and 3. Clayey materials have high PI values (Das, 2010).

Organic content in filler materials is in the literature considered harmful due to its break down and decomposition caused by biochemical processes (Kandhal et al, 1998; Hintz et al, 2010; Melotti et al, 2013). The decomposition affects the soil structure, leading to higher porosity and easier access for infiltration of water. Fillers with high organic content have high moisture holding capacity and poor interfacial adhesion between the filler and the binder (Brady and Weil, 2007). By means of this, it is desirable to have low organic content in filler materials. The organic content can be measured by the loss of ignition (LOI) test, following the procedure in method 14.445 in NPRA R210 and in AASHTO T267. In the LOI test, a sample of filler is oven dried at 110 °C for 1 hour. Thereafter, the sample is then placed in a muffle

furnace at  $455 \pm 10$  °C for 6 hours where the organic materials are burned off. The difference in weight of the sample before and after ignition is reported as the LOI value. NPRA N200 requires that fillers used in asphalt mixtures should not contain any organic contaminants.

The mineralogy of filler materials affects the mastic performance. Asphalt binder bonds better to fillers with certain types of mineral, because the binder adhesion of fillers is dependent on the surface chemistry. Limestone and hydrated lime with high calcium content are typically hydrophobic materials and tend to create strong bonds with bitumen. Siliceous fillers, such as fillers from quartz and granite, are hydrophilic and have greater affinity to water than to bitumen, and the adhesion is impeded by this. Binder films coating hydrophilic fillers may become stripped when water is present. Calcareous materials are hydrophobic and get positively charged when exposed to water, while siliceous fillers get negatively charged. The electric charge affects the adhesion. To improve adhesion, amine can be added as an agent to create better bonds between hydrophilic minerals and bitumen (Roberts et al, 1996).

Since many fillers are composed of several different minerals, they might have both hydrophilic and hydrophobic properties, but to different extents. The reactivity of the fillers can be indicated by the calcium compound. X-ray fluorescence spectrometry is a method to determine the calcium oxide (CaO) content, the calcium hydroxide (Ca(OH)<sub>2</sub>) content and calcium carbonate (CaCO<sub>3</sub>) content (Hintz et al, 2010). In this test, emission of fluorescent X-ray beams from the filler sample is detected and the intensity is analyzed. Studies have shown that slag fillers have high CaO content, while fillers from granites have low CaO content, and as expected, limestone fillers consists of CaCO<sub>3</sub>, while hydrated lime is made up by Ca(OH)<sub>2</sub> (Lerfald, 2000; NCHRP Project 9-45, 2010). The calcium content is of importance for the strength of the filler materials, hence the stiffening effect on the mastic (Anderson, 1979). Wang et al (2011) found correlations between CaO content and rutting potential in asphalt mixtures, where higher CaO content yields less rutting potential.

### **2.2.3 Binder properties**

Bituminous asphalt binders occur in natural deposits or are refined after distillation of crude oil, and mostly all the binders used in production today come from the latter. Depending on the petroleum source, the binder structures are immensely diverse. The main constituents are carbon and hydrogen, while the heteroatoms sulfur, nitrogen and oxygen are present in small amounts. The heteroatoms are attached to carbon constructing molecules with different interior electrochemical forces, thus polar molecules. Due to the polarity, molecular connections are induced within the binder and also with the surface molecules of the aggregates and filler in the mastic (Roberts et al, 1996). There also exist non-polar groups in the binder, which act as solvents for the polar groups. Fritschy and Papirer (1978) state that fillers containing calcium carbonate yields stronger bonds with the polar parts of the binder, while quartz affects better with non-polar parts.

The molecules in the binder are arranged in three main components, i.e. asphaltenes, resins and oils. Asphaltenes are the most polar and interactive component and have the major

contribution in the binder viscosity properties. Binders with low asphaltene content have been associated with tenderness (Roberts et al, 1996). Resins work as the dispersive agents for asphaltenes in the oils, providing homogeneous binders. The nature of the binder is depending on the degree of dispersion of asphaltenes in the oils. High dispersion yields binders with Newtonian behavior, where the viscosity does not change with the flow rate. Conversely, with low dispersion of asphaltenes in the oils, the binders get non-Newtonian flow characteristics (Roberts et al, 1996). Further discussion of the nature of the binder is beyond the scope of this study, but can be found elsewhere in the literature (Roberts et al, 1996; Leseur, 2009).

Bitumen is a temperature susceptible and thermoplastic material, and desired properties of the binder stiffness will to some extent contradict its natural behavior. At low temperatures bitumen is stiff and non-Newtonian, while it becomes soft, Newtonian and fluid at elevated temperatures (Leseur, 2009). Simultaneously, the binder needs to be soft enough to resist cracking at low temperatures, and stiff enough to avoid rutting at high temperatures. Binder stiffness and consistency are therefore of vast importance and are used to classify the binders. Bitumen is a viscoelastic material, and the binder stiffness is the relationship between stress and strain as a function of temperature and loading time (Roberts et al, 1996). The stiffness is represented by the penetration number, which is found by measuring penetration by Method 14.512 in NPRA R210. The penetration number obtained defines the distance a needle vertically penetrates the bitumen sample in 0.1 mm. The temperature is set to 25 °C. The reported value defines penetration grade, which is the upper and lower penetration depth (NPRA R210). As lower the penetration number, as stiffer the binder.

NPRA Handbook N200 specifies the required minimum values for the percentage of binder in asphalt mixtures, and the requirements for Ab 11 are listed in Appendix C, table C.1. Due to variations in aggregate densities for different materials, the minimum value has to be modified by the correction factor in equation (6). As soon as the modified binder content is calculated, the mass of the binder content used in the asphalt mixture is found by equation (7) below (Fwa, 2005). As the equation show, the binder added is at a basis of weight.

$$\alpha = \frac{2.65}{\rho_a} \quad (6)$$

$$M_b = \frac{p_b M_s}{100 - p_b} \quad (7)$$

where  $\alpha$  = correction factor,  $\rho_a$  = aggregate density,  $M_b$  = mass of binder (g),  $M_s$  = mass of the mineral aggregates (g),  $p_b$  = binder content in percentage of total weight (%).

Binders could either be unmodified or modified, and the necessity for modifiers is dependent of the binder use and desired characteristics. Modifiers are added to improve the rheological and mechanical properties of the neat binder. The modifying additives in polymer modified bitumen (PMB) change the physical properties such as softening point and stiffness. The most common types of polymer modifiers are styrene-butadiene-styrene (SBS), polyphosphorous acid (PPA) and ethylene vinyl acetate (EVA). Sengoz and Isikyakar (2008) studied variations

in neat binder and SBS and EVA modifiers, and they proved that the modifying additives give higher adhesion between binder and aggregates. Huang et al (2007) found that hydrated lime fillers can enhance the bonds between aggregates and neat binder, and both hydrated lime and Portland cement can be utilized as anti-stripping agents in asphalt mixtures (Yan et al, 2013).

Neat binders and PMB react differently with different filler materials. NCHRP Project 9-45 (2010) had results showing that SBS binder provides higher mastic viscosity than PPA binder and neat binder. In addition, the mastics with SBS binder had the greatest variability in viscosity with the filler type. There was not any significant difference in mastic viscosity for mastics containing PPA binder and neat binder; even though there were variations due to different filler types (NCHRP Project 9-45, 2010). A noticeable trend was that the natural fillers with low Rigden void content possessed the lowest mastic viscosities, regardless of the use of modifiers or not.

### **2.3 Asphalt mastics**

There are great varieties of the filler materials and asphalt binders. A given binder type reacts differently with different fillers, hence the mastic properties are depending on the combination of filler and binder. Wang et al (2011) conducted a series of tests for evaluating which filler properties had the most influence on the mastic. The outcome showed that Rigden voids had significant impact on the filler stiffening effects in the mastic and the rutting potential of the mixture. CaO content and the fineness modulus FM were also connected to the stiffening effect, but to a less degree than Rigden voids. The relative viscosity of the binder had the most impact on the rutting potential. The impact the filler properties had on the mastic was dependent on the binder type and the gradation of the coarser aggregates (Wang et al, 2011).

The percentage of filler in asphalt mastics is in Norwegian standards a function of the weight of the aggregates in the mixture (NPRA N200). The filler to binder ratio (F/A-ratio) has a major effect of the mastic performance. Due to variations in specific gravity and density of filler materials, a predetermined weight relationship of filler and binder could yield vast volume differences depending on the filler type used in the mastic. If the filler density is low, the filler volume gets high for a given amount of filler by weight, and more binder is needed to coat the filler material. This increases the relative amount of fixed binder leading to less free binder, which results in a dry asphalt mastic and not sufficient coating of the aggregate particles (Faheem and Bahia, 2010). Superpave specifications recommend the F/A-ratio by mass of 0.6 to 1.2 in asphalt mixtures, where the binder content is defined as the free binder content that is not absorbed by the aggregates in the mixture (AASHTO R35). Norwegian standards do not specify F/A-ratio or filler properties beyond mass percentages and a general range of Rigden voids.

The filler works as reinforcement of the binder, and the reinforcement mechanism can be split into reinforcement induced by particle-interaction, by volume-filling and by physiochemical properties of the filler (Buttlar et al, 1999). The particle-interaction reinforcement increases along with increased filler content as the filler material gets closer and forms a skeleton. The

stiffening effect of the volume-filling is a result of rigid filler materials in less rigid mastic, which makes it denser. The physiochemical reinforcement stiffening effect comes from the interfacial bonding between the asphalt binder and the filler, i.e. adsorption, absorption and selective sorption (Buttlar et al, 1999). The major factors affecting the physiochemical properties are the mineral composition, surface texture, surface activity and structural characteristics. The adsorption process is exothermic, and the amount of released heat by the filler-bitumen interaction indicates the adsorption intensity (Anderson and Goetz, 1973).

Ishai and Craus (1996) conducted a series of adsorption tests utilizing a microcalorimeter for determining the amount of released heat for a selection of fillers. 5.0 grams of diluted bitumen was poured into two different reaction cells. 1.0 gram of dry filler was put into a glass ampule, while another glass ampule was unfilled. The reaction cells and the glass ampules were put in a microcalimeter at 35 °C. After 24 hours, the glass ampules were broken inside the reaction cells, and the filler in the first ampules was immersed in the binder. The difference in released heat from the two cells was measured. The study showed that filler with the highest value of released heat per unit area, i.e. the combination of high geometric irregularity and high surface activity, gave strengthening effects on the filler-binder bonds and the ratio of fixed binder to free binder increased. This physiochemical effect gave better consistency of the mastic and higher strength of the asphalt mixtures. Hydrated lime had the highest value of released heat per unit area, followed by limestone and dolomite. Basalt and sandstone had the lowest values of the fillers tested (Ishai and Craus, 1996).

Craus et al (1979) conducted a study on selective sorption of chemical groups in the binder in filler materials. A chromatographic method was used by evaluating percolation of diluted bitumen through columns of different types of filler. The outcome showed that limestone and hydrated lime had highest selective sorption, followed by basalt, while sandstone barely had any capacity of sorption. Siliceous fillers had low surface activity, hence low adsorption intensity. The capacity of selective sorption indicates the filler effect on the adhesion and the stability of the asphalt mixture (Craus et al, 1979).

Another mastic property affected by filler type is the non-recoverable creep compliance  $J_{nr}$ , which indicates the permanent deformation of mastics during repeated loading. The relative  $J_{nr}$  ratio of the mastic to the binder points towards the stiffening effect of the filler in the mastic.  $J_{nr}$  can be measured by a dynamic shear rheometer (DSR) in the multiple stress creep recovery (MSCR) test. The test is originally a part of Superpave Performance Grading asphalt binder specification, but it is also used on mastics (Wang et al, 2011). The purpose of the method is to identify the elastic response under shear creep and recovery at two stress levels at a predetermined temperature. A sample of asphalt mastic is loaded at a constant creep stress of 0.1 kPa for 1 second and 9 seconds of unloaded recovery. The stress and strain shall be recorded for every 0.1 seconds for the creep cycle and every 0.45 seconds for the recovery cycle. This procedure is repeated ten times, followed by the same process with 3.2 kPa creep stress (ASTM D7405:10a). The adjusted strain after each recovery cycle is calculated by:

$$\varepsilon_{10} = \varepsilon_r - \varepsilon_0 \quad (8)$$

where  $\varepsilon_{10}$  = adjusted strain after each recovery cycle,  $\varepsilon_r$  = final strain value after each recovery cycle,  $\varepsilon_0$  = initial strain value.

For each of the ten cycles for the creep stress of 0.1 kPa and 3.2 kPa, the non-recoverable creep compliance is found by equation (9), for  $N = 1$  to 10:

$$J_{nr}(i, N) = \frac{\varepsilon_{10}}{100} \quad (9)$$

where  $J_{nr}$  = non-recoverable creep compliance,  $i$  = creep stress of 0.1 kPa or 3.2 kPa,  $N$  = cycle number,  $\varepsilon_{10}$  = adjusted strain after each recovery cycle.

The test is conducted for the binder and the mastic, and the relative  $J_{nr}$  of the mastic is the ratio of the two values. Wang et al (2011) showed that SBS modified binder had the strongest reaction with the fillers tested. However; there were great variances for all the binders, which indicate that the physiochemical interactions are dependent on the combination of filler and binder. Rigden void content in the fillers had a significant effect on the relative  $J_{nr}$  regardless of the binder type used in the mastic (Wang et al, 2011). Faheem et al (2012) found a negative relationship between Rigden voids and the mastic  $J_{nr}$ , indicating that an increase in mastic  $J_{nr}$  yields a decrease in resistance to rutting. This indicates that binders with low  $J_{nr}$  or fillers with high Rigden void content will increase the resistance to permanent deformation of the mastic.

The DSR apparatus can also be used for evaluating the complex shear modulus  $G^*$  for binders as well as asphalt mastics. This value is a measure of the overall resistance to elastic and plastic deformation when the mastic is exposed for repeated shear stress. The phase angle  $\delta$  is a measure of the elastic response of the material and indicates the lag in the stress response to the applied strain. Purely viscous materials have phase angle of  $90^\circ$ , whereas for purely elastic materials, the phase angle becomes  $0^\circ$  (Lerfald, 2000). The parameter  $G^*/\sin\delta$  is related to rutting and  $G^*\sin\delta$  characterizes fatigue cracking potential (Huang, 2004). Pasetto et al (2014) studied the viscoelastic properties utilizing DSR on mastics with different F/A-ratios. With increasing filler amount in the mastic, the complex shear modulus and the phase angle increased. The mastic stiffness was ten times as high for mastics with filler dosage of 100 % of the weight of the mastic compared to neat binder stiffness. Two spindle sizes were used to reduce the problem of spindle compliance (Pasetto et al, 2014). Yan et al (2013) conducted tests on warm mix asphalt with the purpose of relating  $G^*$  to the F/A-ratio in asphalt mastics. The DSR test was conducted for eight F/A-ratios with a Sasobit modified binder and three types of filler, i.e. limestone, hydrated lime and Portland cement. The outcome showed that as higher the F/A-ratio, the higher the  $G^*$ . Mastics containing hydrated lime yielded highest  $G^*$ , followed by Portland cement and limestone.

Rigden void content in the filler material is of special interest due to its major influence on the rheological property of the mastic (Liao et al, 2012). Mastic is considered a suspension of solid matter in a liquid, that is, filler particles in bitumen, and rheological models could be used to evaluate mastic viscosity. Viscosity of asphalt mastics affects the possibility of

sufficient coating of the aggregates, as well as workability and compatibility. To be able to predict the viscosity is important, however; the viscosity varies with different binder types, filler types and surface interaction, and the viscosity increases with increasing F/A-ratio (Liao et al, 2012). Faheem et al (2012) found that Rigden voids and binder viscosity were the major parameters affecting the viscosity of the mastic. If one or both of the binder viscosity and Rigden void content increased, the relative mastic viscosity and stiffness increased.

The first model describing rheological behavior was proposed by Albert Einstein in 1905 (Einstein, 1905). In his theory, relative viscosity is introduced, which is the increase in viscosity of the suspension as the ratio of the viscosity of the liquid. The filler particle concentration is in this equation defined as the ratio of particle volume to suspension volume, in this case filler volume to the mastic volume. The Einstein model presumes low particle concentration, where the fillers are located far enough from each other so that no particle interaction will occur (Shashidhar and Romero, 1998; Hesami et al, 2012). Equation (10) shows the Einstein equation:

$$\eta_r = 1 + \eta' \phi \quad (10)$$

where  $\eta_r$  = relative viscosity of suspension,  $\eta'$  = intrinsic viscosity,  $\phi$  = filler particle concentration.

The intrinsic viscosity of asphalt mastic is related to filler particle geometry and physical character, as well as the combination of filler type and binder type (Leseur, 2009). It can be treated as a curve fitting parameter depending on the maximum particle concentration (Hesami et al, 2012). The relationship is shown in equation (11):

$$\eta' = \frac{2}{\phi_m} \quad (11)$$

where  $\eta'$  = intrinsic viscosity,  $\phi_m$  = maximum particle concentration by volume.

The value of the intrinsic viscosity, also known as the Einstein coefficient  $K_E$ , is determined to be 2.5 for spherical particles (Einstein, 1905). Shashidhar and Romero (1998) define the coefficient as the stiffening rate of the mastic as a function of the addition of filler. Furthermore, the maximum particle volume concentration  $\phi_m$  in asphalt mastics is the maximum amount of filler that can be added without prompting the appearance of air voids in the mastic. That is, asphalt mastic with maximum particle concentration has no free binder volume (Shashidhar and Romero, 1998). Related to the reinforcement effects of filler in mastics, the maximum particle concentration contributes to the volume-filling stiffening effect. The Einstein coefficient represents the physiochemical reinforcement (Shashidhar and Romero, 1998). The maximum particle concentration in a dry, compacted sample of mastics can be found by equation (12):

$$\phi_m = \frac{V_f}{V_f + V_{b.fixed}} = \frac{V_f}{V_{f.bulk}} \quad (12)$$

where  $\phi_m$  = maximum particle concentration,  $V_f$  = filler volume,  $V_{b.fixed}$  = fixed binder volume,  $V_{f.bulk}$  = filler bulk volume.

As mentioned previously, parts of the fixed binder volume are adhered by the filler and acts as a part of the particle, which gives the filler particles slightly larger radius, as seen in figure 4. The effective radius of the filler particles is the radius of the filler in addition to the thickness of the binder coating the particles. For that reason, the effective filler volume in the mastic becomes greater than the volume of the predetermined volume percentage of the filler added in the mastic (Liao et al, 2012). The compositional filler volume concentration is found by equation (13) and the effective filler volume by equation (14) and (15). The relationship is depicted in figure 5.

$$\phi = \frac{V_f}{V_f + V_{b.fixed} + V_{b.free}} = \frac{V_f}{V_{f.bulk} + V_{b.free}} \quad (13)$$

$$\phi_m = 1 - \frac{V_R}{100} \quad (14)$$

$$\phi_e = \frac{\phi}{\phi_m} \quad (15)$$

where  $\phi$  = filler particle concentration,  $V_f$  = filler volume,  $V_{b.fixed}$  = fixed binder volume,  $V_{b.free}$  = free binder volume,  $V_{f.bulk}$  = filler bulk volume,  $\phi_m$  = maximum particle concentration,  $V_R$  = Rigden void content (%),  $\phi_e$  = effective particle concentration.

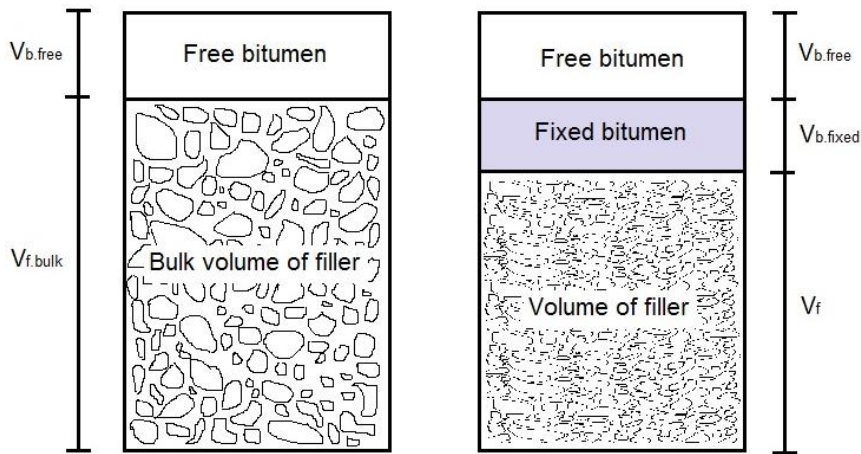


**Figure 5: Schematic of fractional voids in asphalt mastics**

The effective particle concentration is defined as the filler concentration in mastics which provide the same stiffness for different fillers (Lerfald, 2000). The research work by Lerfald (2000) shows that there are great variations in the effective particle concentrations for different filler types used in mastics. Similar results are found by Buttlar et al (1999), where it was shown that two mastics with drastically different filler volume concentrations could yield similar effective volume concentrations and equivalent stiffening ratios. Different effective volume concentration is due to the fact that different fillers have different adsorption properties, Rigden void content, surface area and texture (Buttlar et al, 1999).



Shashidhar and Romero (1998) state that higher binder adsorption gives rise in the actual particle concentration  $\phi$ , and consequently the effective particle concentration increases by equation (15). Table 2.1 below outlines examples of filler mass needed for hydrated lime, limestone and two baghouse dusts to provide three similar effective volume concentrations in soft binder mastic from the study by Lurfald (2000). As the numbers show, there are great variations between hydrated lime and the other filler types tested, and also between the sieved baghouse dusts. This phenomenon is not taken into account if fillers are added based on a weight relationship of the aggregates.

Table 2.1: Filler mass for similar effective volume concentration (Lurfald, 2000)

Filler type, mass (g)	$\varphi_e = 0.1$	$\varphi_e = 0.3$	$\varphi_e = 0.6$
Hydrated lime	6.1	19.8	45.8
Limestone	13.1	47.0	123.0
Sieved baghouse dust, Lia	11.5	38.2	100.4
Sieved baghouse dust, Tau	12.4	42.4	110.8

The effective radius and volume of the filler particles affect the viscosity. The Einstein model for viscosity of suspensions assumes no particle interaction between the fillers within the mastic. The model has to be modified for higher particle concentrations where interaction between filler particles occurs. Several extended theories for the viscosity of suspensions for higher particle percentages have been proposed in the literature, and Hesami et al (2012) emphasize the Frankel model as suitable for asphalt mastics. The equation for the Frankel theory can be seen in equation (16):

$$\eta_r = \left( \frac{\delta}{r} - \frac{h}{r} \right) * N_C * C_1 \quad (16)$$

where  $\eta_r$  = relative viscosity of the suspension,  $r$  = weighted average particle radius,  $\delta$  = thickness of adsorbed binder layer,  $h$  = distance between two effective particles,  $C_1$  = friction coefficient of the system,  $N_C$  = number of particles.

The thickness of the adsorbed binder layer is found by equation (17) by Buttlar et al (1999), while Coussot (2005) derived equation (18) for the distance between two effective particles.

$$\delta = \left( \frac{\phi_e - \phi}{\phi G_m A} \right) \quad (17)$$

$$h = 2r \left( \phi_e^{\frac{1}{3}} - 1 \right) \quad (18)$$

where  $\delta$  = thickness of adsorbed binder layer,  $\phi_e$  = effective particle concentration,  $\phi$  = filler particle concentration,  $\phi_m$  = maximum particle concentration,  $G_m$  = specific gravity of the filler,  $A$  = surface area per weight of the filler particles,  $r$  = weighted average particle radius.

As Leseur and Little (1999) mention in their study, the importance of the variations in maximum particle concentration  $\phi_m$  for different filler types in viscoelastic models has to be emphasized. Leseur and Little (1999) stress the fact that the intrinsic viscosity, or the Einstein coefficient  $K_E$ , is a function of  $\phi_m$ , as seen in equation (11). For hydrated lime,  $\phi_m = 0.2$ , while the average value for most fillers is 0.63. This yields great variations in  $K_E$ , hence the viscosity model for mastics becomes binder and filler specific. Furthermore, Einstein (1905) assumes spherical particles in the proposed rheological model. Most filler materials diverge from this shape, and Leseur and Little (1999) state that flat and elongated particles with 1:10 dimension ratio get  $K_E = 13.6$ . They concluded that additional elements than physiochemical properties of the filler materials are necessary to verify rheological factors for filler-binder interactions in mastics.

Similar results were found by Kavussi and Hicks (1997). Mastics get increased viscosity when filler is added, and this singularity has been shown to be directly related to the particle size, gradation and texture of the filler. The rate of increase is said to be a function of the fineness of the filler, and surface affinity tests revealed that higher viscosity was a result of higher filler absorptivity (Kavussi and Hicks, 1997). Figure 6 depicts the change of mastic viscosity with respect to F/A-ratio by weight and volume. As the figure shows, the kaolin filler yields much higher values than limestone and quartz filler. Kavussi and Hicks (1997) relate this to the fact that kaolin has spherical particles and high fineness, while quartz and limestone have coarser and angular particles.

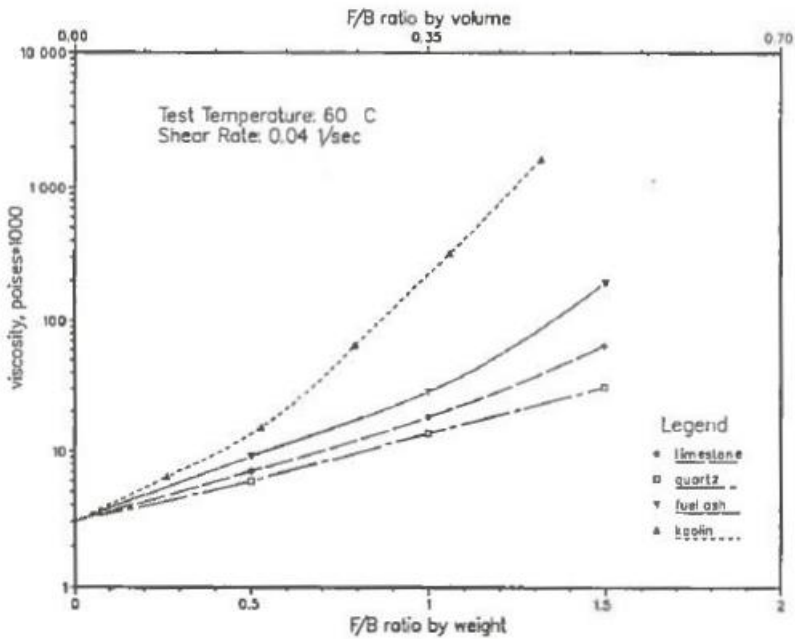


Figure 6: Mastic viscosity with respect to F/A-ratio (Kavussi and Hicks, 1997)

NCHRP Project 9-45 (2010) conducted tests using F/A-ratio by mass of 1:1 to evaluate the change in volume of the mastic. The study uses 17 different fillers blended with 4 different binders creating a total of 68 different mastics. The volumetric fraction of filler to mastic varied between 26 % and 32 %. Both manufactured fillers and natural fillers were tested, and the natural fillers had a range of  $\pm 2$  % of the average of 28 % of the volumetric fraction.

Faheem and Bahia (2009) concluded that when the volumetric filler fraction is less than 40 %, the Rigden voids and the particle size distribution of the filler have greater influence than the volumetric concentration. Rigden voids and volume fraction correlated for the natural fillers, where higher volume fraction yielded higher Rigden voids. Values of the manufactured fillers did not correlate and were scattered. Faheem and Bahia (2009) incorporated Rigden void content in equations for adequate mixture performance based on mastic properties and limits. However; as it is stated in the study, there could be raised questions on how accurate utilization of mastic properties as the connection between filler and mixture performance are on the control of the effect of the fillers in HMA. The proposed models are shown in table 2.2 below, but they need further verification and adjustments for local variations (Faheem and Bahia, 2009).

Table 2.2: *Mastic properties for best mixture performance (Faheem and Bahia, 2009)*

Performance indicator	Mastic property	Mastic limit	Mastic model
Workability	Relative viscosity at 135 °C	Less than 5.0	Mastic viscosity = -8244 + 4.68(binder viscosity) + 205(Rigden void content)
Rutting	$J_{nr}$ at 3.2 kPa and 58 °C	Less than 0.40	Mastic $J_{nr} = 1.01 + 0.160(\text{binder } J_{nr}) - 0.0230(\text{Rigden void content})$

Rigden (1947) proposed a theory stating that the stiffening effect of the filler is affected by the filler fractional voids filled with fixed asphalt binder. Higher Rigden voids yields higher stiffening effect due to the fact that additional binder becomes fixed and has to fill the voids in the filler material. Hence, less binder is available and free for separation amongst filler particles (Anderson, 1987; Harris and Stuart, 1995). However; studies have shown that since Rigden voids are measured in a dry filler sample, the properties of the mastic system as a whole are not taken into account (Shashidhar and Romero, 1998). The study by Landel et al (1965) proved that the maximum particle concentration  $\phi_m$  in a dry compacted filler sample not necessarily is equivalent to the value obtained in presence of liquids, and he recommends  $\phi_m$  in presence of liquids as the parameter for predicting stiffness. Since  $\phi_m$  is closely connected to Rigden void content by equation (14), Shashidhar and Romero (1998) suggest that direct measurements of the  $\phi_m$  and  $K_E$  would be better than Rigden void content as the prediction parameter of the filler stiffening effect in asphalt mastics.

## 2.4 Asphalt mixtures

The filler provides consistency and strength to the mastic and stabilizes the asphalt mixture by filling the voids of the coarser aggregates, which increases the mixture density. The laboratory procedure of obtaining the theoretical maximum specific gravity of asphalt mixtures was developed by James Rice, therefore it is known as Rice density. In American literature, the common way to express the maximum density is by the theoretical maximum specific gravity<sup>2</sup>, symbolized as  $G_{mm}$ . The name could be somewhat misleading, since the calculated value is used as a density measure, not gravity.

<sup>2</sup> Personal communication, Dr. Steve Perkins, March 20, 2014

The theoretical maximum specific density is obtained by multiplying  $G_{mm}$  with the density of water. The procedure is described in Method 14.5633 in NPRA R210. The weight of a beaker in air and in water at temperature 25 °C is found using a balance with 0.1 grams accuracy. A sample of loose asphalt mass is filled in the beaker and weighed in air, before distilled water is added to submerge the asphalt mass. The beaker is then placed in a vacuum desiccator, and vacuum is applied to remove the air in the asphalt mass. Thereafter, the beaker is removed from the apparatus and placed in a water bath at 25 °C until the asphalt mass has 25 °C, since the data of the binder is known at 25 °C. The beaker with the asphalt mass is submerged in water at the same temperature and weighed. The relationship of the Rice density is:

$$G_{mm} = \frac{A}{A+D-E} \quad (19)$$

$$\rho_{max} = G_{mm}\rho_w \quad (20)$$

where  $G_{mm}$  = theoretical maximum specific gravity,  $A$  = sample mass in air (g),  $D$  = mass of beaker in water,  $E$  = mass of beaker filled with sample mass in water (g),  $\rho_{max}$  = maximum theoretical specific density (g/cm<sup>3</sup>),  $\rho_w$  = water density at actual temperature (g/cm<sup>3</sup>).

The mixture needs to have enough stiffness during the construction phase to counteract the downward forces from the gravity leading to mastic drainage. This incidence is called draindown, and it can be evaluated using the NCAT draindown test (Mogawer and Stuart, 1996). In the NCAT draindown test, an asphalt mixture sample is placed in a wire basket on a plate of paper with known weight and put in an oven at elevated temperatures for 60 minutes. The temperature is dependent on the type of asphalt mixture, mastic combination and binder. The paper plate with the draindown is then weighed, and the loss due to draindown is calculated using the equation (21):

$$\text{Loss in percent} = \frac{\text{Final paper mass} - \text{Initial paper mass}}{\text{Initial sample mass}} * 100 \quad (21)$$

Mogawer and Stuart (1996) conducted this test in their study of stone mastic asphalt (SMA), and they showed that draindown did not occur when a stabilizer of cellulose fiber was added to the mixture, and additional investigations are necessary to evaluate different fillers.

Kavussi and Hicks (1997) utilized a measure called *toughness* to compare mixtures containing different types of filler at different F/A-ratios by weight. Toughness is defined as the amount of work per unit volume required to cause failure, and it is determined by integrating the area under the stress-strain curve for the different asphalt mixtures. The test was carried out at various test temperatures, and as higher the temperature, the greater the area under the curve. The study revealed that there is an optimum filler content for each mixture that corresponds to maximum toughness. The toughness increased as the filler concentration increased up to this point. However; for further increase of filler amount, the toughness decreased. At the peak point, the asphalt mixture needs maximum total energy to reach failure. For all the test temperatures, mixtures with limestone had the peak at F/A-ratio of 0.4 by weight. Quartz filler

and fly ash were the most tolerant to variations in F/A-ratio and did not have sharply defined peaks. Regardless of the test temperatures, the maximum toughness corresponds to optimum F/A-ratio by mass between 0.25 and 0.75 for all fillers tested (Kavussi and Hicks, 1997). Huang et al (2007) explain the decrease in toughness when the filler content increases as a result of the asphalt mixture becoming more brittle along with higher filler content. More filler can increase the mixture strength, but this might be compromised with reduced resistance to fatigue cracking (Huang et al, 2007).

Mixture workability is affected by the filler type. Workability and compaction effort can be represented as the number of gyrations needed to reach a predetermined density value by utilizing gyratory compactor in preparation of the mixture samples. NCHRP Project 9-45 (2010) defines the workability indicator as the number of gyrations to 92 % of maximum density. The study showed that coarse graded mixtures are less workable than fine graded mixtures, and the conclusion is that the gradation is significant for mixture workability. The binder type and filler type are less important. The mixture becomes less workable as the relative mastic viscosity increases (NCHRP Project 9-45, 2010).

The Cantabro test described in Method 14.555 in NRPA N200 evaluates the breakdown, durability and quality of asphalt mixtures, as well as resistance to abrasion. The test quantifies the abrasion loss, which is determined as the percent of particle loss of mass from compacted asphalt specimens after 300 revolutions at 30-33 revolutions per minute in the Los Angeles apparatus. After all the revolutions, the mass broken off the test specimen is discarded, and the Cantabro loss is calculated by equation (22) below.

$$CL = 100 \left( \frac{m_1 - m_2}{m_1} \right) \quad (22)$$

where CL = Cantabro loss (%),  $m_1$  = initial weight (g),  $m_2$  = final weight (g).

Method 14.5561 in NRPA R210 outlines the Marshall test, which has the aim of determine the resistance to plastic flow of cylindrical asphalt specimens loaded perpendicular to the radius in a Marshall apparatus. The compacted specimen is conditioned for 1 hour in a water bath until the temperature is 60 °C, before the test is conducted. The Marshall stability is the maximum load that the specimen can carry at the point of failure, and the flow index is the deformation at maximum load. Due to the fast loading rate, the Marshall stability measures the cohesion, and the flow index reports the internal friction (Huang, 2004). Tayebali et al (1998) showed that an increased amount of filler increased the Marshall stability and the unit weight of asphalt mixtures. The optimum binder content for the same filler amount varied with filler type, so the F/A-ratio varied for each mixture. Mixtures containing aggregate blends with 20 % natural sand had higher optimum binder content and higher Marshall stability than mixtures of 100 % crushed granite (Tayebali et al, 1998). Furthermore, the study showed that when the filler content by weight of the aggregates rose from 4 % to 12 %, the optimum binder content decreased with 1.7 % for the blend with 20 % natural sand and 1.4 % for the blend with 100 % crushed granite.

Al-Suhaibani et al (1992) investigated the variety of different optimum binder content for different filler types. Limestone was used as the reference filler, whilst for different mixtures the limestone filler was partly replaced by hydrated lime or Portland cement. Mixtures containing 8 % limestone partly replaced by hydrated lime possessed higher optimum binder content than those replaced with Portland cement. The difference between hydrated lime and Portland cement increased with increasing amount of replacement, and it is explained by the high surface area, high Rigden void content and binder absorption of hydrated lime particles, as well as higher air voids in the asphalt mixture (Al-Suhaibani et al, 1992).

Challenges with different optimum binder content for different filler types and binder types affect the effect of F/A-ratio in the mastics. Zeng and Wu (2008) tested mastics with a standard unmodified binder and a range of F/A-ratio by mass from 0.0 to 1.5. They found that the F/A-ratio of 0.9 for pulverized limestone filler is equivalent to F/A-ratio of 0.75 for Portland cement and 0.4 for hydrated lime filler, when tested as a function of mastic viscosity. Furthermore, the outcome showed that a change in 0.1 in F/A-ratio, the temperatures had to be increased by 3.5 °C for mastics with limestone and 9.3 °C for mastics with hydrated lime to assure necessary mastic viscosity for sufficient mixing and aggregate coating (Zeng and Wu, 2008). Due to this fact, there could be somewhat misleading to compare F/A-ratios directly without including other filler properties in the comparison.

The Prall test described in NS-EN 12697-16:2004 is a method used to determine the abrasion resistance to studded tires and wear of asphalt pavements. A cylindrical specimen cut to a height of 30 mm is conditioned for 5 hours in water of 5 °C. Thereafter, the specimen is placed in the abrasion apparatus, a flat rubber ring is put on top of the specimen and steel balls are put in the ring. The abrasion process lasts for 15 minutes and the steel balls are moving with 950 revolutions per minute. Cooling water is continuously running through the apparatus during the test. The abrasion value is determined by equation (23):

$$Abr_A = \frac{m_1 - m_2}{\rho} \quad (23)$$

where  $Abr_A$  = abrasion value (mL),  $m_1$  = mass of water stored in the specimen surface dry in air before abrasion (g),  $m_2$  = mass of water stored in the specimen surface dry in air after abrasion (g),  $\rho$  = saturated surface dry specimen density (g/mL).

The flow number test determines the resistance to permanent deformation and rutting potential, i.e. the flow number  $F_N$ . The test is run on the Asphalt Mixture Performance Tester (AMPT), and the procedure involves an asphalt specimen subjected to an axial compressive load pulse of 0.1 seconds every 1.0 seconds, with or without confining pressure and a set temperature. The permanent axial strains are measured as a function of time, and  $F_N$  is the number of load cycles corresponding to the minimum rate of change of permanent axial strain (NCHRP Report 629, 2008). Wang et al (2011) conducted the  $F_N$  test on a variety of asphalt mixtures. The results were that mastics with SBS modifier had the highest  $F_N$  values, while neat binders gave mastics with the lowest values. A regression model combining the  $F_N$  value

and the Rigden void content of the mastics as parameters showed that the Rigden void content in the filler material affected the rutting potential of the mixtures. Higher Rigden void content gave higher  $F_N$  value, hence better resistance to rutting and permanent deformation. The effect was more evident for coarse mixtures than fine mixtures (Wang et al, 2011).

Another test method for permanent deformation and rutting is the wheel track test. In this method, a laboratory prepared rectangular test specimen is placed in a wheel track machine, where a tire with 600 kPa load is set in motion and undergoes a predetermined number of load cycles, normally 10 000 cycles. The test can be conducted at various temperatures, but the test specimen must be conditioned for the situation for at least 12 h prior to testing. The rut depth is measured at several spots along the test slab, and the measured proportional rut depth is calculated as sum of the ratios of the local deformations to the specimen height at the corresponding spots (NS-EN 12697-22, 2003).

Al-Suhaibani et al (1992) tested mixes with different filler content in the wheel track test, and the results showed that there seems to be an optimum filler content for the least rut depth. Up to certain filler content, which varied with mixtures and type of filler, the rut depth decreases, whilst it increases beyond this filler content. Furthermore, the rut depth decreases with decreasing binder content due to higher internal particle friction, and it was shown that the binder content had considerably greater effect on rutting resistance than the filler content. Compaction has a vast effect on the mixture behavior, and as mentioned earlier, higher Rigden void content yields stiffer mastics, hence more viscous and less workable mixtures. By having the same compaction effort for all mixtures containing different fillers, the final compaction and density are lower for stiffer mixtures than those with less viscous mastics.

The wheel track test is the reference method in Norwegian standards for determining the resistance to permanent deformation and rutting potential<sup>3</sup>. Juxtaposed with this method, the cyclic compression test is an alternative method for evaluation of permanent deformation resistance. The test is carried out in the Nottingham Asphalt Tester (NAT), where a cylindrical specimen with 15 cm diameter and 60 mm height is placed between two parallel loading plates, whereas the upper plate is 10 cm in diameter. The specimen is subjected to a cyclic axial block-pulse pressure and no additional lateral confinement pressure, and during the load applications the change in height of the specimen is measured. The load pulse has a frequency of 0.5 Hz, and a total of 3600 pulses should be applied. The test temperature is set to 40 °C, and the specimens are conditioned in a thermostatic chamber to the specific temperature 4 to 7 hours prior to testing. The cumulative axial strain as a function number of load applications is represented in a creep curve showing the creep characteristics of the specimen. The cumulative axial strain is calculated by equation (24), while the creep rate and creep modulus is specified by equation (25) and (26) respectively (NS-EN 12697-25:2005, Test Method A).

$$\varepsilon_n = 100 \left( \frac{h_0 - h_n}{h_0} \right) \quad (24)$$

---

<sup>3</sup> Personal communication, Nils Uthus, June 1, 2015

$$f_c = \frac{\varepsilon_{n1} - \varepsilon_{n2}}{n_1 - n_2} \quad (25)$$

$$E_n = \frac{\sigma}{\varepsilon_n} \quad (26)$$

where  $\varepsilon_n$  = cumulative axial strain after  $n$  load cycles (%),  $h_0$  = average height of specimen (mm),  $h_n$  = average height after  $n$  load cycles of specimen (mm),  $f_c$  = creep rate,  $\varepsilon_{n1:n2}$  = cumulative axial strain after  $n_1;n_2$  load cycles,  $n_1;n_2$  = number of repetitive load cycles,  $E_n$  = creep modulus after  $n$  load cycles (MPa),  $\sigma$  = applied stress (kPa).

Figure 7 illustrates a generalized creep curve. Stage 1 is the area where the slope of the curve decreases with increasing number of load cycles. Stage 2 has a quasi-constant slope and the turning point of the curve, denoted as point 4. Stage 3 has increasing slope with increasing number of load cycles. NS-EN 12697-25:2005 states that depending on test conditions and the asphalt mixture, one or more stages may be absent. Other points of interest are the cumulative axial strain at 3600 load cycles and the gradient of the slope in stage 2.

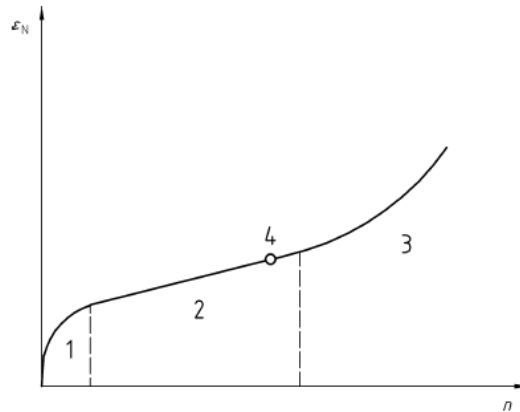


Figure 7: Creep curve with different stages (NS-EN 12697-25:2005)

NS-EN 12697-25:2005 specifies that testing shall not start before 2 days after compaction in the laboratory or on the road, while NPR A N200 requires that the day of testing has to be between 8 and 30 days after the preparation day of cored specimen. If the test is conducted after 30 days, a correction factor has to be applied. The maximum allowed value of cyclic creep in microstrain ( $\mu\varepsilon$ ) with respect to AADT from NPR A N200 are outlined below. In the laboratory procedure, this cyclic creep value should not be exceeded at 3600 load cycles.

Table 2.3: Specifications for cyclic creep

AADT	Less than 1500	1501-3000	3001-5000	5001-10000	More than 10000
Maximum allowed cyclic creep ( $\mu\varepsilon$ )	N/A	40000	30000	25000	20000

The joint study PROKAS suggests producing specimens with height of 10 cm and cut off 2 cm at the top and the bottom for best results in the cyclic compression test when the specimens are compacted with the gyratory compactor (Lerfald et al, 2004). This can be related to the fact that the air void distribution in gyratory compacted specimens is bath tub



shaped, with higher air void content in the top and bottom part of the pucks. Additionally, the gyratory compactor does not produce specimens with parallel top and bottom surfaces. The kneading process in the compaction stops at a certain amount of gyrations, leaving the height of the specimen to vary around the circumference (Ødegård, 2014). By removing the top and bottom part, the specimen will receive a more uniform air void distribution throughout the height and parallel saw kerf surfaces, which again will provide more precise and even results.

Method 14.554 in NPRA R210 describes the procedure of determining indirect tensile strength by utilizing the Marshall apparatus. In this test, a cylindrical asphalt specimen with diameter 10 cm is loaded by two steel loading strips with concave surface with the same radius of curvature as the specimen. The temperature of the specimen during the test should be 5 °C or 25 °C. Load is applied vertically with a deformation rate of  $50 \pm 2$  mm/min until failure, and the maximum load is recorded. The indirect tensile strength is found by:

$$S_t = \frac{2000P}{\pi t D} \quad (27)$$

where  $S_t$  = indirect tensile strength (kPa),  $P$  = maximum load at failure (N),  $t$  = specimen height (mm),  $D$  = specimen diameter (mm).

Huang et al (2007) employed the indirect tensile strength test to determine the tensile strength and strain of different asphalt mixtures at failure. The study showed that the increase in filler content led to an increase in the indirect tensile strength. Filler strength is greater than binder strength, and when the mastic contains more filler, the mastic strength will increase. Inevitably this results in a mixture strengthening effect and higher indirect tensile strength of the asphalt specimen. The trend showed that hydrated lime and manufactured sand had similar strength values, while gravel filler had the lowest value for the lowest filler content and the highest value for the highest filler content (Huang et al, 2007). This is in agreement with the results of Al-Suhaibani et al (1992). The results proved that the filler type had little effect on the indirect tensile strength, but the filler content was the critical parameter. Higher filler content gave higher tensile strength (Al-Suhaibani et al, 1992).

In the study by Huang et al (2007) the effects of fillers on optimum binder content and indirect tensile strength were also investigated. Hydrated lime, manufactured sand and gravel were the fillers tested. The study used Marshall mix design procedure to find the optimum binder content for each asphalt mixture with different filler type and filler content. Increased amount of filler yielded slightly lower optimum binder content, because less binder is needed with increasing filler content to form the same amount of mastic. The variance in optimum binder content for the different fillers was  $\pm 0.3\%$ . However; there was no consistency in which filler needed the highest value for different filler content (Huang et al, 2007).

Along with the indirect tensile strength, the resilient modulus  $M_R$  is an important parameter, which is the elastic modulus based on the recoverable strain under repeated load (Huang, 2004). The resilient modulus for asphalt specimens is found by a repeated load indirect tensile

strength test, where a haversine compressive load is applied in the vertical diametric plane with duration of 0.1 seconds and 0.9 seconds rest period (ASTM D4123). The horizontal recoverable deformation is measured, and the resilient modulus is calculated by equation (28):

$$M_R = \frac{\sigma_d}{\varepsilon_r} \quad (28)$$

where  $M_R$  = resilient modulus (MPa),  $\sigma_d$  = deviator stress (MPa),  $\varepsilon_r$  = recoverable strain.

The difference between indirect tensile strength test and the resilient modulus test is that the latter is not loaded until failure. The stress level is 5 % to 20 % of the indirect tensile strength (Roberts et al, 1996). It has been shown that the resilient modulus increases with increasing filler amount, and that the filler type is critical. Mixtures with 20 % natural sand yields higher resilient modulus than mixtures containing 100 % crushed granite, due to higher average unit weight for mixtures with natural sand (Tayebali et al, 1998). Al-Suhaibani et al (1992) tested the filler effects on the resilient modulus by partly replacing limestone filler with hydrated lime or Portland cement. The study showed that the increase in the amount of replaced limestone by either hydrated lime or Portland cement reduced the resilient modulus. This was explained by the fact that hydrated lime and Portland cement may have extended the binder rather than stiffen it, which resulted in lower resilient modulus (Al-Suhaibani et al, 1992).

The modulus of rupture is a measure of the flexural strength of asphalt mixtures. For low temperatures, high modulus of rupture, along with low stiffness modulus, is desirable to ensure sufficient tensile strength and avoid brittleness. Kavussi and Hicks (1997) evaluated dense graded asphalt mixtures containing different F/A-ratios by weight and four different filler types, i.e. limestone, fly ash, quartz and kaolin. For all filler types, both the mixture stiffness and the modulus of rupture increased as the F/A-ratio increased. The modulus of rupture test is carried out on simply supported beams of asphalt mixtures where two point loads are applied on 1/3 of either side of the beam. The modulus of rupture is calculated by:

$$S_r = \frac{m_2^h}{I} \quad (29)$$

where  $S_r$  = modulus of rupture,  $m$  = bending moment,  $h$  = height of the beam,  $I$  = moment of inertia.

Faheem and Bahia (2009) studied the effect of diluted and concentrated mastics. In a diluted solution, filler particles are suspended and float freely in the binder, while in concentrated solutions there is not enough binder to coat the entire filler amount, and the mastic cohesion starts to weaken. The critical filler concentration has the maximum binder influence, and it corresponds to the filler volume where there is just enough binder to coat the filler, i.e. the optimum binder content. The critical filler concentration represents the point where the cohesive strength of mastics starts to reduce. Figure 8(a) shows fillers in diluted mastics and figure 8(b) is the critical filler concentration and the border between diluted and concentrated region. Figure 8(d) depicts the concentration where the mastic has maximum stiffening effect.

The repulsion phase is shown in figure 8(e), where there is no free binder and the mastic system struggles with holding together (Tunnicliff, 1962; Faheem and Bahia, 2009).

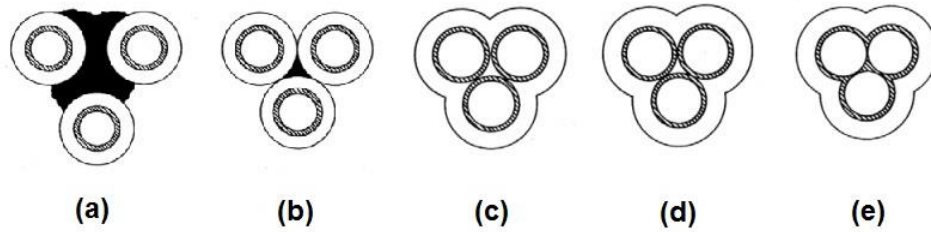


**Figure 8: Packing of filler in mastics (Tunnicliff, 1962)**

In the study by Faheem and Bahia (2010) it was found that the critical filler concentration could be represented as a function of the Rigden void content and the methylene blue value of the filler material, where the resulting prediction parameter tested was the relative complex shear modulus  $G_r^*$  and stiffness of the mastic. The relationship for the critical filler content can be seen in equation (30). The equation is validated for several filler and binder types, including limestone and hydrated lime, neat and modified binders, and the estimated values of the relative complex shear modulus compared to the measured values were lying within a range of  $\pm$  one standard deviation.

$$\phi_c = 83.2V_R + 4.79MBV \quad (30)$$

where  $\phi_c$  = critical volumetric filler concentration,  $V_R$  = Rigden void content (%), MBV = methylene blue value.

A property with vast importance to the mixture performance is aggregate coating, hence the asphalt film thickness. Evaluation of asphalt binder film thickness is not a part of the Marshall mixture design procedure used in Norway (NPRA N200). However; it is an important factor for asphalt mixture durability and performance. If the binder film gets too thin, the binder will more rapidly oxidize leading to hardening, brittleness and failure. The thickness of the binder film is a function of the binder content and the particle size of the aggregates, where the thickness of the binder film decreases as the particle diameter of the aggregate particles decreases (Roberts et al, 1996). Additionally, the film thickness varies depending on the asphalt mixture type, and also within the mixture type in different specimens (Lerfald, 2000).

Huang et al (2007) emphasize the statement that asphalt mixtures should be considered as a system of mastic coated aggregates rather than binder coated aggregates only. Zeng and Wu (2008) suggest that mastic viscosity should be the basis for mixing and compaction temperature, not binder viscosity. As of today, there are no standardized restrictions for mastic properties in Norwegian standards. NPRA N200 set requirements for the properties for the binder used in the asphalt mixture, but not for the mastic. Anderson and Goetz (1973) state that to assume the binder properties in turn will specify the mastic properties is equivalent to indicate that the consistency of the binder is unaffected by the filler in the mastic, and that filler-binder interaction does not influence the mastic properties.

# CHAPTER 3: METHODOLOGICAL DESIGN

## 3.1 General

This research experiment is undertaken to evaluate the different fillers used in asphalt mastics and to relate the filler properties and F/A- ratios to mixture performance. The sieving curve has been kept constant for all series to reduce the number of variables, since mastic properties are results of filler types, binder types, surface interaction and the ratio of filler to binder. Keeping the filler content by mass constant will still provide varieties in F/A-ratios by volume, since the density, Rigden void content and particle geometry vary between the fillers.

## 3.2 Type of asphalt

Asphalt concrete with maximum aggregate size of 11.2 mm (Ab 11) has been chosen as the type of asphalt in this study. Ab 11 is a well-graded asphalt mixture commonly used in Norway as a surface course and binder course on roads with high traffic volume and strict requirements for stability (NPRA N200). Requirements for Ab 11 are found in NPRA N200, provided in table C.1 in Appendix C. The sieving curve chosen for the asphalt mixture lies halfway between the upper and lower limits, see figure 9 below. The obtained sieving curve and the ratios of the different fractions were determined utilizing the Solver application in Excel. The ratios will be discussed in chapter 3.3.1, while details of the sieving curve are attached as table C.2 in Appendix C.

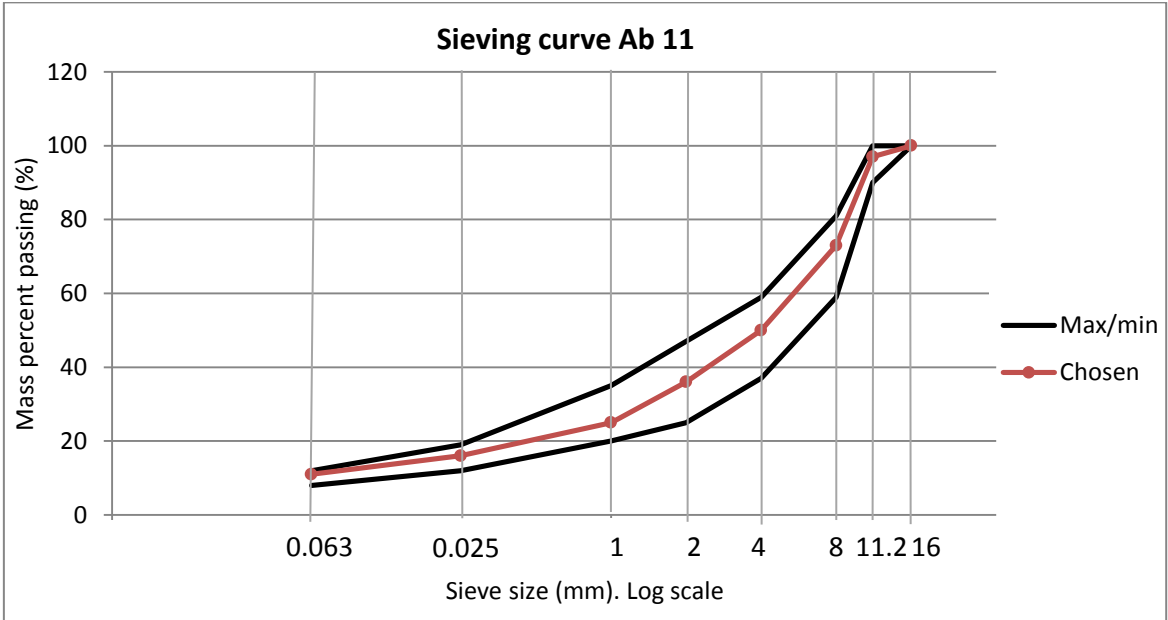


Figure 9: Sieving curve for Ab 11

### 3.2.1 Aggregates and filler

The aggregates in all mixture batches are Steinkjer 0-4, Steinkjer 4-8 and Steinkjer 8-11, where Steinkjer is the place of origin and the figures are the lower and upper limits of the aggregate sizes in each fraction. The fines passing the 0.063 mm sieve were removed from the

Steinkjer 0-4 fraction by dry sieving utilizing a quadratic sieve with 0.063 mm mesh size followed by washing and drying the retained aggregates in a heating cabinet. Excluding the dust particles from the aggregates yields a controlled mixture that isolates the effect of the added filler particles. The coarser fractions were not sieved or washed due to very low percentage of fines. The sieving curves of the Steinkjer aggregate fractions are attached in table D.1, Appendix D. The density of Steinkjer is  $\rho = 2.71 \text{ g/cm}^3$ . The aggregate is made of meta-sandstone, meta-greywacke and quartzite, and it is an acidic and hydrophilic type of rock (Nålsund, 2014). As mentioned previously, hydrophilic minerals create weak bonds with bitumen. However; it was decided not to add amine to improve the adhesion in the mixture. This decision was made in order to have more isolated evaluations of the filler effects.

Four types of filler have been tested; limestone, hydrated lime and sieved dust passing sieve 0.063 mm from Steinkjer 0-4 fraction and Vassfjell 0-4. Vassfjell is a meta-gabbro and cataclasite, and it is a strong base with relatively good affinity to bitumen (Nålsund, 2014). Approximately 15 grams of the sieved filler fraction of Steinkjer and Vassfjell were sent to SINTEF Materials and Chemistry for determining the filler density. The results are shown in Appendix D, table D.2. Properties for limestone and hydrated lime were provided in the datasheet by the producer and are attached in Appendix D, table D.3 and D.4.

The Rigden void content of the fillers was found by Method 14.4282 in NPRA R210, as explained in chapter 2.2.1. The inside cross section area of the apparatus was  $500.9 \text{ mm}^2$ . The desiccator where the sample was cooled is shown to the left in figure 10, while the Rigden apparatus is to the right. The Rigden apparatus is placed on a lightweight expanded clay block on a wooden countertop in level to avoid vibrations. Three parallel tests were conducted for the sieved fillers and hydrated lime. Limestone had Rigden void content specified in the datasheet in table D.3, Appendix D and was not further tested.



Figure 10: Desiccator and Rigden apparatus

### 3.2.2 Bitumen

The binder used in the mixture had a stiffness of 70/100. The binder was stored in 10 L containers, and to be able to divide it into smaller buckets it had to be heated in the heating cabinet until it was in liquid state. The cabinet was set at  $160 \text{ }^\circ\text{C}$ . When the bitumen reached

its liquid state it was poured into metal cans, where each can contained approximately 0.5 L. The preheating may have caused the binder to be slightly stiffer than 70/100. Since the binder consistency changes with temperature, it is essential to keep the temperature at a level where the properties are known when evaluating the asphalt specimens. At 25.0 °C the binder density is  $\rho_b = 1.01 \text{ g/cm}^3$ .

The minimum binder content for Ab 11 is specified in NPRA N200, see Appendix C table C.1. The minimum value is 5.8 % of the total mass of the asphalt mixture. The applied value of the binder content, after multiplying by the correction factor in equation (6), was rounded up to 5.8 % of the total mass of the asphalt mixture, presented in table 3.1 below.

Table 3.1: *Applied binder content in the asphalt mixture*

Property	Amount
Minimum binder content (%)	5,80
Steinkjer aggregate density $\rho_a \text{ (g/cm}^3\text{)}$	2,71
Correction factor $\alpha$	0,98
Adjusted binder content (%)	5,67
Used binder content (%)	5,80

### 3.3 Sample preparation

The gyratory compactor was chosen as the compaction method due to its ability to compact specimens with the best approximations to real placed asphalt (Robert et al, 1996). The compaction procedure follows the guidelines in Method 14.5533 in NPRA R210. The gyratory molds were preheated at 160 °C the night before compaction. The aggregates and the filler were weighed, mixed and heated in the same cabinet as the molds. Bitumen and the iron mixing pot were heated at 140 °C for two hours prior to compaction. The top gyratory compaction disc was not heated. The binder was added to the aggregates and filler, and the mixture was blended in the iron pot by an automatic mixer and divided into mixing bowls.

The gyratory apparatus was set to 17 mrad gyratory angle and the pressure was 600 kPa. According to NPRA N200, the air void content for Ab 11 should be between 2.0 % and 5.5 % for the surface course layer when the AADT is less than 5000. The target air void content was 3.0 % and a test batch of four specimens was used to determine the number of gyrations needed. It was decided to continue with 60 gyrations to reach an air void content of approximately 3.0 %. The gyratory molds were filled with the target weight of asphalt mixture and put in the heating cabinet at 160 °C for 30 minutes. Successively the specimens were compacted, jacked out of the molds and put to rest. The initial temperature before compaction was  $140 \pm 5 \text{ °C}$ .

The test batch produced consisted of the original fractions, where the filler dust was not removed from the Steinkjer 0-4 fraction, and the added filler was limestone. The test batch was not further tested, since all the parameters varied from each specimen, i.e. number of gyrations, air void content and weight. For the remaining series, the sieved Steinkjer 0.063-4

fraction was used. Due to the variations in particle gradation in limestone and hydrated lime, the ratios of the aggregate fractions had to be adjusted for the different series, even though the sieving curves are equivalent for all of them. While the sieved dust has 0.063 mm as the upper particle size, limestone and hydrated lime have 0.125 mm. Therefore, the filler fraction is higher and the Steinkjer 0.063-4 fraction is lower for series C and D. The ratios of aggregates for the test batch and the other series are outlined in table 3.2 below.

Table 3.2: *Ratios of the aggregate fractions in the different mixture series*

<b>Aggregates</b>	<b>Test batch</b>	<b>Series A</b>	<b>Series B</b>	<b>Series C</b>	<b>Series D</b>
Steinkjer 8-11	0,439	0,439	0,439	0,438	0,392
Steinkjer 4-8	0,055	0,051	0,051	0,073	0,141
Steinkjer 0.063-4	0,458	0,403	0,403	0,376	0,326
Steinkjer filler		0,107			
Vassfjell filler			0,107		
Limestone	0,048			0,113	
Hydrated lime					0,141
Total ratio	1,000	1,000	1,000	1,000	1,000

All series consist of three batches with three parallel samples in each batch, making up a total of nine specimens per series. The specimens in the first two batches were prepared in 10 cm diameter molds, target weight of 1300 grams and height around 6.8 cm for the indirect tensile strength test and the Cantabro test. The third round was prepared in 15 cm diameter molds, target weight of 3100 grams and a height of roughly 7.4 cm for the cyclic compression test. Because of limited amount of sieved dust from Vassfjell, in addition to large quantity needed of Steinkjer 0.063-4 fraction which had required additional time sieving and washing, it was decided to aim for specimen height of approximately 7.4 cm for the cyclic compression test. The required specimen height in the test is 6.0 cm. According to the PROKAS study (Lerfald et al, 2004) the target height should be 10.0 cm and 2.0 cm cut off from the top and bottom of the specimen for best results in the cyclic compression test. In this study, the height was set to 7.4 cm and 0.7 cm was cut off from each side of the puck with a diamond bladed saw.

The first two batches for each series were compressed with 60 gyrations in 10 cm diameter molds. Due to undesirably low air void content for some of these specimens, it was decided to reduce the amount of gyrations from 60 to 40 for the last batch with 15 cm diameter molds.

When producing the first batch of series D with hydrated lime, the mixture became extremely dry. There was not sufficient amount of binder to make up for the volume of fines. It was decided to add additional binder into the mixture until it visually looked similar to series A through C. The mixture became sticky and gristly and had a considerably different behavior than the other mixtures. Adjustments were done for the binder content for the other two batches of series D. The first batch in series D had 8.4 % binder content, whereas this amount was reduced to 7.9 % for batch d.2 and d.3.

### 3.4 Asphalt mixture

#### 3.4.1 Rice density

The maximum theoretical density of the asphalt mixtures was found using the Rice density procedure, following Method 14.5633 in NPR A R210. This procedure is described previously. For determining the maximum theoretical density, two parallel tests of each series were conducted. The loose asphalt mixture was placed in beakers and put in the vacuum desiccator, as seen in figure 11. The initial pressure in the apparatus was 1020 mBar, while the final pressure was to 50 mBar to remove all the air in the sample mass.

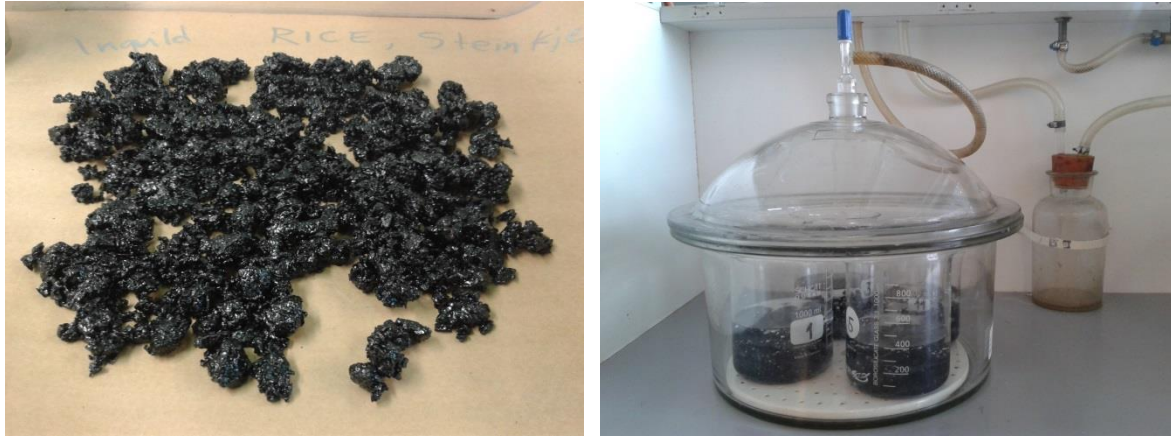


Figure 11: Loose asphalt mixture and vacuum desiccator for determining Rice density

#### 3.4.2 Air void content

The air void content of the compacted specimens was found by the saturated surface dry method described in Method 14.5623 in NPR A R210, which is the method required by NPR A N200. The method involved weighing the specimens in dry condition with a balance of 0.1 grams accuracy. Then the specimens were immersed in water at 25 °C for approximately 5 minutes until the submerged weight had stabilized. Subsequently the asphalt puck was taken out of the water, and the surface was dried with a damp cloth. The saturated surface dry weight was measured. The density and air void content are found by equation (31) and (32).

$$\rho = \frac{\rho_w m_3}{m_2 - m_1} \quad (31)$$

$$AV = \left(1 - \frac{\rho}{\rho_{max}}\right) * 100 \% \quad (32)$$

where  $\rho$  = density of the specimen ( $\text{g}/\text{cm}^3$ ),  $\rho_w$  = water density at the actual water temperature ( $\text{g}/\text{cm}^3$ ),  $m_3$  = dry weight of specimen (g),  $m_2$  = saturated surface dry weight of specimen (g),  $m_1$  = submerged weight of specimen (g), AV = air void content (%),  $\rho_{max}$  = maximum theoretical density, i.e. Rice density ( $\text{g}/\text{cm}^3$ ).



### 3.5 Testing procedures for the compacted specimens

Three detrimental tests have been chosen to evaluate fundamental asphalt mixture properties and pavement life indicators. The indirect tensile strength test defines the indirect tensile strength of the mixture, the Cantabro test puts number on the resistance against particle loss, while the cyclic compression test evaluates the cyclic creep and permanent deformation. Three specimens from each of the four series have been tested in the three test procedures.

#### 3.5.1 Indirect tensile strength test

The indirect tensile strength test was carried out on the Marshall apparatus. The specimens were dry conditioned in an incubator at 25 °C for 1 hour. The height and diameter of the specimens tested were measured with a caliper eight times each and averaged, and during the test the crack occurrence was noted. After the specimens had gone to failure, the cracks were examined to visually evaluate the binder and mastic coating of the aggregates.

#### 3.5.2 Cantabro test

The Cantabro test was conducted following the procedure explained in chapter 2.4. The specimens were tested at room temperature, and the test was conducted with 300 revolutions at a rate of 33 revolutions per minute. The Los Angeles machine used is seen to the left figure 12 below. The specimens before and after the test are to the right.



Figure 12: Los Angeles machine and specimens before and after the Cantabro test

#### 3.5.3 Cyclic compression test

The cyclic compression test is described previously, and the test was conducted following Test Method A – Uniaxial cyclic compression test with confinement with the Nottingham Asphalt Tester (NAT). The specimens were 15 cm in diameter, and the top and bottom of each specimen were cut off giving the specimens parallel surfaces and height of 60 mm. The initial height of the specimens were measured with a caliper eight times around the circumference and averaged. The specimens were conditioned 4 to 6 hours prior to testing at 40 °C in a thermostatic chamber. White grease paste was applied in a thin layer on the top surface of the specimens on the interface of the 10 cm top disk and the specimen surface. The specimens were put in level perpendicular to the two linear variable displacement transformers (LVDT). The top plate was placed centrally on top of the specimen, and the

LVDTs were adjusted to the top disk and reset to zero displacement. The setup is illustrated in figure 13. Preloading with 10 kPa was applied for 10 minutes, and the cyclic compression test was carried out under the following conditions:

- Stress: 100 kPa
- Number of load cycles: 3600 sec
- Duration of load pulse: 1 sec
- Frequency of load pulses: 0.5 Hz
- Test duration: 7200 sec
- Temperature: 40 °C

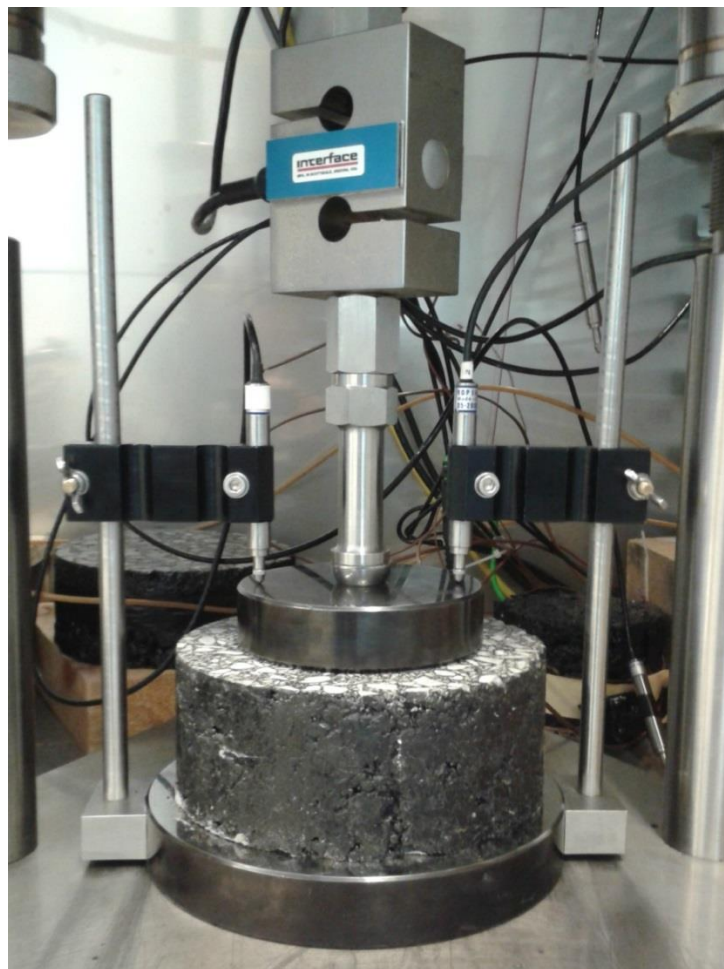


**Figure 13: Setup for cyclic compression test in the NAT machine**

#### **3.5.4 Statistical analysis**

To be able to evaluate the statistical significance of the test results, a two-tailed t-test has been conducted in Excel for the output data. The test uses two samples and assumes unequal variances. Hypothesized mean difference is believed to be zero, and the significance level is set to 5.0 %, i.e. the alpha value is 0.05. If the value of t-stat is greater than t-critical for the two-tail or t-stat is less than the negative value of t-critical two-tail, the null hypothesis is rejected and the average values of the output data are too different to make a statistical significant conclusion.

## CHAPTER 4: RESULTS

### 4.1 Filler and mixture properties

Table 4.1 outlines the filler density and the Rigden void content for the filler materials and the Rice density for the mixtures containing the respective filler. Calculations are attached in Appendix D, table D.5 through D.7, and Appendix E, table E.1. Since the binder content in series D with hydrated lime was adjusted, there are two different values of the Rice density, i.e. the average value for the different batches was not calculated due to different binder content. Specimen densities, air void contents and additional preparation information are shown in table E.2 and E.3, Appendix E. The volumetric particle concentrations of filler in the mastics are calculated by the method on page 16 and listed in table 4.2 below.

Table 4.1: *Filler density, Rigden void content and Rice density*

Filler type	Filler density (g/cm <sup>3</sup> )	Rigden void content (%)	Rice density (g/cm <sup>3</sup> )
Steinkjer filler	2,76	37,7	2,440
Vassfjell filler	3,06	42,9	2,472
Limestone	2,7	30,5	2,454
Hydrated lime, batch d.1	2,04	44,6	2,337
Hydrated lime, batch d.2 and d.3	2,04	44,6	2,325

Table 4.2: *Volumetric filler particle concentrations in the mastics*

Filler type	Filler particle concentration (%)	Maximum particle concentration (%)	Effective particle concentration (%)
Steinkjer	38,87	62,30	62,40
Vassfjell	36,45	57,10	63,84
Limestone	40,71	69,50	58,57
Hydrated lime, batch d.1	43,32	55,40	78,19
Hydrated lime, batch d.2 and d.3	44,79	55,40	80,84

The F/A-ratio by mass was intended to be kept equal in all mixture series. For the sieved dust from Steinkjer and Vassfjell, the filler was sieved on 0.063 mm mesh size. Limestone and hydrated lime had sieving curves starting at 0.125 mm. The F/A-ratios for the last two are adjusted to the actual percent passing the 0.063 mm sieve. Additional binder was added in the hydrated lime series due to a very dry and unworkable mixture with the initial 5.8 % binder content by mass. The F/A-ratios for all series and batches are shown in table 4.3. The ratios for series C and D are adjusted for the actual amount of filler passing the 0.063 mm sieve.

Table 4.3: *F/A-ratio by mass and volume for the three batches in the four different series*

Series	Filler type	Filler content passing 0.063 mm sieve (%)	Binder content (%)	F/A-ratio by mass	F/A-ratio by volume
a.1	Steinkjer	10,700	5,8	1,738	0,636
a.2					
a.3					
b.1	Vassfjell	10,700	5,8	1,738	0,574
b.2					
b.3					
c.1	Limestone	10,283	5,8	1,670	0,625
c.2					
c.3					
d.1	Hydrated lime	10,442	8,4	1,142	0,556
d.2			7,9	1,212	0,600
d.3			7,9	1,212	0,600

## 4.2 Indirect tensile strength test

The specimens used in the indirect tensile strength test were conditioned for 1 hour at 25 °C in the incubator. For series A, B and C containing Vassfjell, Steinkjer and limestone filler respectively, the crack occurrence was diametrical and vertical from the point of load application. A few cracks appeared as an upside down letter Y, but this was arbitrary and independent on the series. For series D with hydrated lime, the cracking was inconsistent and concave. Furthermore, the axial deformation until failure appeared noticeably more ductile for hydrated lime than the other series. The results are shown in table F.1, Appendix F and illustrated in figure 14 and 15, while the output data is attached in Appendix G. As the results show, the tensile strength for hydrated lime lies much higher than those of sieved dusts and limestone. This will be discussed in the next chapter. The load distribution coefficient is according to NPRA N200 required to be 3.0 for Ab 11 with 70/100 binder, and the obtained value should not exceed 0.75 over the requirement. The series with hydrated lime and two of the Vassfjell specimens exceeded this limit, as seen in table F.1, Appendix F.

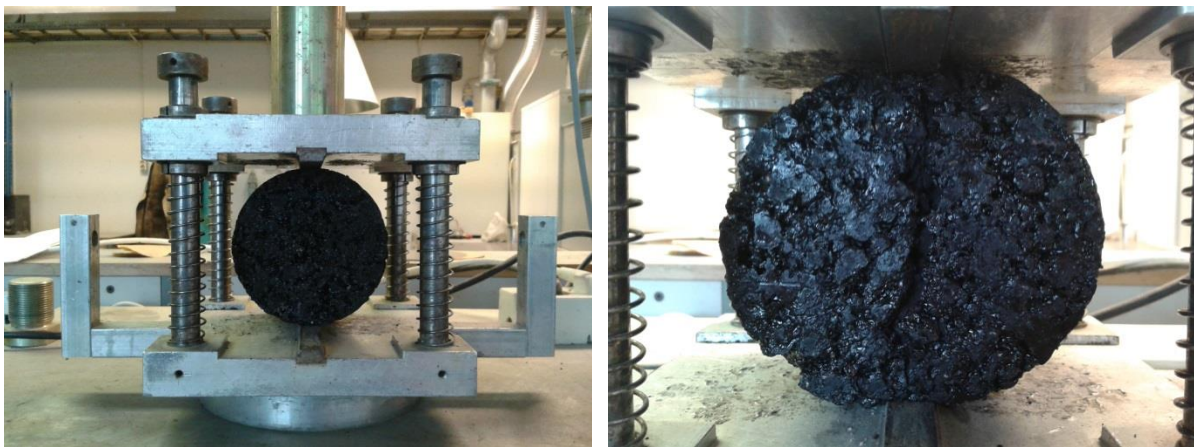


Figure 14: Indirect tensile strength test

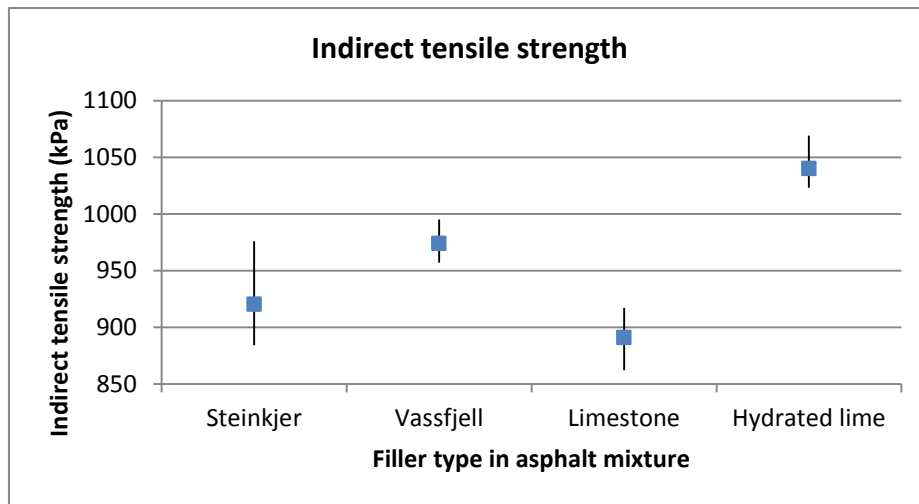


Figure 15: Range of indirect tensile strength values, including average values

### 4.3 Cantabro test

The results from the Cantabro test are attached in table F.2 in Appendix F. The Cantabro loss had a range of 4.40 % to 8.31 % for all the specimens tested. The range of the Cantabro loss and the average values are shown in figure 16.

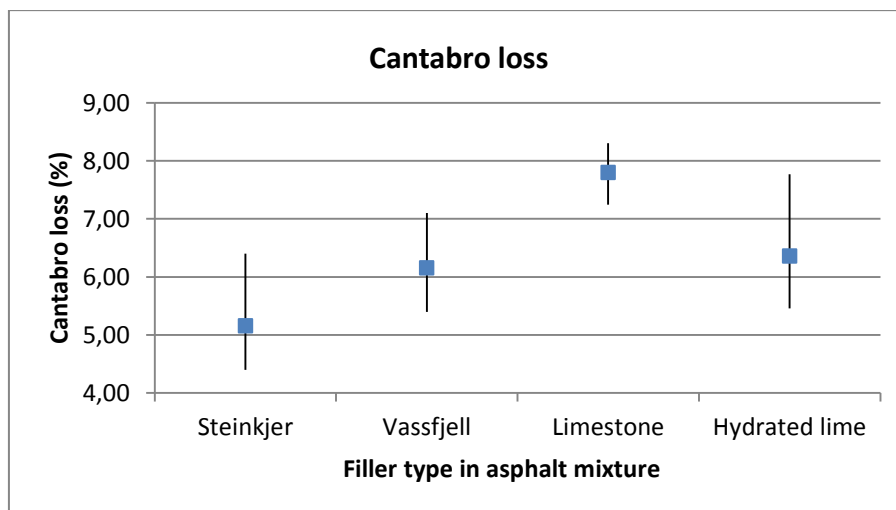


Figure 16: Range of Cantabro loss values, including average values

### 4.4 Cyclic compression test

The output files from NAT program was raw data that needed considerably processing. The conscientiously logging of the load and the displacement of the LVDTs every 0.1 seconds yielded relatively large text files of 31 MB for each of the twelve specimens tested. A program code in Excel was developed to seek for the rows containing the logged values, and the program filtered out every 11<sup>th</sup> row of the approximately 860.000 rows in the spreadsheets and put them in a separate sheet for further calculations. The data filtered out was the load, the displacements of the LVDTs and the time for every 0.1 seconds. The time was converted to load cycles by multiplying by the frequency of 0.5 Hz.

The load pulse in the NAT was set to 100 kPa during load time and 10 kPa during rest time. However; the logged values varied between approximately 8 kPa and 98 kPa as a result of undefined noise in the system. This is illustrated to the left in figure 17. In addition, during each cycle the applied load oscillated, as seen in the waveform chart to the right in figure 17.

The displacement values from the two LVDTs oscillated due to the frequency and load pulse, so in the following analysis the average value of the two LVDTs for each measure point of 0.1 seconds has been used. To reduce the size of the file and be able to evaluate the data, groups of every 100 adjacent measure points were formed and averaged. It was decided to take the average of the whole specter to get the middle value of the oscillations, not the top nor the bottom values only, and this is depicted in figure 18. The bulk average of the group of 100 measure points of the average values of the two LVDTs induced displacement values for approximately every 10 seconds, hence every 5 load cycle. These values were then used in the calculations of the cumulative axial strain.



Figure 17: Variations in the applied load pulse due to noise in the system

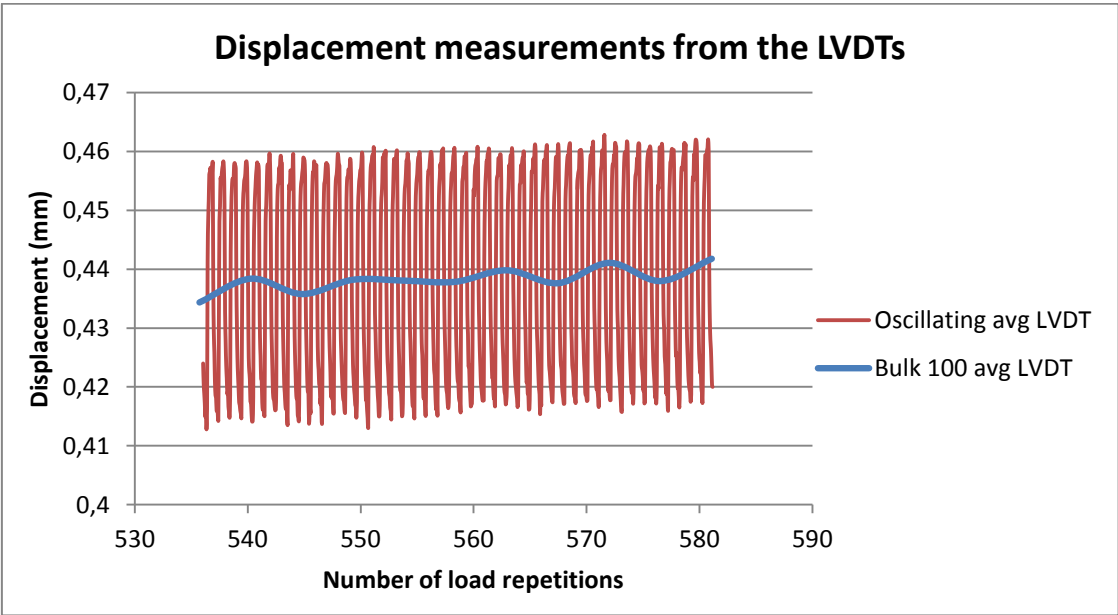


Figure 18: Displacement measurements from the LVDTs

The series with Steinkjer, Vassfjell and hydrated lime had unnoticeably surface deflection and no decayed area. The limestone series had prominently deflections in the surface, which can be seen in figure 19 and 20. The displacement was deeper on one side for specimen c.3.2, which could be due to inhomogeneous aggregate distribution throughout the specimen.



Figure 19: Final surface displacement for specimen c.3.2 with limestone

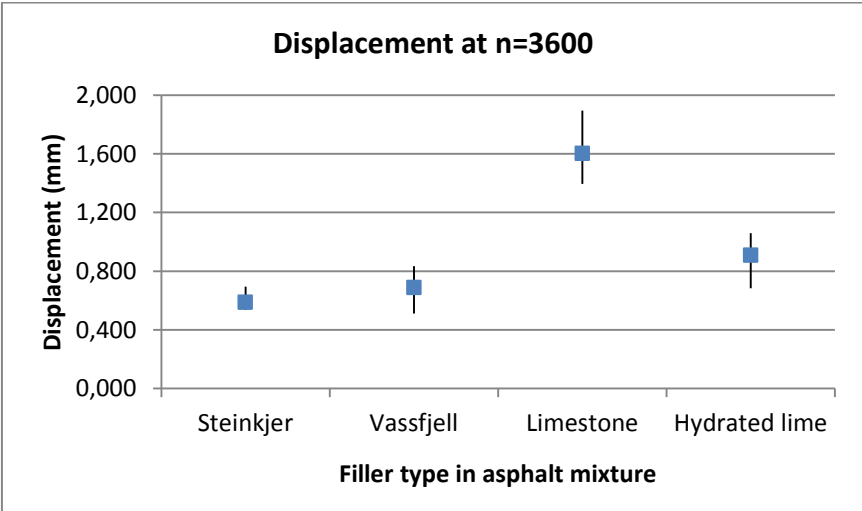
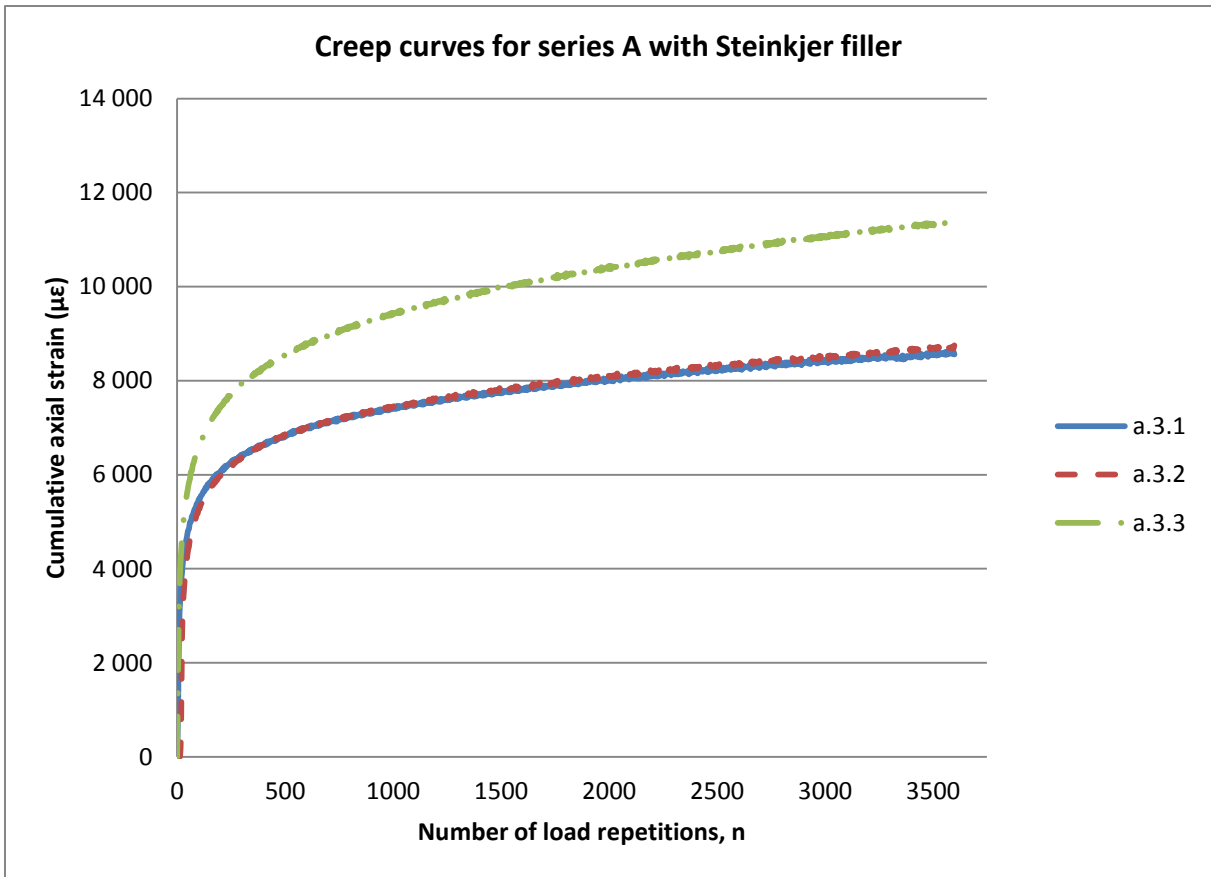
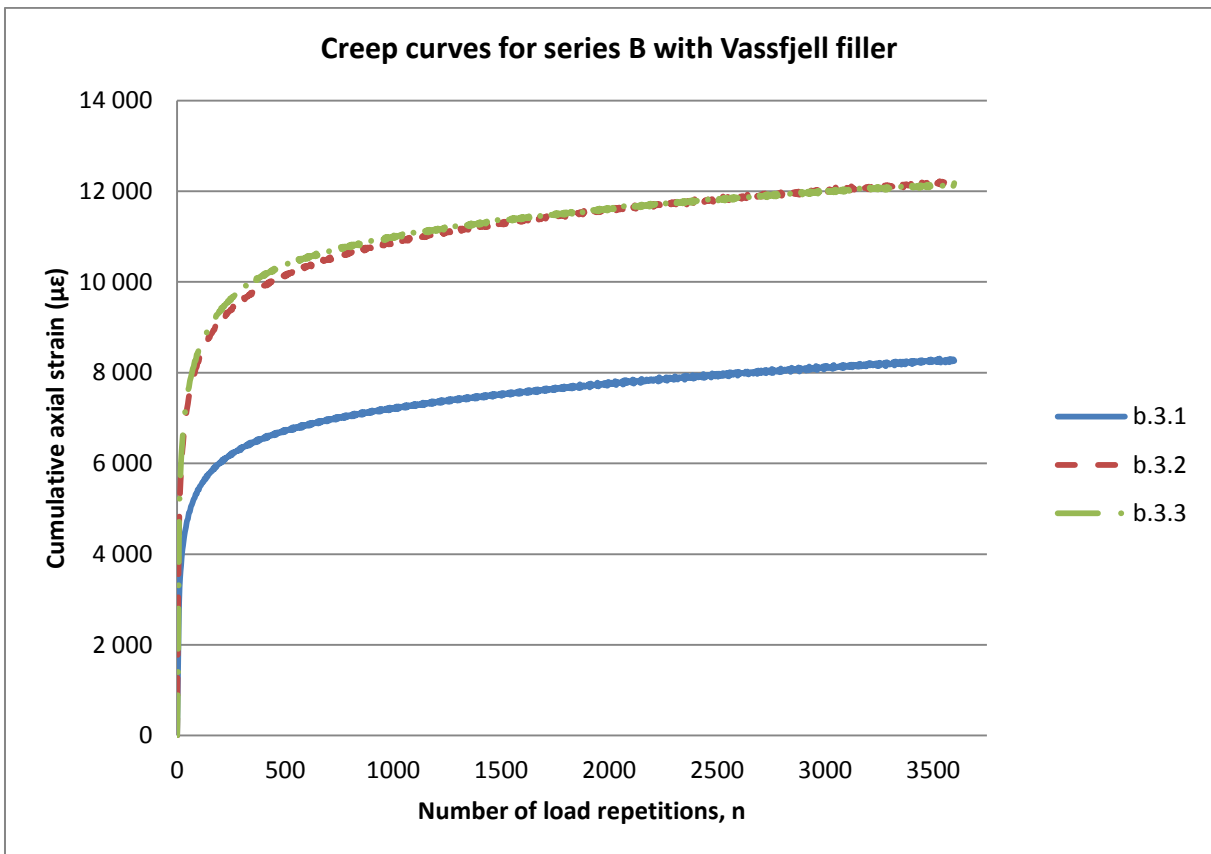


Figure 20: Displacement at 3600 load cycles

Figure 21 through 24 present the obtained creep curves for the specimens tested in the four series. Compared to figure 7 on page 24, stage 3 is absent in these figures. Remark the different scale on the ordinate in the illustrations. The preloading is not a part of the creep curves. The deformation measured from the LVDTs at the end of the preloading is subtracted from the deformations during testing, which is resulting in relative zero cumulative axial strain at the beginning of the test when  $n = 0$ . Data of interest and the permanent deformation from the cyclic compression test is attached in Appendix H. Generally, the limestone series had the most extreme result values for all the measures evaluated, with over twice as much permanent deformation after ended test procedure than the other series.



**Figure 21: Creep curves for series A with Steinkjer filler**



**Figure 22: Creep curves for series B with Vassfjell filler**



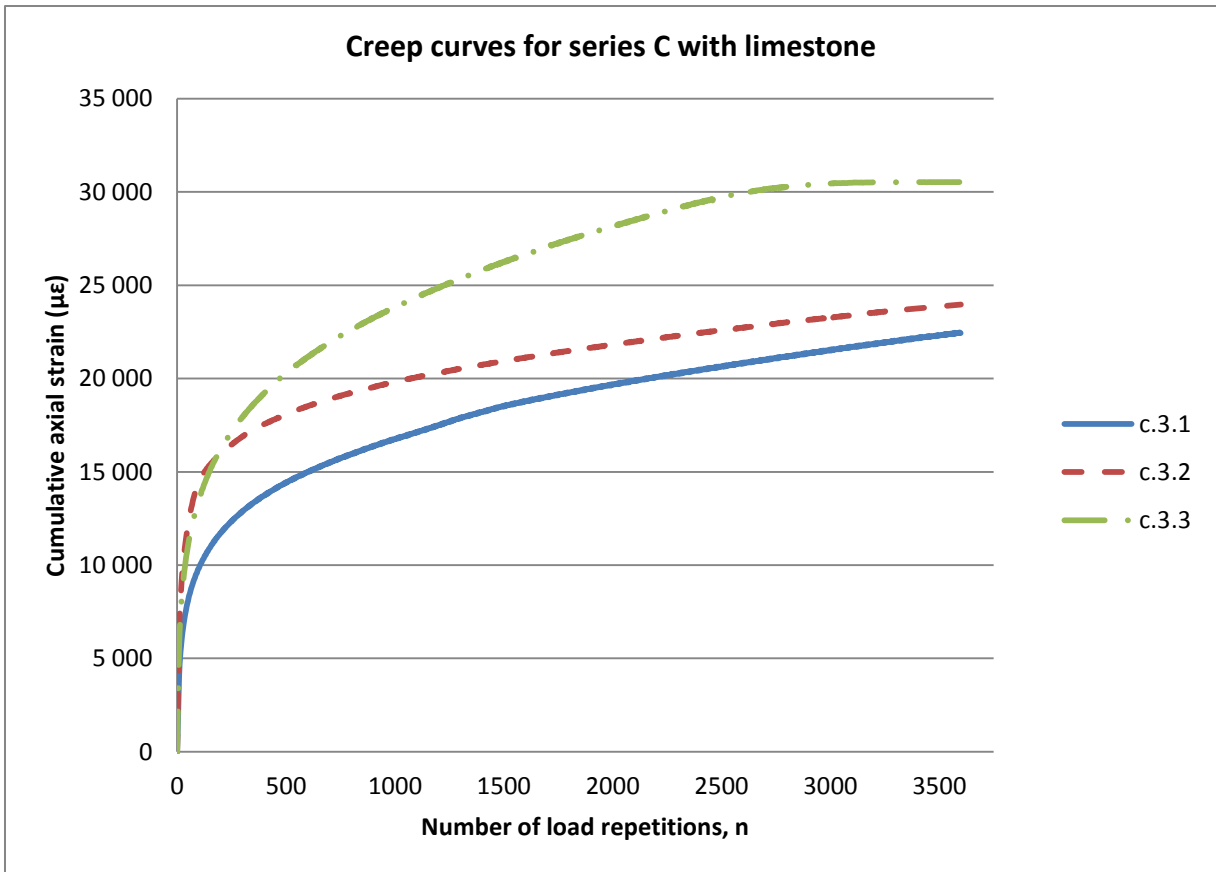


Figure 23: Creep curves for series C with limestone

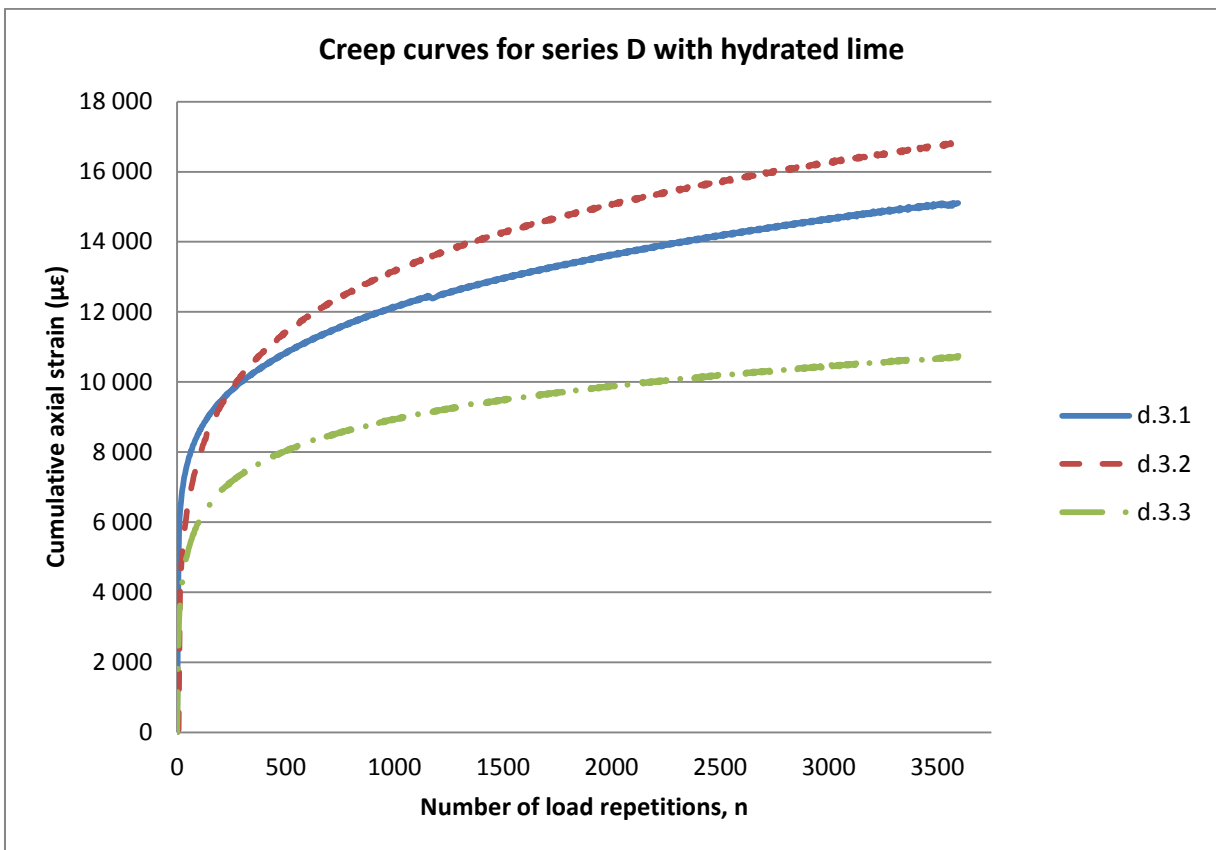


Figure 24: Creep curves for series D with hydrated lime

The cyclic compression test for specimen c.3.2 was stopped too early, and it ended at load cycle n=3326. Due to this incidence the cumulative axial strain value at load cycle n=3600 was not obtained. The creep rate in stage 2 was therefore used to extrapolate the conceivable value of the cumulative axial strain.

After the preloading and 117 load cycles for specimen c.3.3, the LVDT2 got jammed and stopped oscillating and measuring the displacement. By means of this, the values of LVDT2 were neglected, the average LVDT was not calculated and the displacement of LVDT1 was used in the calculations. The same happened to specimen d.3.1, but with LVDT1 getting jammed. Therefore, the displacement of LVDT2 has been used in further calculations for this specimen.

The maximum allowed cyclic creep specified in NPRA N200 is listed in table 2.3 in chapter 2, page 24 previously. The obtained cyclic creep values for the four series are within the requirement for AADT less than 5000, where the maximum limit is 30000  $\mu\epsilon$ . For AADT 5001-10000 and greater than 10000, the maximum values are 25000  $\mu\epsilon$  and 20000  $\mu\epsilon$  respectively. The specimens with limestone exceed this limit, while the others are within the criteria. Values are presented in figure 25.

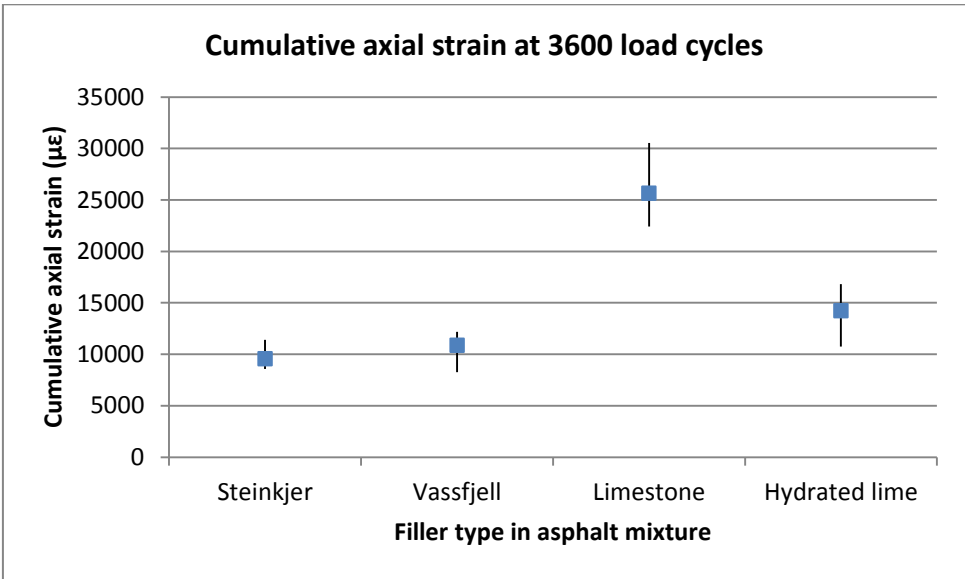


Figure 25: Cumulative axial strain at 3600 load cycles

#### 4.5 Two-tailed t-test

The tables 4.4 through 4.7 show the results from the two-tailed t-test assuming unequal variances, while the statistical analysis is listed in Appendix I. The null hypothesis with zero mean differences is rejected if one of the allegations is not met. The allegations are as follow:

- $t\text{-stat} > t\text{-critical}$ , two-tail
- $t\text{-stat} < - t\text{-critical}$ , two-tail

As table 4.4 show, most of the results from the indirect tensile strength test must be rejected. The only samples that are statistical significant are the specimens containing Steinkjer filler when compared to Vassfjell filler. In the Cantabro loss in table 4.5, limestone and Steinkjer filler are not comparable, while the others are. Table 4.6 and 4.7 there are no statistical significant relationship between limestone and the natural sieved fillers.

Table 4.4: *t-test indirect tensile strength*

	<b>Steinkjer</b>	<b>Vassfjell</b>	<b>Limestone</b>	<b>Hydrated lime</b>
<b>Steinkjer</b>	N/A	Do not reject	Do not reject	Reject
<b>Vassfjell</b>	Do not reject	N/A	Reject	Reject
<b>Limestone</b>	Do not reject	Reject	N/A	Reject
<b>Hydrated lime</b>	Reject	Reject	Reject	N/A

Table 4.5: *t-test Cantabro loss*

	<b>Steinkjer</b>	<b>Vassfjell</b>	<b>Limestone</b>	<b>Hydrated lime</b>
<b>Steinkjer</b>	N/A	Do not reject	Reject	Do not reject
<b>Vassfjell</b>	Do not reject	N/A	Do not reject	Do not reject
<b>Limestone</b>	Reject	Do not reject	N/A	Do not reject
<b>Hydrated lime</b>	Do not reject	Do not reject	Do not reject	N/A

Table 4.6: *t-test cumulative axial strain at 3600 load cycles*

	<b>Steinkjer</b>	<b>Vassfjell</b>	<b>Limestone</b>	<b>Hydrated lime</b>
<b>Steinkjer</b>	N/A	Do not reject	Reject	Do not reject
<b>Vassfjell</b>	Do not reject	N/A	Reject	Do not reject
<b>Limestone</b>	Reject	Reject	N/A	Do not reject
<b>Hydrated lime</b>	Do not reject	Do not reject	Do not reject	N/A

Table 4.7: *t-test creep rate in stage 2 of the creep curve*

	<b>Steinkjer</b>	<b>Vassfjell</b>	<b>Limestone</b>	<b>Hydrated lime</b>
<b>Steinkjer</b>	N/A	Do not reject	Reject	Do not reject
<b>Vassfjell</b>	Do not reject	N/A	Reject	Do not reject
<b>Limestone</b>	Reject	Reject	N/A	Do not reject
<b>Hydrated lime</b>	Do not reject	Do not reject	Do not reject	N/A

## CHAPTER 5: DATA ANALYSIS

### 5.1 Indirect tensile strength test

Figure 26 and 27 depict the results from the indirect tensile strength test as a function of F/A-ratio by mass and volume. As mentioned before, the series with hydrated lime has higher binder content than the other series, yielding lower F/A-ratio by mass. Due to low filler density, high surface area and porosity for hydrated lime, the F/A-ratio by volume becomes less extreme. Nevertheless, the t-test showed that the hydrated lime values are statistical insignificant in relation to the other values. The plots illustrate that the series with Vassfjell filler yields higher indirect tensile strength than the series with Steinkjer filler and limestone. Steinkjer and limestone had indirect tensile strength in the lower range.

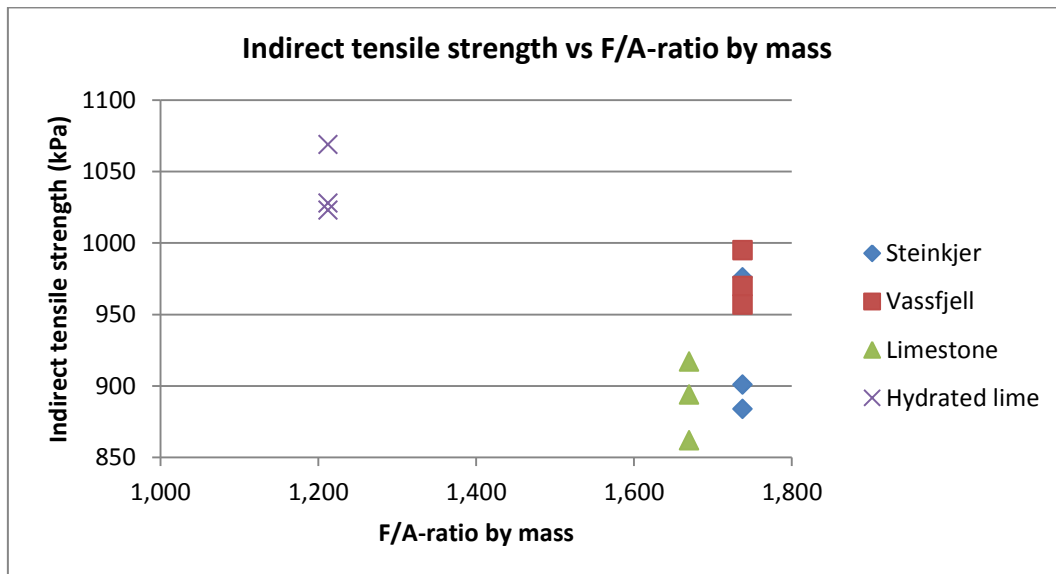


Figure 26: Indirect tensile strength vs F/A-ratio by mass

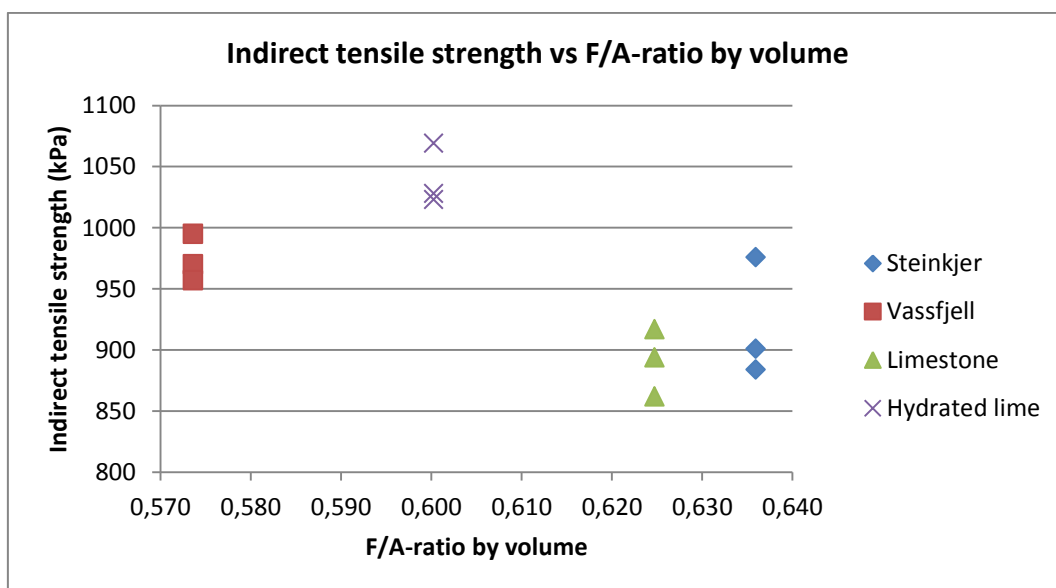


Figure 27: Indirect tensile strength vs F/A-ratio by volume

If the indirect tensile strengths of hydrated lime are neglected in figure 26, the remaining values are concentrated in a small area and no trend is seen between F/A-ratio by mass and the indirect tensile strength. However; by including the hydrated lime values, it could be argued that the indirect tensile strength decreases as the F/A-ratio by mass increases, but this conclusion would be based on a marginal number and narrow range of values, and it is in this context considered insignificant. The plot of indirect tensile strength as a function of F/A-ratio by volume is scattered, but by drawing a line between the Vassfjell values through the Steinkjer and limestone values, it give the impression of that the indirect tensile strength decreases with increasing F/A-ratio by volume.

Figure 28 is a plot of the indirect tensile strength as a function of Rigden void content in the filler. The trend shows that as higher the Rigden void content, as higher the indirect tensile strength. The indirect tensile strength as a function of the air void content in the compacted specimen is plotted in figure 29, and higher air void content yields lower indirect tensile strength. It has to be said that the range of air void content is rather narrow, and all specimens are considered dense, but the trend is notably for this selection.

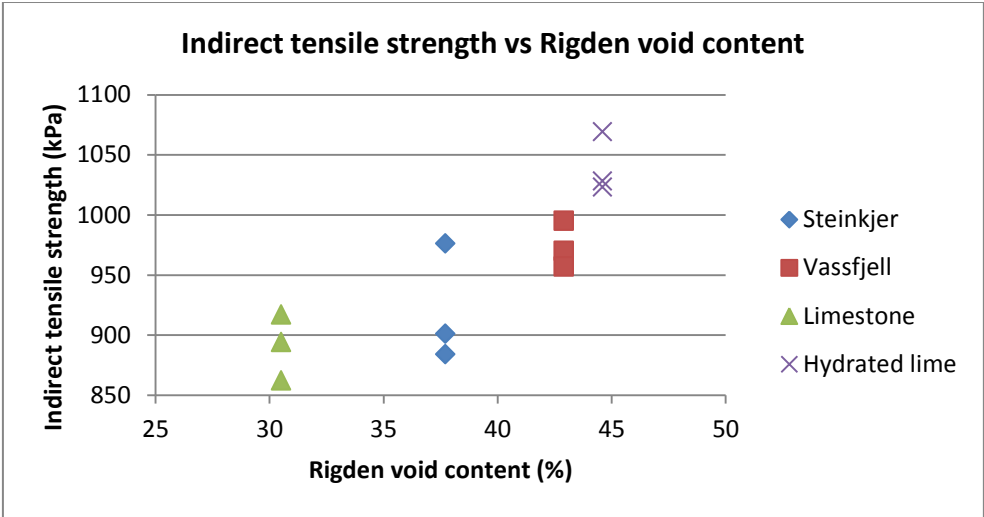


Figure 28: Indirect tensile strength vs Rigden void content

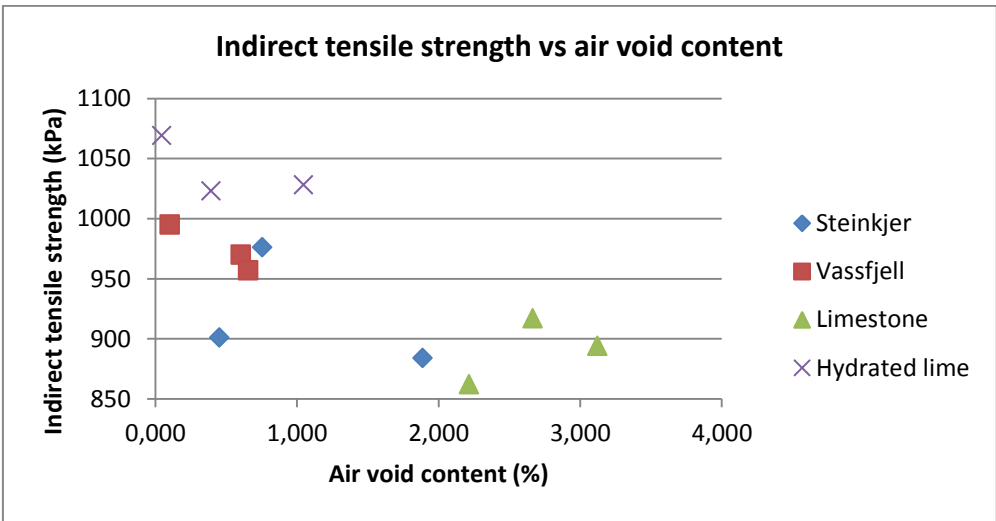


Figure 29: Indirect tensile strength vs air void content

## 5.2 Cantabro test

Plots of the Cantabro loss with respect to F/A-ratio by mass and volume are shown in figure 30 and 31. The tendency is that none of the F/A-ratios can directly be related to the loss, whereas both high and low F/A-ratios yield similar Cantabro loss values. The Cantabro loss lied between 4.40 % and 8.31 % for all specimens tested. The mixture with limestone filler had the overall highest Cantabro loss, with an average of 7.80 %. The other series had average values of 5.16 %, 6.16 % and 6.36 % for Steinkjer, Vassfjell and hydrated lime respectively. The t-test showed that comparing values of limestone to Steinkjer filler is not significant. By neglecting the limestone values, the Cantabro loss seems to decrease by increasing F/A-ratio by volume. However; the opposite trend occurs for a trend line neglecting the Steinkjer values.

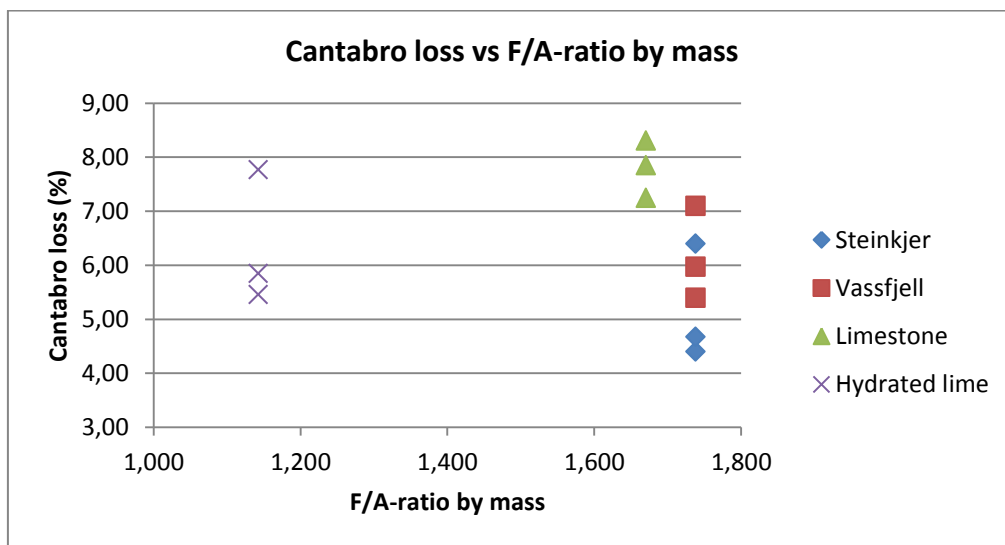


Figure 30: Cantabro loss vs F/A-ratio by mass

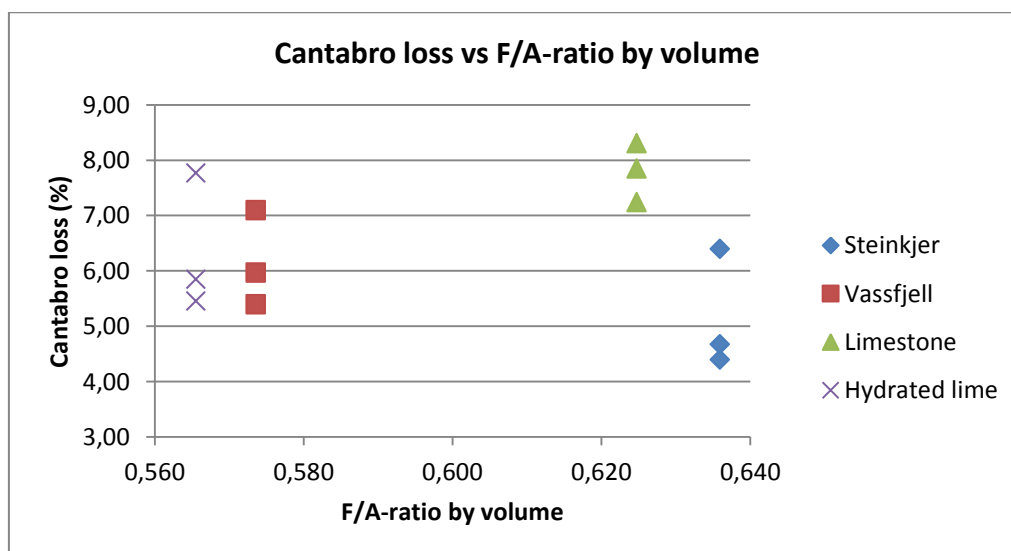


Figure 31: Cantabro loss vs F/A-ratio by volume

Figure 32 illustrates the Cantabro loss with respect to Rigden void content. Since Steinkjer and limestone are two samples with statistical insignificant relationship, one of them should be neglected in potential trend lines, since they are points adjacent to each other in figure 32.

Limestone stands out as a deviation for a tendency of higher Cantabro loss with higher Rigden void content. By ignoring Steinkjer, the opposite trend is visible, where higher Rigden void content yields lower Cantabro loss. The major impact on the Cantabro loss is the air voids in the specimens, as presented in figure 33. Higher air void content yields higher Cantabro loss. The high air void content in the limestone mixture could explain the discrepancy in figure 32, where the particle loss for limestone differs from the trend of higher Cantabro loss with higher Rigden void content. This can imply that the effects of the air void content overrule the effects of the Rigden void content.

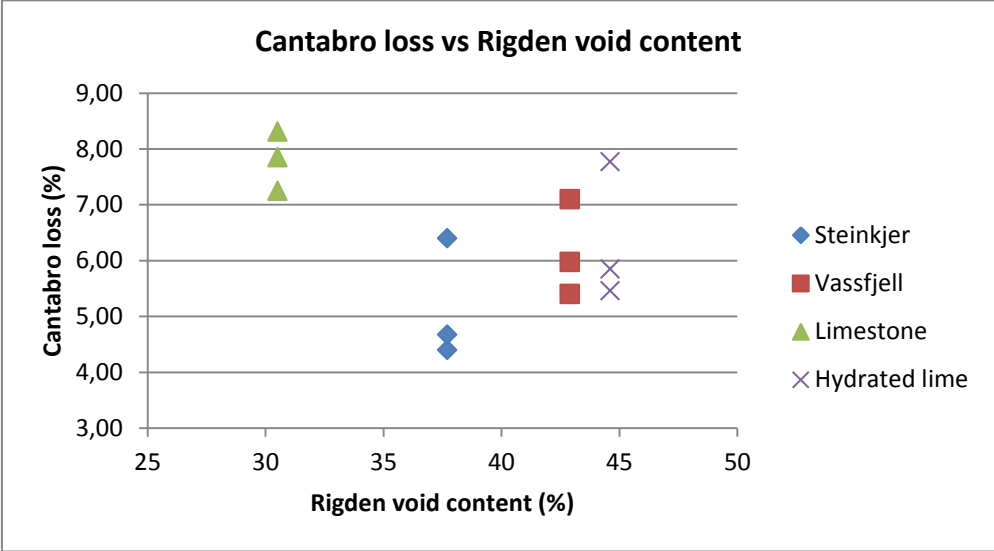


Figure 32: Cantabro loss vs Rigden void content

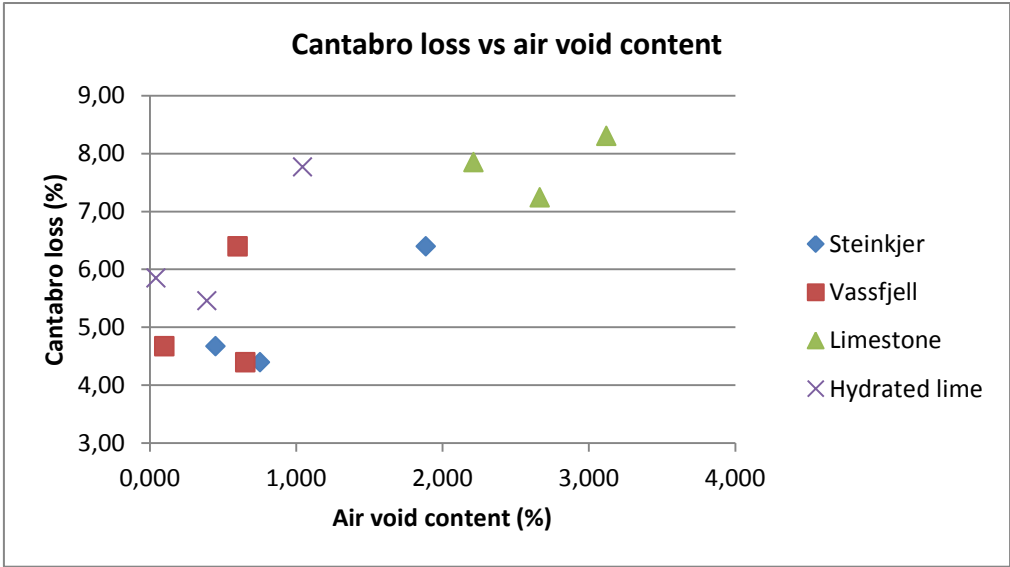


Figure 33: Cantabro loss vs air void content

### 5.3 Cyclic compression test

Figure 34 and 35 illustrate the cumulative axial strain at 3600 load cycles as a function of F/A-ratio by mass and volume. As for Steinkjer and Vassfjell filler, both high and low F/A-ratios by volume yield similar cumulative axial strain. The results were identical when plotted

to F/A-ratio by mass. The specimens containing limestone lack similarities to the other series and should be rejected as a result of the t-test. Hydrated lime had slightly higher values than the sieved fillers. There are no evident trends to be drawn between the maximum creep value and the F/A-ratios, and by ignoring the limestone values the cumulative axial strain at 3600 load cycles seems independent of the F/A-ratios.

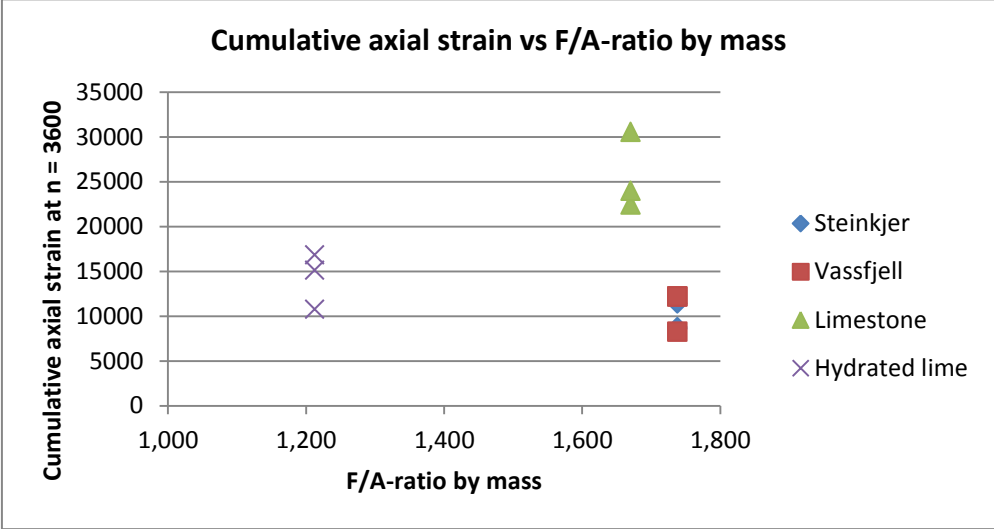


Figure 34: Cumulative axial strain at 3600 load cycles vs F/A-ratio by mass

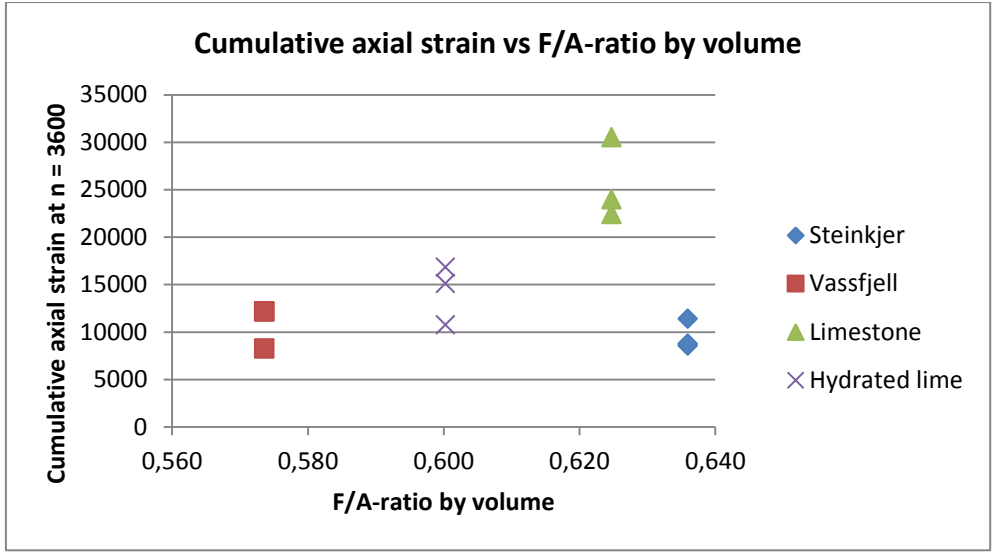


Figure 35: Cumulative axial strain at 3600 load cycles vs F/A-ratio by volume

Figure 36 is the cumulative axial strain at 3600 load cycles plotted as a function of Rigden void content. The Steinkjer and Vassfjell series yield similar results, despite the different Rigden void content. Specimens containing hydrated lime have marginally higher cumulative axial strain than the natural fillers, but there is no evident trends based on these values and the cumulative axial strain occurs unaffected by the Rigden void content.

The parameter in figure 37 is the air void content. Steinkjer, Vassfjell and hydrated lime specimens have air void contents concentrated in an area less than 2.0 %, while limestone has air void content around 6.0 %. The limestone values are not statistically significant compared



to the natural fillers, and the range of air void content of the remaining values is too narrow to give any reasonable assumptions of the relationship presented in the plot. If all specimens are included in the evaluation, then the trend of the cumulative axial strain is that higher air void content yields higher cumulative axial strain at 3600 load cycles.

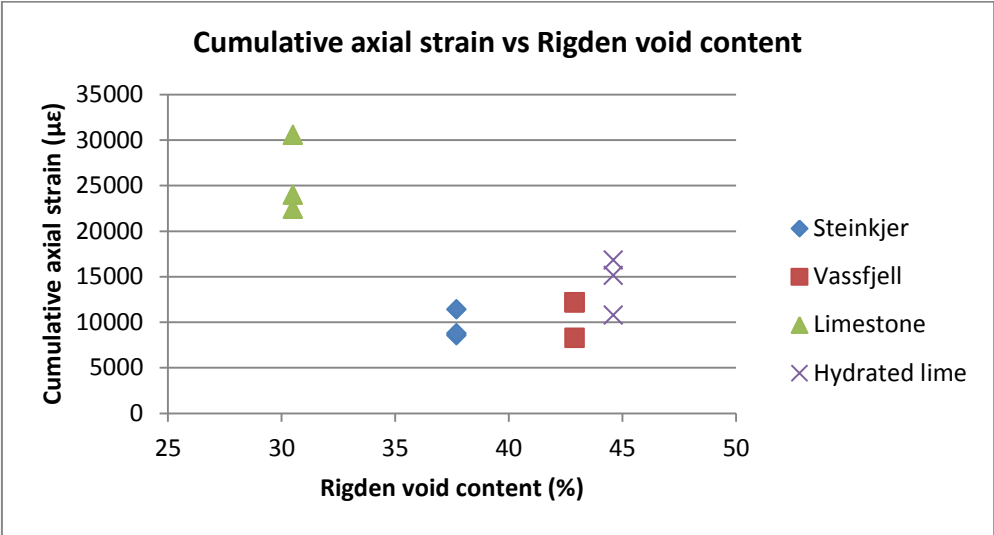


Figure 36: Cumulative axial strain at 3600 load cycles vs Rigden void content

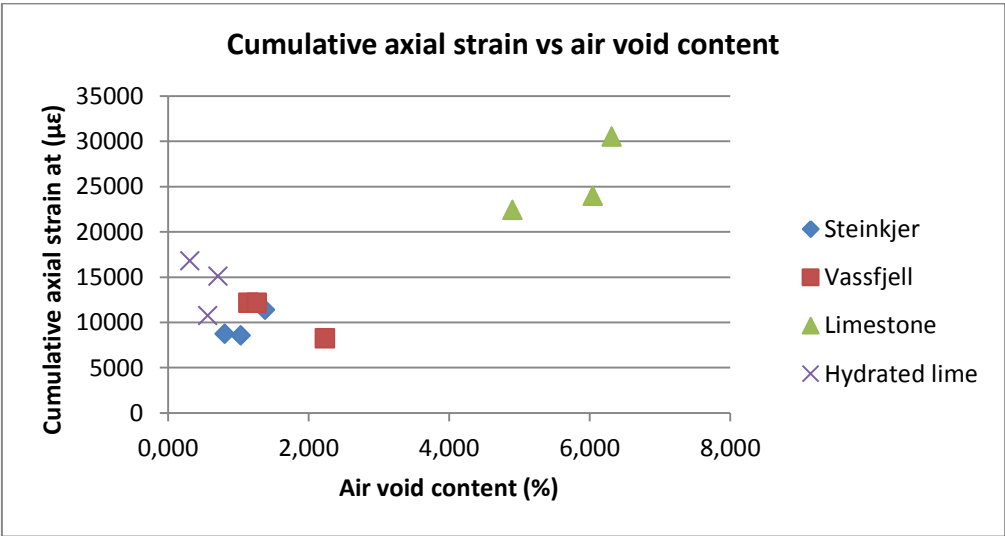


Figure 37: Cumulative axial strain at 3600 load cycles vs air void content

### 5.4 Additional evaluations

#### 5.4.1 Coating

When the specimens used in the indirect tensile strength test had reached failure, it was possible to visually investigate the coating of the coarser aggregates in the cracks. The series containing Steinkjer filler, Vassfjell filler and limestone had a thin binder film coating the coarser aggregates, as seen in the upper right and left and bottom left in figure 38. The specimen with hydrated lime had a sticky crack surface, and the film felt thicker and more ductile than the others, which is as expected due to much higher binder content. The bottom

right part of figure 38 shows the hydrated lime specimen. Comparisons of the specimens were also made for the top saw kerf surfaces on the specimens used in the cyclic compression test, as seen in figure 39. It was challenging to differentiate among the specimens, and the hydrated lime was the only mixture where the binder film and coating appeared slightly thicker.



**Figure 38: Aggregate coating. From left to right: Steinkjer and Vassfjell on top, limestone and hydrated lime on the bottom**



**Figure 39: Saw kerf surface for evaluation of the aggregate coating**

### 5.4.2 Rigden void content

The plot in figure 40 reveals that the Rigden void content has an effect on the air void content. All the series of specimens with diameter 10 cm were compacted with the same number of gyrations, i.e. 60 gyrations. The 15 cm diameter specimens had all 40 gyrations. This is the reason for the wide range of air void content within each series. By taking all specimens into account, there is a negative relationship between the Rigden void content and the air void content, where increasing Rigden void content reduces the air void content. However; by neglecting the upper extremal points of the limestone specimens in figure 40, the remaining specimens are considered massive and dense with air void content less than 3.0 %. Among these specimens, there are challenging to see any clear relationship between the Rigden void content and the air void content in the compacted specimen.

Figure 41 illustrates the relationship between F/A-ratio by mass and volume and the Rigden void content. The hydrated lime batches have 7.9 % and 8.4 % binder content, while the other series have 5.8 %. Based on this fact, the values of hydrated lime specimens in figure 41 might be ignored when the F/A-ratios are evaluated, since that ratio represents a singular case in relation to the other ratios.

If the points of hydrated lime in the F/A-ratio by mass are neglected, it seems to be a slightly increase in F/A-ratio by mass with increasing Rigden void content. Conversely, by adding additional filler to one of the series, the F/A-ratio by mass would increase and annul this trend, since the Rigden void content will unchanged. The interesting part is the F/A-ratio by volume as a function of Rigden void content, since an increase in Rigden void would generate more volume and possibly lead to changes in the volumetric mastic composition. As seen in figure 41, the F/A-ratio by volume is stable when the Rigden void content in the fillers increases and seems unaffected by the filler fractional voids. However; there are too few data points for an adequate evaluation of the current effect and make any proper assumptions.

The effective volumetric filler particle concentrations in the mastics, from table 4.2 on page 35, are plotted as a function of Rigden void content in figure 42. The trend for all of the filler types is that as the Rigden void content rises, the effective volumetric concentration rises. Even though the mass percentages of filler are equal, the effective volumetric particle concentrations are a lot different. This indicates that the same amount of filler by weight takes different amount of space in the mastic based on the concentration of filler. This phenomenon was not seen in figure 41 when the Rigden void content was plotted to the F/A-ratio by weight and volume. For the manufactured filler hydrated lime, the effective volumetric concentration is much higher than the other values. The irregularity of the hydrated lime is conceivably a result of higher binder content, since the effective particle concentration is a function of the actual volumetric filler concentration in the mastic and the maximum volumetric particle concentration, as seen in equation (13) and (14). Hydrated lime needed much more binder than the other series to be workable, and therefore the effective volumetric particle concentration is affected by this.

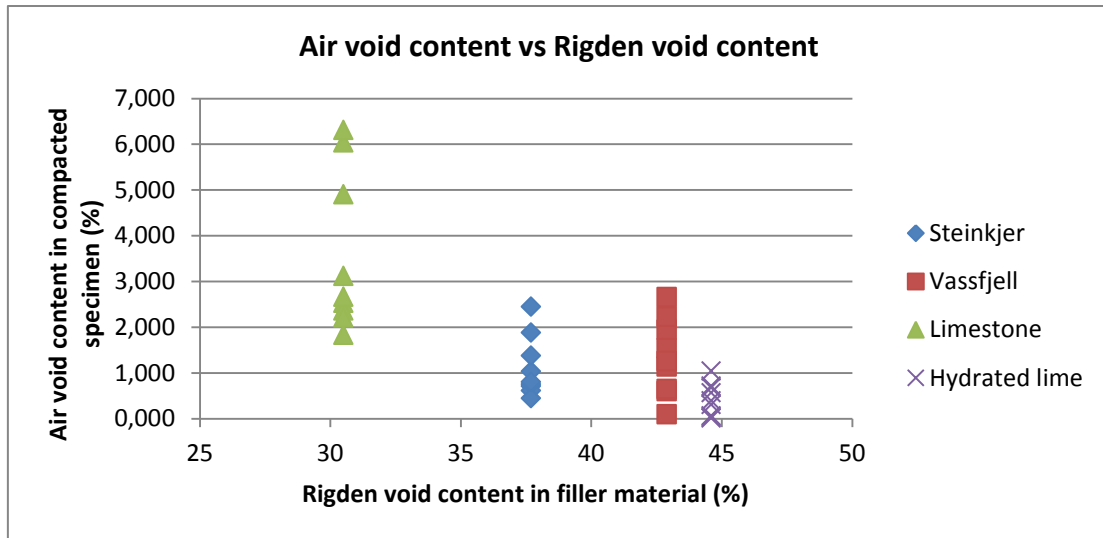


Figure 40: Air void content vs Rigden void content

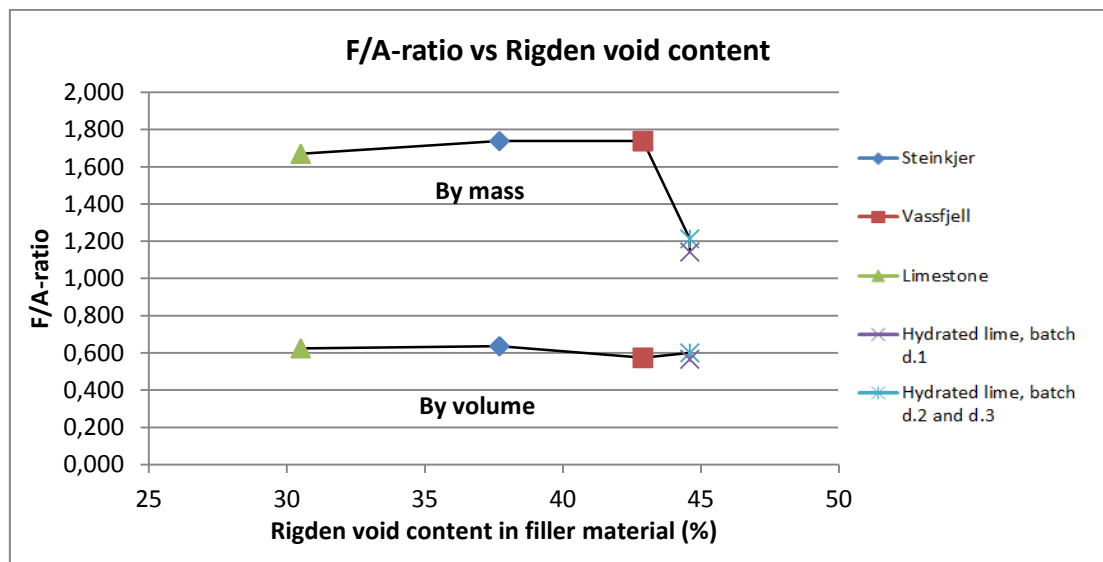


Figure 41: F/A-ratio by mass and volume vs Rigden void content

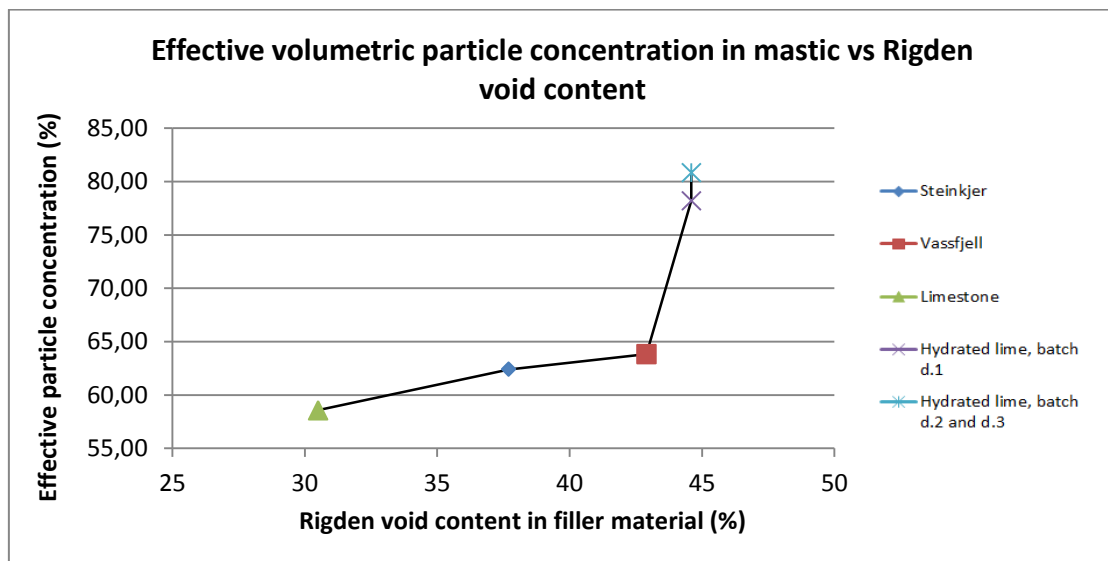


Figure 42: Effective volumetric particle concentration in mastic vs Rigden void content

## CHAPTER 6: DISCUSSION OF FINDINGS

### 6.1 Effects of mixture properties

#### 6.1.1 F/A-ratio

The intention in the mixing process was to keep the binder content constant for all mixtures. This was not possible for the hydrated lime series, because the mixture become extremely dry and impossible to blend. Due to high porosity, surface area and Rigden void content, the hydrated lime mixtures had the need for additional binder. This led to much lower F/A-ratio by mass for hydrated lime than the other series. However; the F/A-ratios by volume did not differ more than  $\pm 0.050$  among the four series.

The outcome of the analysis did not title any clear relationship between the F/A-ratio and the mixture performance in the conducted tests. The data points in the indirect tensile strength test were scattered when plotted against the F/A-ratio, both by weight and volume. This indicates that the indirect tensile strength is independent of the F/A-ratios. Similar findings were observed in the Cantabro test, where there was no evident connection between the F/A-ratio by mass or volume and the Cantabro loss.

The data from the cyclic compression test plotted against the F/A-ratios is scattered. The specimens with limestone filler yield much higher cumulative axial strain and deformation at 3600 load cycles and the creep rate in stage 2 are significantly steeper than those of the other series. By means of the outcome of the t-test, the limestone values are rejected. The Steinkjer and Vassfjell specimens had the same results, and as figure 34 and 35 showed, the F/A-ratios and the final creep seem independent, since both high and low ratios gave similar cumulative axial strain. The much lower F/A-ratio by weight for the hydrated lime series does not contribute to any significant change in the final cumulative axial strain value. The value is slightly higher than the outcome for natural fillers, but not as extreme as limestone. Yan et al (2013) found that the creep stiffness in mastics for warm mix asphalt is dependent on the F/A-ratio by mass, where higher F/A-ratio gave higher creep stiffness. It could be questioned whether there is a relationship between creep stiffness in mastic and creep stiffness in asphalt mixture, and furthermore if the results of warm mix asphalt can be related to hot mix asphalt, but the findings are of interest. In this study, this particular tendency was not visible.

Faheem and Bahia (2009) found that if the volumetric concentration of filler particles in the mastic is less than 40 %, the Rigden voids and the particle gradation are of more importance for the mixture performance than the volumetric relationship (Faheem and Bahia, 2009). Table 4.2 on page 35 outlined the actual volumetric particle concentration, and the range was between 36 % and 44 %, so according to Faheem and Bahia (2009) the Rigden void content should be the most influential factor along with particle gradation. This coincides with this study, as there were more noticeable relationships when Rigden void content was the parameter rather than F/A-ratio by volume.

### 6.1.2 Air void content

The number of gyrations was based on the test batch, which consisted of the original aggregate fractions with dust and limestone. The target air void content was 3.0 %, but the results showed that the air void content were lower than expected, as seen in Appendix E, table E.2. Even though the compaction effort and number of gyrations were kept constant, the obtained density and air void content varied significantly. Series C containing limestone filler yielded higher air void content than the other series. A theory that might explain this incidence is the particle gradation and the fineness modulus in the filler material. NCHRP Project 9-45 (2010) found that the particle size distribution is an important filler property and affects the physical aspect of the mixture. In the study by Brown (1990) it is stated that the degree of compaction, hence the overall density and air void content, is the most dominant parameter that affects the pavement performance, and that the air void content is the single most important factor of asphalt mixtures. This could explain the discrepancy and the statistical insignificance of the outcome of the values of the limestone series.

All series in this research, except hydrated lime series, contains the same percentage of binder. Depending on the Rigden void content in the fillers, the relative amount of fixed and free binder will vary. While Steinkjer and Vassfjell filler have 37.7 % and 42.9 % Rigden voids respectively, limestone has 30.5 %. This indicates that the mastics with Steinkjer and Vassfjell have less free binder than the limestone mastic. It is known that higher amount of free binder makes the compaction easier, leading to less air void content (Faheem et al, 2012). Despite the mentioned effect, the limestone series has notably higher air void content than the other series. A plausible reason for this can be attributed to the potential of the Steinkjer and Vassfjell filler to work as an extender of the binder. In terms of binder extension, the relative free binder content increases in the mastic, which again leads to improved workability, better compaction and lower air void content. This phenomenon was also the case for Kandhal et al (1998) when the specimens in their study regarding filler characterization were compacted.

Steinkjer and Vassfjell fillers are sieved natural aggregate dusts containing several minerals. Limestone consists of more than 99 % calcium carbonate (Lerfald, 2000). The calcium compound can increase the stiffening effect of the filler in mastics (Hintz et al, 2010; NCHRP Project 9-45, 2010; Wang et al, 2011). This singularity might contribute to explain why the specimens containing natural sieved fillers experience better compaction than the series containing limestone. Hydrated lime is a manufactured type of filler with significantly different behavior than the natural fillers and limestone. Due to high Rigden void content, surface area and other filler properties, there was necessary with additional binder to be able to blend the mixture properly. Hydrated lime is known for the stiffening effect, which results in more viscous mastics (Buttlar et al, 1999).

In the indirect tensile strength, higher air void content indicated lower indirect tensile strength. This is in correspondence with other studies, where it has been found that high air void content causes asphalt mixtures to have lower strength and higher deformation than mixtures with lower air void content (Huang et al, 1995). Gubler et al (2005) did also see a negative relationship between indirect tensile strength and air void content. As the air void

content increased, the indirect tensile strength decreased. This was the case for both dense-graded and open-graded mixtures in wet and dry condition.

Air void content was the major factor affecting the Cantabro loss of the parameters tested. With increasing air void content, the Cantabro loss increased. This coincides with the results found by Vivar and Haddock (2006), where lower density and higher air void content in the mixture decreased the performance and durability. Gubler et al (2005) found that the percentage of weight loss in the Cantabro test increases as the air void content in the specimens increases. The open-graded mixtures were more prone to the abrasion than the dense-graded mixture, and the Cantabro loss was significantly higher when the specimens were in wet condition than in dry condition.

For the cyclic creep, the results showed that the series with limestone yielded significantly higher cumulative axial strain and displacement at 3600 load cycles. The gradient of the slope in stage 2 was steeper than the other curves, indicating that the permanent deformation occurred at a faster rate than the other series. The limestone specimens have greater air void content than the Steinkjer, Vassfjell and hydrated lime, which could be the reason for the greater deformation depth in the limestone series. The effect of the air void content on the cumulative strain is supported by Natu et al (2001). In their study it was found that the permanent shear strain in asphalt specimens is sensitive to the air void content and the binder content, and that the aggregate gradation is of less importance. The recommendation by the PROKAS study (Lerfald et al, 2004) is 10 cm specimen height and 2 cm cutoff on each side. This was adjusted to 7.4 cm height and 0.7 cm cutoff on each side in this study, and could possibly have affected the results, as well as the noise in the load pulse in the NAT.

## **6.2 Effects of filler properties**

The different fillers had great variations in Rigden void content and specific density. Steinkjer has low density and relatively low Rigden void content compared to the limits in NPRA N200. Vassfjell is a dense filler with higher Rigden void content. Hydrated lime had the lowest density and highest Rigden void content. Limestone had values similar to Steinkjer filler.

The effect of the Rigden void content on the indirect tensile strength was evident. Higher Rigden void content resulted in higher indirect tensile strength. The limestone series had lowest indirect tensile strength, and the transition to the values of other series was linear, as the indirect tensile strength increased with higher Rigden void content in the filler. The results of the series containing hydrated lime showed that the specimens from this mixture yielded the highest indirect tensile strength. This corresponds well with the data found in the literature. Leseur and Little (1999) designated hydrated lime as an active filler material which provides significant improvement to aggregate coating, mixture strength and reducing the permanent deformation.

The plot of the Cantabro loss as a function of Rigden void content does not indicate any clear relationship when all series are taken into account. The loss is greatest for the limestone specimens. By rejecting these results, there is a tendency towards higher Rigden void content in the filler results in higher Cantabro loss for the specimen. However; when Cantabro loss was plotted against air void content, the results of the limestone specimens followed the proposed trend. It is worth mentioning that the limestone specimens have higher air void content, and this may point towards that the air void content in the specimens has grander influence than the Rigden void content and overrules the effect of the filler fractional voids on the Cantabro loss.

There was an apparent correlation between the Rigden voids and the effective volumetric filler fraction in mastics for natural fillers, where higher Rigden void content yielded higher volumetric particle concentration. Faheem and Bahia (2009) found relationship between actual volumetric particle concentration and Rigden void content, where higher Rigden void content gave higher volumetric filler particle concentration. The hypothesis of higher Rigden void content with higher volumetric filler fraction in the mastics is reasonable, since compacted filler samples with higher Rigden void content takes up more volume than samples with lower Rigden void content. Moreover, the relationship explained did not coincide for manufactured fillers in the study by Faheem and Bahia (2009). This complements the findings in this study, where hydrated lime had notably higher values between Rigden void content and volumetric particle concentration than the other series.

When the air void content in the specimens was plotted as a function of Rigden void content in the respective fillers, it was an observable trend that higher Rigden void content yielded lower air void content, which is seen in figure 40. If the extremal points were neglected, there were not any clear trends. Faheem et al (2012) found a positive relationship between air void content and Rigden void content by bridging mastic viscosity to mixture workability. As the relative mastic viscosity increased, the asphalt mixture got less workable and more difficult to compact to the desired density and air void content. Furthermore, the mastic viscosity correlated with Rigden void content, where increasing Rigden void content yielded increasing mastic viscosity. The increase in mastic viscosity due to higher amount of Rigden voids is advocated by the fact that the relative amount of fixed binder increases along with higher Rigden void content. This was also found by Mogawer and Stuart (1996), where the free binder content was lower for asphalt mastics containing filler with high Rigden void content than filler with low Rigden void content. If less binder is free to lubricate the mastic suspension, both the mastic becomes stiffer and more viscous.

The results of the cyclic compression test were scattered. The plot of the cumulative axial strain at 3600 load cycles as a function of the Rigden void content gave marginally any correlation at all. Mogawer and Stuart (1996) tested the correlation between Rigden void content and rutting potential and did not see any connection between them. This result was supported in the study by Huang et al (2007), where there was no relationship between Rigden void content and permanent deformation and rut depth in the asphalt mixtures.



The Steinkjer aggregate is an acidic type of rock, which indicates weaker binder affinity than alkaline and basic aggregates, such as the Vassfjell aggregate. No amine was added to improve the bonds between the filler and binder in the mastic for the series containing Steinkjer filler. However; when comparing the cracks from the indirect tensile strength test, there were no visibly dissimilarities of the mastic coating the coarser aggregates for the Steinkjer, Vassfjell and limestone series. The hydrated lime specimens had more ductile and sticky cracks. This may be explained by the fact that hydrated lime can be used as anti-stripping agents to improve asphalt rutting potential, whereas the binder and the mastic are better attached to the aggregates (Buttlar et al, 1999). Furthermore, the hydrated lime had much higher binder content than the other series.

## CHAPTER 7: CONCLUSION AND FURTHER INVESTIGATIONS

### 7.1 Conclusion and recommendations

The essential part of this thesis has been to assemble information concerning properties of filler types used in asphalt production, as well as requirements and relevant test methods. Efforts have been made to relate differences in asphalt mixture performance to filler properties and variations mastic constituents, volumetric composition and filler-binder ratios.

Based on the findings in the literature and in the laboratory research, the filler properties greatly affect the properties of the asphalt mixture, and different mastic compositions have a major impact on the mixture performance. The Rigden void content in the filler was found to be the single most important filler property, and this measure has an effect on the mastic stiffness and viscosity, hence the mixture workability, as well as the air void content in the compacted specimen. Higher Rigden void content increases the resistance of permanent deformation for mastics and mixtures, and higher Rigden void content yields higher indirect tensile strength and a tendency to increase the abrasion resistance in the Cantabro test, if the dominant effect of the air void content is overlooked. Furthermore, the Rigden void content has a major effect on the effective volumetric particle concentration in mastics. It was shown that higher Rigden void content yields higher effective volumetric particle concentration. This phenomenon is not visible when filler is added in the mixture on a weight relationship basis.

Hydrated lime acts noticeably different from the other fillers in the mixing process and needs additional binder compared to natural sieved fillers to avoid too dry mixtures. Limestone tends to give softer mixtures with higher air void content which are more prone to permanent deformation. Limestone does not need additional binder like hydrated lime. The two natural fillers sieved on the 0.063 mm sieve from Steinkjer and Vassfjell aggregates have the same behavior and need the same amount of binder. As a conclusion regarding binder content, it can be stated that fillers with similar properties within a given range need the same amount of binder, but it is obvious that the specific density, Rigden void content, surface area and the ability to absorb binder greatly affect the necessity for additional binder content, regardless whether the fillers are natural, added or manufactured.

The relationship between indirect tensile strength and air void content was scattered and statistical insignificant based on the t-test. However; a trend of decreasing indirect tensile strength with higher air void content was clear. This is despite the fact that the indirect tensile strength test assumes homogeneous, isotropic and elastic hot mix asphalt (Roberts et al, 1996). The distribution of air voids throughout gyratory compacted specimens is not homogeneous, which was discussed in the specialization project by Ødegård (2014). The recommendation by the PROKAS study (Lerfald et al, 2004) with specimen heights of 10 cm and 2 cm cutoff on each side might be an overestimation, and it could possibly moderated without affecting the results too much.

The air void content is related to the Rigden void content. Results found in the literature showed that as the Rigden void content increases, the air void content in the compacted specimen increases. The trend was not evident in this study, which could be explained by the rather narrow range of air void content. The lowest was 0.04 % air voids for the 10 cm mold hydrated lime specimen to the highest of 6.32 % for the 15 cm mold limestone specimen. To be able to draw any conclusions, there is need for a larger specter of air void contents.

For more adequate comparison of the cyclic compression test and permanent deformation, the load pulse should be validated and the noise in the system should be investigated. Better understanding of these variations can contribute to isolate the effect of the actual asphalt mixture tested, because identical conditions are crucial in tests where the rate of change is on micro level. Even though the system noise yields inherent variations and the relative differences between the specimens might be equalized to each other, when compared to other test methods measuring the same parameters this could lead to great deviations. The standard NS-EN 12697-25:2005 (2005) specifies that the cyclic compression test should be conducted at least 2 days after compaction, while the handbook NPRA N200 requires testing between 8 and 30 days after specimen preparation. One of these values should be adjusted to match the other under the next update and revision.

The results from this study, both the literature review and the laboratory research, can encourage introducing additional requirements for the filler properties and mastic phase of the asphalt mixture. The Rigden void content is an important factor for mastic and mixture properties, and it has a major effect on the effective particle concentration, which again affects the mastic viscosity. Increasing Rigden void content gives higher mastic viscosity, and viscous mastics yield mixtures that are less workable and more difficult to compact. The ability of coating the aggregates suffer from this, which impose a greater chance for stripping of the coarser aggregates in the surface course. Additional requirements for the Rigden void content could be specified to ensure adequate performance between filler and binder. The National Cooperative Highway Research Program in the US suggests a range of filler to binder ratio of 0.6 to 1.2 by mass and proposed to introduce requirements for the mastic viscosity in the revised version of Superpave standard. Shashidar and Romero (1998) suggest that direct measurements of the maximum volumetric particle concentration and the intrinsic viscosity would give good estimations of the filler stiffening effect in asphalt mastics.

Another recommendation is to look into the effective volumetric particle concentration in the mastics and preferably implement this as an additional factor for the filler fraction in the mixture design. The effective volumetric particle concentration is related to the maximum volumetric particle concentration, which is recommended as a prediction parameter by Shashidhar and Romero (1998), but the effective volumetric particle concentration does also consider the actual amount by volume of filler added. Introducing specification on the effective volumetric particle concentration can be a step towards changing the mixture design to a volumetric based requirement for the filler content, which would also include additional filler properties, such as Rigden void content, filler density and mastic viscosity, rather than just the weight of the filler fraction as of today.

## 7.2 Further investigations

Further research on the effective volumetric particle concentration of filler in mastics is necessary if there should be set additional requirements for the filler materials on this basis. Validations are needed to connect Rigden void content, density and mastic viscosity to the effective volumetric particle concentration in asphalt mastics. Relating pavement life indicators to the variations in the effective volumetric particle concentration is crucial to justify choices of upper and lower limits.

It could be interesting to gain better insight into particle gradation and fineness modulus of the fillers and see to what extent these properties affect the pavement life indicators. Furthermore, finer filler particles might react different with the binder in the mastic than coarser fines, and it could be of interest to relate the filler particle size distribution to the binder content needed in the asphalt mixture. The optimum binder content for the different fillers could also be important, and possibly relate this value to the Rigden void content and the effective volumetric particle concentration.

Additional investigations on the cyclic creep and permanent deformation should be conducted utilizing the wheel track test. This test is the reference test in NPRA N200 and might provide more applicable output data than the cyclic compression test.

The surface area of filler and the absorptiveness of the binder for different filler types could be of interest to evaluate. The absorptiveness is an important parameter for mastic constituents, because it affects the effective particle diameter and the free binder content in the mastic, which again is related to the effective volumetric particle concentration and the mastic viscosity.

The intention in this study was to have an additional mixture series containing mica as the type of filler. Mica is a soft and relatively weak mineral with flaky structure and high specific surface, which would represent an extremal point of the fillers tested. Due to late shipment, the evaluation of mica was disregarded, but it could be interesting to include it in later studies.

Another aspect could be to relate mastic properties to mixture properties, and to seek possibilities of connecting factors affecting mastic performance to the properties of compacted asphalt mixture. Faheem and Bahia (2012) bridged filler properties to asphalt mixture properties through mastic viscosity and mastic creep compliance. The same authors found relationship between the critical volumetric particle concentration in mastics and Rigden void content and the methylene blue value, as seen in equation (30) on page 27 (Faheem and Bahia, 2010). However; both studies need validation and adjustments for local variations, and additional investigations could be valuable.

## REFERENCES

### Literature

- Al-Suhaibani, A., Al-Mundaiheem, J., Al-Fozan, F. (1992): *Effects of Filler Type and Content on properties of Asphalt Concrete Mixes*. ASTM STP 1147, Meininger, R. C.; *Effects of Aggregates and Mineral Fillers on Asphalt Mixture Performance*, ISBN 0803114680
- Anderson, D.A., Goetz, W.H. (1973): *Mechanical behavior and reinforcement of mineral filler-asphalt mixtures*. Proceedings for the Association of Asphalt Paving Technologists, Vol, 42, pp. 37–66
- Anderson, D. A. (1987): *Guidelines for use of dust in hot-mix asphalt concrete mixtures*. Proceedings for the Association of Asphalt Paving Technologists, Vol. 56, pp. 492-516
- Brady, N. C., Weil, R. R. (2007): *The Nature and Properties of Soils. Fourteenth Edition*. Pearson Prentice Hall, ISBN 9780132279383
- Brown, E. R (1990): *Density of Asphalt Concrete – How much is needed?* NCAT Report Number 90-3 for the National Center for Asphalt Technology, Auburn University, AL, USA
- Buttlar, W. G., Bozkurt, D., Al-Khateeb, G. G., Waldhoff, A. S. (1999): *Understanding Asphalt Mastic Behavior through Micromechanics*. Transportation Research Record 1681, paper No. 99-1229, pp. 157-169
- Coussot, P. (2005): *Rheometry of pastes, suspensions, and granular materials*. John Wiley & Sons, ISBN 9780471653691
- Craus, J., Ishai, I., Por, N. (1979): *Selective Sorption in Filler-Bitumen Systems*. Journal of Material Science Vol. 14 No. 9, pp.2195–2204
- Das, B. M. (2010): *Principles of Foundation Engineering. Seventh Edition*. Cengage Learning. ISBN 9780495668107
- Einstein, A. (1905): *On the movement of small particles suspended in stationary liquids required by the molecular-kinetic theory of heat*. Annalen der Physik 17, pp. 549-560. Available through: *Investigations on the Brownian Movement*. Dover Publications Inc., 1956, ISBN 0486603040
- Faheem, A., H. Bahia (2009): *Conceptual Phenomenological Model for Interaction of Asphalt Binders with Mineral Fillers*. Journal of the Association of Asphalt Paving Technologists, Vol. 78
- Faheem, A. F., Bahia, H. U. (2010): *Modelling of Asphalt Mastic in Terms of Filler-Bitumen Interaction*. Road Materials and Pavement Design, Vol. 11 Sup. 1, pp. 281-303
- Faheem, A. F., Hintz, C., Bahia, H., Al-Quadi, I. L., Glidden, S. (2012): *Influence of Filler Fractional Voids on Mastic and Mixture Performance*. Journal of the Transportation Research Board Vol. 2294, pp. 74-80
- Fritschy, G., Papirer, E. (1978): *Interactions between a bitumen, its components and model fillers*. Fuel, Vol. 57 Issue 11, pp. 701-704
- Fwa, T. F. (2005): *The Handbook of Highway Engineering*. CRC Press, ISBN 9870849319860
- Geber, R., Gömse, L. A. (2010): *Characterization of mineral materials as asphalt fillers*. Materials Science Forum, Vol. 659, pp. 471-476

- Gubler, R., Partl, M. N., Canestrari, F., Grilli, A. (2005): *Influence of water and temperature on mechanical properties of selected asphalt pavements*. Materials and Structures, Vol. 38, pp 523-532
- Harris, B. M., Stuart, K. D. (1995): *Analysis of Mineral Fillers and Mastics Used in Stone Matrix Asphalt*. Journal of the Association of Asphalt Paving Technologists Vol. 64, pp. 54-95
- Haynes, W. M., Bruno, T. J. and Lide, D. R. (2014): *Handbook of Chemistry and Physics, 95<sup>th</sup> Edition*. CRC Press, ISBN 1114498106
- Hesami, E., Jelagin, D., Kringos, N., Birgisson, B. (2012): *An empirical framework for determining asphalt mastic viscosity as a function of mineral filler concentration*. Construction and Building Materials Vol. 35, pp. 23-29
- Hintz, C., Faheem, A., Bahia, H. U. (2010): *Use of Additives and Fillers in Hot Mix Asphalt*. Presented at CUPGA 2010 Workshop Program, Edmonton, Canada. Part of NCHRP Project 9-45.
- Huang, S., Tia, M., Ruth, B. E. (1995): *Evaluation of aging characteristics of modified asphalt mixtures*. ASTM Special Technical Publication, No. 1265, pp. 128-145
- Huang, Y. (2004): *Pavement Analysis and Design*. Pearson Education, Inc., ISBN 0131424734
- Huang, B., Shu, X., Chen, X. (2007): *Effects of mineral fillers on hot-mix asphalt laboratory-measured properties*. International Journal of Pavement Engineering, Vol. 8 No. 1, pp. 1-9
- Ishai, I., Craus, J. (1996): *Effects of Some Aggregate and Filler Characteristics on Behavior and Durability of Asphalt Paving Mixtures*. Transportation Research Record 1530, pp. 75-85
- Kandhal, P. S., Lynn, C., Parker, F. (1998): *Characterization Tests for Mineral Fillers Related to Performance of Asphalt Paving Mixtures*. Transportation Research Record 1638, Paper No. 98-0224, pp. 101-110
- Kavussi, A., Hicks, R. G. (1997): *Properties of bituminous mixtures containing different fillers*. Journal of the Association of Asphalt Paving Technologists, Vol. 66, pp. 153-186
- Landel, R. F., Moser, B. G., Bauman, A. J. (1965): *Rheology of Concentrated Suspensions: Effect of a Surfactant*. Proceedings, 4th International Congress of Rheology, Part 2, New York, p. 663.
- Lerfald, B. O. (2000): *A study of Ageing and Degradation of Asphalt Pavements on Low Volume Roads*. Ph.D. thesis 2000:49 submitted at Norwegian University of Science and Technology, Department of Civil and Transport Engineering
- Lerfald, B. O., Andersen, E. O., Aurstad, J., Bragstad, R., Jørgensen, T., Lange, G. (2004): *PROKAS Project Report No. 1*. SINTEF Teknologi og samfunn, Veg og samferdsel. ISBN 8214036038
- Leseur, D., Little, D. N. (1999): *Effect of hydrated lime on the rheology, fracture and ageing of bitumen*. Transportation Research Record 1661, Paper No. 99-1399, pp. 93-105
- Lesueur, D. (2009): *The colloidal structure of bitumen: Consequences on the rheology and on the mechanisms of bitumen modification*. Advances in Colloid and Interface Science Vol. 145 Issue 1-2, pp. 42-82
- Liao, M., Chen, J., Tsou, K. (2012): *Fatigue Characteristics of Bitumen-Filler Mastics and Asphalt Mixtures*. Journal of Civil Engineering Vol. 24 No. 7, pp. 916-923

- Melotti, R., Santagata, E., Bassani, M., Salvo, M., Rizzo, S. (2013): *A preliminary investigation into the physical and chemical properties of biomass ashes used as aggregate fillers for bituminous mixtures*. Waste Management 33, pp. 1906-1917
- Mogawer, W. S., Stuart, K. D. (1996): *Effects of Mineral Fillers on Properties of Stone Matrix Asphalt Mixtures*. Transportation Research Record 1530, pp. 86-94
- Natu, G., Guada, I., Tayebali, A. A. (2001): *Evaluation of the Sensitivity of Repeated Simple Shear Test at Constant Height Based in Laboratory Rutting*. Aggregate Contribution to HHMA Performance, ASTM STP 1412, pp. 72-94
- NCHRP Project 9-45 (2010): *Test Methods and Specification Criteria for Mineral Filler used in HMA*. Revised draft final report used in National Cooperative for Highway Research Program. Available through: [http://onlinepubs.trb.org/onlinepubs/nchrp/docs/NCHRP09-45\\_FR.pdf](http://onlinepubs.trb.org/onlinepubs/nchrp/docs/NCHRP09-45_FR.pdf) [Accessed February 26, 2015]
- NCHRP Report 629 (2008): *Ruggedness Testing of the Dynamic Modulus and Flow Number Tests with the Simple Performance Tester*. Transportation Research Board NCHRP Project 9-29, ISBN 9780309117586
- Nålsund, R. (2014): *Railway Ballast Characteristics, Selection Criterion and Performance*. Ph.D thesis 2014:259 submitted at Norwegian University of Science and Technology, Department of Civil and Transport Engineering
- Pasetto, M., Barbati, S. D., Giacomello, G (2014): *An experimental study on viscoelastic behavior of bituminous mastics*. Asphalt Pavements, Taylor & Francis Group, ISBN 9781138026933
- Ridgen, P. J. (1947): *The Use of Fillers in Bituminous Road Surfacing. A Study of Filler-Binder System in Relation to Filler Characteristics*. Journal of Society of Chemical Industry, Vol. 66 Issue 9, pp. 299–309
- Roberts, F. L., Kandhal, P. S., Brown, E. R., Lee, D. and Kennedy, T. W. (1996): *Hot Mix Asphalt Materials, Mixture Design and Construction. Second Edition*. NAPA Education Foundation, ISBN 0914313010
- Santamarina, J.C., Klein, K.A., Wang, Y.H., Prencke, E. (2002). *Specific surface: Determination and relevance*. Canadian Geotechnical Journal, Vol. 39, pp. 233-241
- Sengoz, B., Isikyakar, G. (2008): *Evaluation of the properties and microstructure of SBS and EVA polymer modified bitumen*. Construction and Building Materials, Vol 22, pp. 1897-1905
- Shashidar, N., Romero, P. (1998): *Factors Affecting the Stiffening Potential of Mineral Fillers*. Transport Research Record 1638, Paper No. 98-0989, pp. 94-100
- Sing, K. S. W. (1998): *Adsorption methods for the characterization of porous materials*. Advances in Colloid and Interface Science Vol. 76-77, pp. 3-11
- Tayebali, A. A., Malpass, G. A., Khosla, N. P. (1998): *Effects of Mineral Filler Type and Amount on Design and Performance of Asphalt Concrete Mixtures*. Transportation Research Record 1609, Paper No. 98-0296, pp.36-43

Tunnickliff, D. A. (1962): *A review of mineral filler*. Proceeding for Association of Asphalt Paving Technologists, Vol 31, pp. 118-150

Vivar, E. P., Haddock, J. E. (2006): *HMA Pavement Performance and Durability*. Final report of the Joint Transportation Research Program for Federal Highway Administration, JTRP Project Number C36-31N, Purdue University, IN, USA

Wang, H., Al-Qadi, I. L., Faheem, A. F., Bahia, H. U., Yang, S., Reinke, G. H. (2011): *Effect of Mineral Filler Characteristics on Asphalt Mastic and Mixture Rutting Potential*. Journal of the Transportation Research Board No. 2208, pp. 33-39

Woodward, D., Woodside, A., Jellie, J. (2002): *Clay in rocks*. Society in Chemical Industry, Vol. 124, pp. 1-12

Yan, K., Xu, H., Zhang, H. (2013): *Effect of mineral filler on properties on warm asphalt mastic containing Sasobit*. Construction and Building Materials, Vol. 48, pp. 622-627

Zeng, M., Wu, C. (2008): *Effect of Type and Content of Mineral Filler on Viscosity of Asphalt Mastic and Mixing and Compaction Temperatures of Asphalt Mixtures*. Journal of the Transportation Research Board No. 2051, pp. 31-40

Ødegård, I. (2014): *Methods for measuring Air Void Content in Asphalt Mixtures*. Specialization project for the course TBA4541 Highway Engineering at Norwegian University of Science and Technology

## **Standards and handbooks**

American Standard AASHTO R35-14 (2014): *Standard Practice for Superpave Volumetric Design for Hot-Mix Asphalt*

American Standard AASHTO T267-86 (2008): *Standard Method of Test for Determination of Organic Content in Soils by Loss of Ignition*.

American Standard AASHTO T330-07 (2011): *Standard Method of Test for the Qualitative Detection of Harmful Clays of the Smectite Group in Aggregates Using Methylene Blue*

American Standard AASHTO TP79-13 (2013): *Standard Method of Test for Determining the Dynamic Modulus and Flow Number for Hot Mix Asphalt Using the Asphalt Mixture Performance Tester*

American Standard ASTM C125 (2014): *Standard Terminology Relating to Concrete and Concrete Aggregates*

American Standard ASTM D4123-82 (1995): *Standard Test Method for Indirect Tension Test for Resilient Modulus of Bituminous Mixtures*

American Standard ASTM D7405:10a (2010): *Standard Test Method for Multiple Stress Creep and Recovery of Asphalt Binder Using a Dynamic Shear Rheometer*

European Standard NS-EN 12697-16 (2004): *Bituminous mixtures - Test methods for hot mix asphalt - Part 16: Abrasion by studded tires*



European Standard NS-EN 12697-22:2003+A1:2007 (2003): *Bituminous mixtures. Test methods for hot mix asphalt, part 22: Wheel tracking*

European Standard NS-EN 12697-25:2005 (2005): *Bituminous mixtures. Test methods for hot mix asphalt, part 25: Cyclic compression test.*

European Standard NS-EN 13043:2002+NA:2008 (2002): *Aggregates for bituminous mixtures and surface treatments for roads, airfields and other trafficked areas*

NPRA Handbook N200 (2014): *Road Construction*

NPRA Handbook R210 (2014): *Laboratory Examinations*



## **APPENDIX**

Appendix A – Problem statement .....	iii
Appendix B – Water density versus water temperature .....	vii
Appendix C – Requirements for Ab 11 .....	viii
Appendix D – Properties of the aggregates and filler material .....	ix
Appendix E – Asphalt mixture properties .....	xiii
Appendix F – Data from the Cantabro and the indirect tensile strength tests.....	xvi
Appendix G – Indirect tensile strength outputs.....	xvii
Appendix H – Data from the cyclic compression test.....	xxiii
Appendix I – Two-sample t-test assuming unequal variances .....	xxv



## MASTEROPPGAVE

(TBA4940, Veg, masteroppgave)

VÅREN 2015

for

Ingvild Ødegård

### **Effects of mastic ingredients and composition on asphalt mix properties**

#### **BACKGROUND**

All asphalt mixes consist of a blend of mineral aggregates, a bituminous binder and possibly additives of different kinds, for example in the form of agents to improve the bond between aggregates and binder, and/or constituents to improve the binder properties, for example by the use of polymer modification, which is usually considered part of the binder itself. Most asphalt mixtures contain fine aggregate fractions, filler, which usually consists of both dust from the coarser aggregate(s) and some introduced added filler, e.g. limestone.

Mastic is a term used for the mixture of fine mineral aggregate or filler and asphalt binder. However, it is a dispute whether the filler should be considered as part of the aggregate or as part of the mastic. Anyhow, the filler plays an important role in the asphalt mix, not the least as different filler materials have different specific surface area and thereby to varying degree bind varying amount of binder. Therefore, the same amount by weight of different filler materials occupies different volumes, and thereby leaves different air void contents in the mix. It is also beyond doubt that the filler serves as reinforcement of the binder, preventing binder drainage, and the binder provides tensile strength to the asphalt and coating of the aggregates, and acts as glue in the mix.

In asphalt mix design, usually the weight relationships of different aggregate fractions and binder which provides the desired properties are determined. The result is a recipe which describes the proposed composition of the asphalt mixture, but in practice there will be variations in the composition of the asphalt produced.

The particular area of interest here is variations in the mineral aggregates that can be considered part of the mastic. Different types of filler materials have different properties in terms of size distribution, density, mineralogy, specific surface area and interaction with the binder. Uncontrolled variations in this composition may therefore lead to binder drainage due to insufficient reinforcement or a “dry” mixture with insufficient coating of the aggregates.

#### **TASK**

##### **Description of the task**

This master task deals with filler materials for asphalt concrete, and how different types and amounts of filler materials affect the asphalt properties and volumetric composition. Especially, the

effects of limestone filler and hydrated lime should be investigated, and compared to the effects of natural aggregate dust.

#### **Objective and purpose**

An important objective is to study the impact different filler types might have on the volumetric distribution of the «ingredients» (included here also the air void content) in the asphalt concrete mix. This will be an important «correction» to the currently dominating requirements for asphalt concrete mixes in the Norwegian guidelines, and will act as an important assessment basis for a possible change towards a volumetric based requirement for the filler part of the aggregate or the mastic as a whole.

Also, the impact the different filler materials might have on the results of different asphalt mix tests should be investigated. This should at least comprise tests describing different pavement life aspects. If no or limited impact is measurable for normal variations of filler and/or binder content, it should for some tests be considered to go beyond the normal variation limits.

#### **Subtasks and research questions**

Important subtasks will be:

- A literature survey to describe relevant tests and requirements in other countries, which can give ideas to further testing
- To study whether different filler types require different binder contents for asphalt concrete. The effect of different filler types, both aggregate dust and added filler of different kinds, should be investigated.
- To carry out detrimental tests like Indirect tensile strength, Cantabro, and possibly NAT or Wheel-track testing, to investigate whether the different filler types affect different pavement life indicators differently.
- To check film thickness of coarse aggregates.
- To visually assess possible differences, “manually” or by image processing.
- To judge whether the results might encourage a change towards a volumetric based requirement for filler content, and in case how, if possible.

### GENERELT

Oppgaveteksten er ment som en ramme for kandidatens arbeid. Justeringer vil kunne skje underveis, når en ser hvordan arbeidet går. Eventuelle justeringer må skje i samråd med faglærer ved instituttet.

Ved bedømmelsen legges det vekt på grundighet i bearbeidningen og selvstendighet i vurderinger og konklusjoner, samt at framstillingen er velredigert, klar, entydig og ryddig uten å være unødig voluminøs.

Besvarelsen skal inneholde

- standard rapportforside (automatisk fra DAIM, <http://daim.idi.ntnu.no/>)
- tittelside med ekstrakt og stikkord (mal finnes på siden <http://www.ntnu.no/bat/skjemabank>)
- forord
- sammendrag på norsk og engelsk (studenter som skriver sin masteroppgave på et ikke-skandinavisk språk og som ikke behersker et skandinavisk språk, trenger ikke å skrive sammendrag av masteroppgaven på norsk)
- innholdsfortegnelse inklusive oversikt over figurer, tabeller og vedlegg
- om nødvendig en liste med beskrivelse av viktige betegnelser og forkortelser benyttet
- hovedteksten
- referanser til kildemateriale som ikke er av generell karakter, dette gjelder også for muntlig informasjon og opplysninger.
- oppgaveteksten (denne teksten signert av faglærer) legges ved som Vedlegg 1.
- besvarelsen skal ha komplett paginering (sidenummerering).

Besvarelsen kan evt. utformes som en vitenskapelig artikkel. Arbeidet leveres da også med rapportforside og tittelside og om nødvendig med vedlegg som dokumenterer arbeid utført i prosessen med utforming av artikkelen.

Se forøvrig «Råd og retningslinjer for rapportskrivning ved prosjektarbeid og masteroppgave ved Institutt for bygg, anlegg og transport». Finnes på <http://www.ntnu.no/bat/skjemabank>

### Hva skal innleveres?

Rutiner knyttet til innlevering av masteroppgaven er nærmere beskrevet på <http://daim.idi.ntnu.no/>. Trykking av masteroppgaven bestilles via DAIM direkte til Skipnes Trykkeri som leverer den trykte oppgaven til instituttkontoret 2-4 dager senere. Instituttet betaler for 3 eksemplarer, hvorav instituttet beholder 2 eksemplarer. Ekstra eksemplarer må bekostes av kandidaten/ eksternt samarbeidspartner.

Ved innlevering av oppgaven skal kandidaten levere besvarelsen i digital form i pdf- og word-versjon med underliggende materiale (for eksempel datainnsamling) i digital form (f. eks. excel). Videre skal kandidaten levere innleveringsskjemaet (fra DAIM) hvor både Ark-Bibl i SBI og Fellestjenester (Byggsikring) i SB II har signert på skjemaet. Innleveringsskjema med de aktuelle signaturene underskrives av instituttkontoret før skjemaet leveres Fakultetskontoret.

Dokumentasjon som med instituttets støtte er samlet inn under arbeidet med oppgaven skal leveres inn sammen med besvarelsen.

Besvarelsen er etter gjeldende reglement NTNUs eiendom. Eventuell benyttelse av materialet kan bare skje etter godkjenning fra NTNU (og eksternt samarbeidspartner der dette er aktuelt). Instituttet har rett til å bruke resultatene av arbeidet til undervisnings- og forskningsformål som om

det var utført av en ansatt. Ved bruk ut over dette, som utgivelse og annen økonomisk utnyttelse, må det inngås særskilt avtale mellom NTNU og kandidaten.

**(Evt) Avtaler om ekstern veiledning, gjennomføring utenfor NTNU, økonomisk støtte m.v.**  
Det er inngått avtale om økonomisk utgiftsdekning fra Statens vegvesen, Vegdirektoratet. Det vises til avtaleteksten for de betingelsene som må være oppfylt for at avtalt beløp utbetales. Se <http://www.ntnu.no/bat/skjemabank> for avtaleskjema.

**Helse, miljø og sikkerhet (HMS):**

NTNU legger stor vekt på sikkerheten til den enkelte arbeidstaker og student. Den enkeltes sikkerhet skal komme i første rekke og ingen skal ta unødige sjanser for å få gjennomført arbeidet. Studenten skal derfor ved uttak av masteroppgaven få utdelt brosjyren "Helse, miljø og sikkerhet ved feltarbeid m.m. ved NTNU".

Dersom studenten i arbeidet med masteroppgaven skal delta i feltarbeid, tokt, befarings, feltkurs eller ekskursionsjoner, skal studenten sette seg inn i "Retningslinje ved feltarbeid m.m.". Dersom studenten i arbeidet med oppgaven skal delta i laboratorie- eller verkstedarbeid skal studenten sette seg inn i og følge reglene i "Laboratorie- og verkstedhåndbok". Disse dokumentene finnes på fakultetets HMS-sider på nettet, se <http://www.ntnu.no/ivt/adm/hms/>.

Studenter har ikke full forsikringsdekning gjennom sitt forhold til NTNU. Dersom en student ønsker samme forsikringsdekning som tilsatte ved universitetet, anbefales det at han/hun tegner reiseforsikring og personskadeforsikring. Mer om forsikringsordninger for studenter finnes under samme lenke som ovenfor.

**Oppstart og innleveringsfrist:**

Oppstart og innleveringsfrist er i henhold til informasjon i DAIM.

**Faglærer ved instituttet:** Helge Mork

**Medveileder ved instituttet:** Andreas Kjosavik

**Veileder hos ekstern samarbeidspartner:** Nils Uthus, Statens vegvesen

Institutt for bygg, anlegg og transport, NTNU

Dato: 8.1.2015, (revidert: 21.04.2015)

Underskrift



Faglærer



## Appendix B – Water density versus water temperature

Table B.1: Water density ( $\text{g/cm}^3$ ) versus water temperature ( $^{\circ}\text{C}$ ). (Haynes et al., 2014)

$t/^{\circ}\text{C}$	$\rho/\text{g cm}^{-3}$	$t/^{\circ}\text{C}$	$\rho/\text{g cm}^{-3}$	$t/^{\circ}\text{C}$	$\rho/\text{g cm}^{-3}$	$t/^{\circ}\text{C}$	$\rho/\text{g cm}^{-3}$	$t/^{\circ}\text{C}$	$\rho/\text{g cm}^{-3}$
20.1	0.9981860	25.3	0.9969696	30.5	0.9954967	35.7	0.9937899	49.0	0.98848
20.2	0.9981652	25.4	0.9969436	30.6	0.9954660	35.8	0.9937549	50.0	0.98804
20.3	0.9981443	25.5	0.9969176	30.7	0.9954352	35.9	0.9937199	51.0	0.98758
20.4	0.9981233	25.6	0.9968914	30.8	0.9954044	36.0	0.9936847	52.0	0.98712
20.5	0.9981022	25.7	0.9968651	30.9	0.9953734	36.1	0.9936495	53.0	0.98665
20.6	0.9980810	25.8	0.9968387	31.0	0.9953424	36.2	0.9936142	54.0	0.98617
20.7	0.9980596	25.9	0.9968123	31.1	0.9953113	36.3	0.9935788	55.0	0.98569
20.8	0.9980382	26.0	0.9967857	31.2	0.9952801	36.4	0.9935434	56.0	0.98521
20.9	0.9980167	26.1	0.9967591	31.3	0.9952488	36.5	0.9935078	57.0	0.98471
21.0	0.9979950	26.2	0.9967324	31.4	0.9952175	36.6	0.9934722	58.0	0.98421
21.1	0.9979733	26.3	0.9967055	31.5	0.9951860	36.7	0.9934365	59.0	0.98371
21.2	0.9979514	26.4	0.9966786	31.6	0.9951545	36.8	0.9934007	60.0	0.98320
21.3	0.9979295	26.5	0.9966516	31.7	0.9951228	36.9	0.9933649	61.0	0.98268
21.4	0.9979074	26.6	0.9966245	31.8	0.9950911	37.0	0.9933290	62.0	0.98216
21.5	0.9978853	26.7	0.9965973	31.9	0.9950593	37.1	0.9932929	63.0	0.98163
21.6	0.9978630	26.8	0.9965700	32.0	0.9950275	37.2	0.9932569	64.0	0.98109
21.7	0.9978407	26.9	0.9965426	32.1	0.9949955	37.3	0.9932207	65.0	0.98055
21.8	0.9978182	27.0	0.9965151	32.2	0.9949635	37.4	0.9931844	66.0	0.98000
21.9	0.9977956	27.1	0.9964875	32.3	0.9949313	37.5	0.9931481	67.0	0.97945
22.0	0.9977730	27.2	0.9964599	32.4	0.9948991	37.6	0.9931117	68.0	0.97890
22.1	0.9977502	27.3	0.9964321	32.5	0.9948668	37.7	0.9930753	69.0	0.97833
22.2	0.9977273	27.4	0.9964043	32.6	0.9948344	37.8	0.9930387	70.0	0.97776
22.3	0.9977044	27.5	0.9963763	32.7	0.9948020	37.9	0.9930021	71.0	0.97719
22.4	0.9976813	27.6	0.9963483	32.8	0.9947694	38.0	0.9929654	72.0	0.97661
22.5	0.9976582	27.7	0.9963202	32.9	0.9947368	38.1	0.9929286	73.0	0.97603
22.6	0.9976349	27.8	0.9962920	33.0	0.9947041	38.2	0.9928917	74.0	0.97544
22.7	0.9976115	27.9	0.9962637	33.1	0.9946713	38.3	0.9928548	75.0	0.97484
22.8	0.9975881	28.0	0.9962353	33.2	0.9946384	38.4	0.9928178	76.0	0.97424
22.9	0.9975645	28.1	0.9962068	33.3	0.9946055	38.5	0.9927807	77.0	0.97364
23.0	0.9975408	28.2	0.9961783	33.4	0.9945724	38.6	0.9927435	78.0	0.97303
23.1	0.9975171	28.3	0.9961496	33.5	0.9945393	38.7	0.9927063	79.0	0.97241
23.2	0.9974932	28.4	0.9961208	33.6	0.9945061	38.8	0.9926689	80.0	0.97179
23.3	0.9974692	28.5	0.9960920	33.7	0.9944728	38.9	0.9926316	81.0	0.97116
23.4	0.9974452	28.6	0.9960631	33.8	0.9944394	39.0	0.9925941	82.0	0.97053
23.5	0.9974210	28.7	0.9960341	33.9	0.9944060	39.1	0.9925565	83.0	0.96990
23.6	0.9973968	28.8	0.9960050	34.0	0.9943724	39.2	0.9925189	84.0	0.96926
23.7	0.9973724	28.9	0.9959758	34.1	0.9943388	39.3	0.9924812	85.0	0.96861
23.8	0.9973480	29.0	0.9959465	34.2	0.9943051	39.4	0.9924434	86.0	0.96796
23.9	0.9973234	29.1	0.9959171	34.3	0.9942713	39.5	0.9924056	87.0	0.96731
24.0	0.9972988	29.2	0.9958876	34.4	0.9942375	39.6	0.9923677	88.0	0.96664
24.1	0.9972740	29.3	0.9958581	34.5	0.9942035	39.7	0.9923297	89.0	0.96598
24.2	0.9972492	29.4	0.9958285	34.6	0.9941695	39.8	0.9922916	90.0	0.96531
24.3	0.9972243	29.5	0.9957987	34.7	0.9941354	39.9	0.9922534	91.0	0.96463
24.4	0.9971992	29.6	0.9957689	34.8	0.9941012	40.0	0.9922152	92.0	0.96396
24.5	0.9971741	29.7	0.9957390	34.9	0.9940669	41.0	0.99183	93.0	0.96327
24.6	0.9971489	29.8	0.9957090	35.0	0.9940326	42.0	0.99144	94.0	0.96258
24.7	0.9971236	29.9	0.9956790	35.1	0.9939982	43.0	0.99104	95.0	0.96189
24.8	0.9970981	30.0	0.9956488	35.2	0.9939637	44.0	0.99063	96.0	0.96119
24.9	0.9970726	30.1	0.9956185	35.3	0.9939291	45.0	0.99021	97.0	0.96049
25.0	0.9970470	30.2	0.9955882	35.4	0.9938944	46.0	0.98979	98.0	0.95978
25.1	0.9970213	30.3	0.9955578	35.5	0.9938597	47.0	0.98936	99.0	0.95907
25.2	0.9969955	30.4	0.9955273	35.6	0.9938248	48.0	0.98893	99.974	0.95837

## Appendix C – Requirements for Ab 11

Table C.1: Requirements for Ab 11 (NPRA N200)

Grensekurver (tilsiktet utgående sammensetning)					
	Gjennomgang i masseprosent				
ISO-sikt	Ab 4	Ab 8	Ab 11	Ab 16	Ab 22
31,5 mm					100
22,4 mm				100	90-100
16 mm			100	90-100	70-95
11,2 mm		100	90-100	56-80	54-75
8 mm		90-100	59-81	45-66	
5,6 mm	100				
4 mm	90-100	53-75	37-59		
2 mm	55-68	38-55	25-47	23-43	21-40
1 mm	37-49	29-45	20-35	18-33	17-32
0,25 mm	19-27	17-22	12-19	10-19	10-19
0,063 mm	11-16	9-13	8-12	7-12	7-11
Minimum bindemiddelinhold tilsiktet utgående sammensetning <sup>2)</sup>					
Slitelag <sup>1)</sup>	6,4%	6,2%	5,8%	5,6%	5,2%
Bindlag <sup>1)</sup>	6,0%	5,8%	5,6%	5,4%	5,2%

- 1) Minimum bindemiddeltisetning i % av totalvekt asfaltmasse korrigeres med hensyn på steinmaterialets densitet ved å multiplisere med faktoren  $\alpha = \frac{2,650}{\rho_a}$ , hvor  $\rho_a$  er steinmaterialets densitet i megagram pr kubikkmeter ( $\text{Mg/m}^3$ ), bestemt i henhold til NS-EN 1097-6. Bindemiddelinholdet inkluderer bitumen i gjenbruk og naturasfalt når det benyttes.
- 2) For massetyper med  $D < 16\text{mm}$  vil bindemiddelinholdet normalt måtte ligge ca. 0,2 % over minimum bindemiddeltisetning. Bindemiddelinhold kan økes ytterligere ved å tilsette fiber e.l.
- 3) For  $\text{ADT} < 300$  settes kravet til  $\text{LA} \leq 40$ . For  $\text{ADT} \leq 1500$  er kravet til mølleverdi  $\leq 19$ .

Table C.2: Sieving curve for Ab 11 asphalt mixture

Mass percent passing (%) for Ab 11				
Sieve (mm)	Requirement N200 max	Requirement N200 min	Chosen value	Obtained by Solver
31,5				
22,4				
16	100	100	100	100,0
11,2	100	90	97	98,4
8	81	59	73	71,6
4	59	37	50	51,6
2	47	25	36	37,2
1	35	20	25	25,1
0,25	19	12	16	15,9
0,063	12	8	11	11,1

## Appendix D – Properties for the aggregates and filler materials

Table D.1: Sieving curves for the aggregates and the filler

Mass percent passing (%). Average numbers							
Sieve (mm)	Steinkjer 8-11	Steinkjer 4-8	Steinkjer 0-4	Steinkjer 0.063-4	Sieved filler, Steinkjer and Vassfjell filler	Limestone	Hydrated lime
31,5							
22,4							
16	100,00	100,00	100	100,00	100	100	100
11,2	96,33	100,00	100	100,00	100	100	100
8	35,35	98,91	100	100,00	100	100	100
4	2,08	17,53	96,77	97,01	100	100	100
2	1,38	1,59	67,34	64,00	100	100	100
1	1,17	1,00	41,13	34,24	100	100	100
0,25	1,04	0,92	22,98	11,53	100	100	96,33
0,063	0,88	0,75	13,71	0,00	100	91	74

Table D.2: Density of the sieved 0.063 mm fillers (SINTEF Materials and Chemistry)



## SPESIFIKK VEKT

**Prover fra:** Inst.for bygg, anlegg og transport-veg og samferdsel  
v/Lisbeth Johansen, 2015-05-13

Prøve	Innvekt ( g )	Spesifikk vekt ( g / cm <sup>3</sup> )
Vassfjell egenfiller	7,028	3,06
Steinkjer egenfiller	8,171	2,76

**SINTEF Materialer og kjemi**

Table D.3: Sieving curve for limestone filler (Franzefoss miljøkalk, produktdatablad)


Produktdatablad BITUFILL VK									
Franzefoss Miljøkalk AS Postboks 53 NO-1309 Rud Telefon : +47 05255      miljokalk@kalk.no Fax : +47 67 15 20 01      www.kalk.no									
Materiale: Kalkstein CaCO <sub>3</sub>		Produsent: Verdalskalk AS, avd Havna		Råmateriale: Kalkstein fra Tromsdalen i Verdal					
Reg.nr.: CE godkjent REACH nr		1111-CPD-0108 -		Fremstilt: Nedmaling av kalkstein					
Anvendelse: Filler for bituminøse masser og overflatebehandling for veger, flyplasser og andre trafikkarealer									
Krav: NS-EN 13043									
Parameter	Metode	Enhet	Statistikk		Krav				
			Snitt	s	L	H	Toleranse +/-		
CaO	Kalsiumoksid	WD-XRF	%	55,4	0,13	-	-		
MgO	Magnesiumoksid		%	0,3	0,11	-	-		
Ca	Kalsium	Beregnet fra	%	40	-	-	-		
Mg	Magnesium	WD-XRF	%	0,2	-	-	-		
Vanninnhold		NS-EN 12048	%	0,1	-	-	1,0		
Masstetthet		Pyknometer	[kg/dm <sup>3</sup> ]	2,7	-	-	-		
Rigden hulrom		NS-EN 1097-4	%	30,5	-	-	-		
0,001 mm			%	3,8	0,3	-	-		
0,002 mm			%	10	0,6	-	-		
0,005 mm			%	22	1,0	-	-		
0,010 mm			%	33	1,3	-	-		
0,020 mm			%	51	1,5	-	-		
0,045 mm			%	79	2,0	-	-		
0,063 mm			%	91	2,0	70	100		
0,125 mm			%	99	0,7	85	100		
0,200 mm			%	100	0,3	-	-		

Table D.4: Sieving curve for hydrated lime filler (Franzefoss miljøkalk, produktdatablad)


Produktdatablad BITUFILL H100									
Franzefoss Miljøkalk AS Postboks 53 NO-1309 Rud Telefon : +47 05255      miljokalk@kalk.no Fax : +47 67 15 20 01      www.kalk.no									
Materiale: Hydratkalk Ca(OH) <sub>2</sub>		Produsent: Verdalskalk AS, avd Hylla		Råmateriale: Kalkstein fra Tromsdalen i Verdal					
Reg.nr.: Produktregistrert REACH nr		075233 01-2119475325-36-0043		Fremstilt: Brenning av CaCO <sub>3</sub> til CaO (1000°C i sjaktovn) og lesking av CaO til Ca(OH) <sub>2</sub>					
Anvendelse: Filler for bituminøse masser og overflatebehandling for veger, flyplasser og andre trafikkarealer									
Krav: NS-EN 13043									
Parameter	Metode	Enhet	Statistikk		Krav				
			Snitt	s	L	H	Toleranse +/-		
Ca(OH) <sub>2</sub>	Våtkjemisk	%	95	1,6	-	-			
CaO <sub>total</sub>	Kalsiumoksid	WD-XRF	%	74	0,6	-		-	
MgO	Magnesiumoksid		%	0,5	0,04	-		-	
Vanninnhold		Karl Fisher	%	0,7	0,3	-	1,0		
Masstetthet		Pyknometer	[kg/dm <sup>3</sup> ]	2,04	-	-	-		
Rigden hulrom		NS-EN 1097-4	%	*	-	-	-		
0,001 mm			%	3	0,4	0,2	-		
0,002 mm			%	8	0,9	0,7	-		
0,005 mm			%	27	2,4	5,6	-		
0,010 mm			%	46	3,7	13,4	-		
0,020 mm			%	57	4,0	15,5	-		
0,045 mm			%	68	3,8	13,7	-		
0,063 mm			%	74	3,6	13	100		
0,125 mm			%	88	2,8	85	100		
0,200 mm			%	96	1,3	-	-		
0,350 mm			%	100	0,0	-	-		

Table D.5: *Rigden void content calculation, sieved dust Steinkjer 0.063 mm*


 Norwegian University of Science and Technology Department of Civil and Transport Engineering	<b>Bestemmelse av hulrom i tørr komprimert filler</b>		
	Standard: NS-EN 1097-4		
	Trondheim, 2015.04.28		
Utført av: Ingvild Ødegård			
<b>Materiale: Steinkjer filler, sieved 0.063 mm</b>			
Sted:			
Analysert for:			
Relativ densitet for fillermateriæ 2,76			
Prøvenummer	1	2	3
Høyde tom m/filterpapir (mm)	26,85	26,82	26,98
Høyde m/komprimert filler (mm)	38,38	38,30	38,38
Vekt av sylinder m/filterpapir (g)	524,62	524,64	524,64
Vekt av sylinder med komp. filler (g)	534,39	534,51	534,59
Vekt av komprimert filler (g)	9,77	9,87	9,95
Hulrom (%)	38,6	37,7	36,8
<b>Rigdenhulrom:</b>		<b>37,7</b>	

Table D.6: *Rigden void content calculation, sieved dust Vassfjell 0.063 mm*



 Norwegian University of Science and Technology Department of Civil and Transport Engineering	<b>Bestemmelse av hulrom i tørr komprimert filler</b>		
	Standard: NS-EN 1097-4		
	Trondheim, 2015.04.28		
Utført av: Ingvild Ødegård			
<b>Materiale: Vassfjell filler, sieved 0.063 mm</b>			
Sted:			
Analysert for:			
Relativ densitet for fillermateriæ 3,06			
Prøvenummer	1	2	3
Høyde tom m/filterpapir (mm)	26,81	26,86	26,86
Høyde m/komprimert filler (mm)	38,12	38,12	38,11
Vekt av sylinder m/filterpapir (g)	524,64	524,63	524,64
Vekt av sylinder med komp. filler (g)	534,57	534,41	534,48
Vekt av komprimert filler (g)	9,93	9,78	9,84
Hulrom (%)	42,6	43,2	42,8
<b>Rigdenhulrom:</b>		<b>42,9</b>	

Table D.7: *Rigden void content calculation, hydrated lime*

 Norwegian University of Science and Technology Department of Civil and Transport Engineering	<b>Bestemmelse av hulrom i tørr komprimert filler</b>		
	Standard: NS-EN 1097-4		
	Trondheim, 2015.04.28		
Utført av: Ingvild Ødegård			
Materiale: <b>Hydrated lime</b>			
Sted:			
Analysert for:			
Relativ densitet for filler materiale: 2,04			
Prøvenummer	1	2	3
Høyde tom m/filterpapir (mm)	26,79	26,73	26,75
Høyde m/komprimert filler (mm)	44,54	44,53	44,34
Vekt av sylinder m/filterpapir (g)	524,66	524,64	524,65
Vekt av sylinder med komp. filler (g)	534,60	534,70	534,70
Vekt av komprimert filler (g)	9,94	10,06	10,05
Hulrom (%)	45,1	44,6	44,0
<b>Rigdenhulrom:</b>		<b>44,6</b>	

## Appendix E – Asphalt mixture properties

Table E.1(a): *Calculations for Rice density*

	Test batch		Steinkjer filler, series A		Vassfjell filler, series B	
	1	2	1	2	1	2
Beaker (g)	245,4	243,2	243,2	264,3	256,6	235,0
Beaker in water (g)	135,2	134	134	146,1	141,3	129,5
Sample mass + beaker (g)	482	497,3	491,5	475,9	512,1	423,2
Sample mass + beaker in water (g)	276,2	285,3	280,9	271,2	293,6	241,9
Weight of submerged sample mass (g)	141	151,3	146,9	125,1	152,3	112,4
Weight of dry sample mass (g)	236,6	254,1	248,3	211,6	255,5	188,2
Temperature (deg C)	25,0	25,0	24,9	24,9	24,9	24,9
Water density (g/cm <sup>3</sup> )	0,997047	0,997047	0,997073	0,997073	0,997073	0,997073
Maximum specific gravity	2,475	2,472	2,449	2,446	2,476	2,483
Rice density (g/cm <sup>3</sup> )	2,468	2,464	2,442	2,439	2,469	2,476
<b>Average (g/cm<sup>3</sup>)</b>	<b>2,466</b>		<b>2,440</b>		<b>2,472</b>	

Table E.1(b): *Calculations for Rice density*

	Limestone, series C		Hydrated lime, series D	
	1	2	1	2
Beaker (g)	243,2	264,3	256,6	235
Beaker in water (g)	134	146,1	141,3	129,5
Sample mass + beaker (g)	421,1	493,3	588,9	545,8
Sample mass + beaker in water (g)	239,5	282,2	331,8	307
Weight of submerged sample mass (g)	105,5	136,1	190,5	177,5
Weight of dry sample mass (g)	177,9	229	332,3	310,8
Temperature (deg C)	25	25,1	25	25,1
Water density (g/cm <sup>3</sup> )	0,997047	0,997021	0,997047	0,997021
Maximum specific gravity	2,457	2,465	2,343	2,332
Rice density (g/cm <sup>3</sup> )	2,450	2,458	2,337	2,325
<b>Average (g/cm<sup>3</sup>)</b>	<b>2,454</b>		<b>N/A</b>	

Table E.2: Air void content of the specimens

Specimen	Filler type	Dry weight (g)	Weight in water (g)	Saturated surface dry (g)	Water temp. (°C)	Water density (g/cm <sup>3</sup> )	Specimen density (g/cm <sup>3</sup> )	Air void content (%)
a.1.1	Steinkjer	1295,5	755,0	1297,6	25,1	0,9970213	2,380	2,453
a.1.2		1295,7	763,8	1297,0	25,1	0,9970213	2,423	0,717
a.1.3		1299,0	765,9	1299,9	25,1	0,9970213	2,425	0,614
a.2.1		1298,9	759,3	1300,2	25,0	0,997047	2,394	1,887
a.2.2		1298,8	764,9	1299,6	24,9	0,9970726	2,422	0,754
a.2.3		1297,9	766,4	1299,1	24,9	0,9970726	2,429	0,450
a.3.1		3096,6	1822,1	3100,5	25,1	0,9970213	2,415	1,036
a.3.2		3095,0	1823,0	3097,8	25,1	0,9970213	2,421	0,808
a.3.3		3092,8	1814,6	3095,9	25,0	0,997047	2,407	1,379
b.1.1	Vassfjell	1297,7	761,7	1299,4	25,1	0,9970213	2,406	2,662
b.1.2		1298,7	767,8	1299,8	25,1	0,9970213	2,434	1,544
b.1.3		1300,4	766,8	1301,7	25,0	0,997047	2,424	1,947
b.2.1		1300,0	773,4	1300,9	25,0	0,997047	2,457	0,602
b.2.2		1297,8	771,8	1298,7	24,9	0,9970726	2,456	0,654
b.2.3		1297,6	774,3	1298,2	24,9	0,9970726	2,470	0,101
b.3.1		3092,1	1819,8	3095,4	25,0	0,997047	2,417	2,232
b.3.2		3086,0	1828,7	3087,8	24,9	0,9970726	2,444	1,144
b.3.3		3088,7	1828,7	3090,4	24,9	0,9970726	2,441	1,261
c.1.1	Limestone	1299,3	762,7	1300,5	25,0	0,997047	2,409	1,833
c.1.2		1297,7	758	1299,0	25,0	0,997047	2,392	2,534
c.1.3		1299,2	760,4	1301,1	24,9	0,9970726	2,396	2,365
c.2.1		1297,6	760,3	1299,5	24,9	0,9970726	2,399	2,214
c.2.2		1295,2	756,4	1297,1	24,9	0,9970726	2,388	2,665
c.2.3		1297,0	755,7	1299,7	24,9	0,9970726	2,377	3,121
c.3.1		3079,6	1771,0	3086,9	24,9	0,9970726	2,333	4,905
c.3.2		3084,1	1761,8	3095,6	24,9	0,9970726	2,305	6,044
c.3.3		3089,0	1761,1	3100,9	24,9	0,9970726	2,299	6,316
d.1.1	Hydrated lime	1297,4	740,7	1298,1	25,1	0,9970213	2,321	0,679
d.1.2		1296,2	743,5	1296,7	25,1	0,9970213	2,336	0,017
d.1.3		1297,5	743,9	1297,9	25,1	0,9970213	2,335	0,062
d.2.1		1301,5	742,1	1302,5	25,1	0,9970213	2,316	0,392
d.2.2		1298,7	738,4	1301,3	25,0	0,997047	2,300	1,045
d.2.3		1298,8	742,5	1299,8	25,0	0,997047	2,324	0,043
d.3.1		3100,8	1764,2	3103,7	25,0	0,997047	2,308	0,713
d.3.2		3093,4	1764,5	3095,4	25,0	0,997047	2,317	0,310
d.3.3		3097,7	1763,6	3099,8	24,9	0,9970726	2,312	0,565



Table E.3: *Compaction and test information of the specimens*

Specimen	Filler type	Number of compaction cycles	Preparation day	Day of testing	Test
a.1.1	Steinkjer	60	April 29, 2015	May 12, 2015	Cantabro
a.1.2		60	April 29, 2015	May 12, 2015	
a.1.3		60	April 29, 2015	May 12, 2015	
a.2.1		60	April 29, 2015	May 11, 2015	Indirect tensile strength
a.2.2		60	April 29, 2015	May 11, 2015	
a.2.3		60	April 29, 2015	May 11, 2015	
a.3.1		Cyclic creep	40	May 8, 2015	May 18, 2015
a.3.2			40	May 8, 2015	May 19, 2015
a.3.3			40	May 8, 2015	May 19, 2015
b.1.1	Vassfjell	60	April 29, 2015	May 15, 2015	Cantabro
b.1.2		60	April 29, 2015	May 15, 2015	
b.1.3		60	April 29, 2015	May 15, 2015	
b.2.1		60	April 29, 2015	May 11, 2015	Indirect tensile strength
b.2.2		60	April 29, 2015	May 11, 2015	
b.2.3		60	April 29, 2015	May 11, 2015	
b.3.1		Cyclic creep	40	May 8, 2015	May 20, 2015
b.3.2			40	May 8, 2015	May 20, 2015
b.3.3			40	May 8, 2015	May 20, 2015
c.1.1	Limestone	60	May 7, 2015	May 15, 2015	Cantabro
c.1.2		60	May 7, 2015	May 15, 2015	
c.1.3		60	May 7, 2015	May 15, 2015	
c.2.1		60	May 7, 2015	May 11, 2015	Indirect tensile strength
c.2.2		60	May 7, 2015	May 11, 2015	
c.2.3		60	May 7, 2015	May 11, 2015	
c.3.1		Cyclic creep	40	May 12, 2015	May 25, 2015
c.3.2			40	May 12, 2015	May 25, 2015
c.3.3			40	May 12, 2015	May 25, 2015
d.1.1	Hydrated lime	60	May 7, 2015	May 15, 2015	Cantabro
d.1.2		60	May 7, 2015	May 15, 2015	
d.1.3		60	May 7, 2015	May 15, 2015	
d.2.1		60	May 7, 2015	May 11, 2015	Indirect tensile strength
d.2.2		60	May 7, 2015	May 11, 2015	
d.2.3		60	May 7, 2015	May 11, 2015	
d.3.1		Cyclic creep	40	May 12, 2015	May 26, 2015
d.3.2			40	May 12, 2015	May 26, 2015
d.3.3			40	May 12, 2015	May 26, 2015

## Appendix F – Data from the Cantabro and the indirect tensile strength tests

Table F.1: Results from the indirect tensile strength test

Specimen	Diameter avg. (mm)	Height avg. (mm)	E modulus (MPa)	Tensile strength (kPa)	Load distribution coefficient
a.2.1	99,93	70,13	5493	884	3,65
a.2.2	99,8	69,11	6056	976	3,77
a.2.3	99,81	69,14	5598	901	3,67
b.2.1	99,68	68,21	6017	970	3,76
b.2.2	99,91	67,78	5939	957	3,75
b.2.3	99,87	67,25	6167	995	3,79
c.2.1	99,89	69,75	5360	862	3,62
c.2.2	99,7	69,79	5691	917	3,69
c.2.3	99,71	70,54	5553	894	3,66
d.2.1	99,83	71,70	6339	1023	3,83
d.2.2	99,89	72,58	6373	1028	3,84
d.2.3	99,84	71,70	6624	1069	3,89

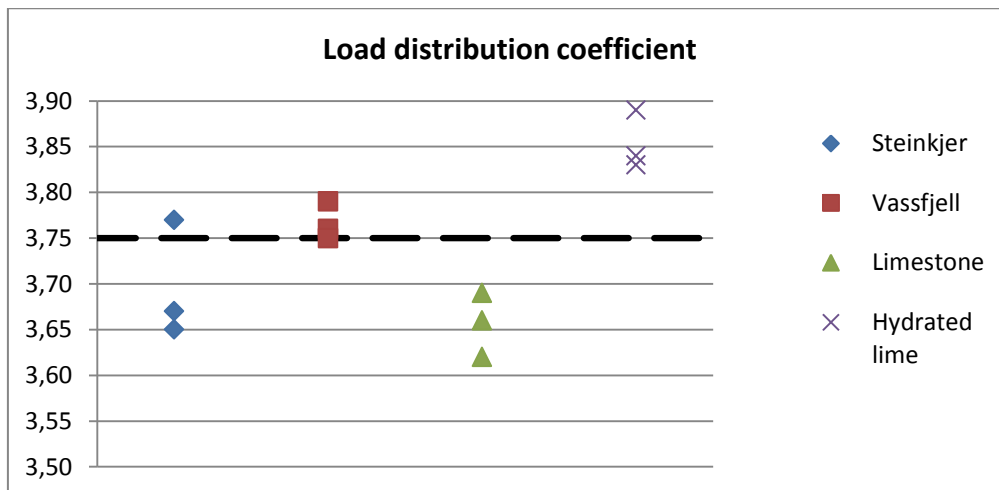


Figure F.1: Load distribution coefficients and maximum value of 3.75

Table F.2: Results from the Cantabro test

Specimen	Initial weight (g)	Final weight (g)	Cantabro loss (%)
a.1.1	1295,5	1212,6	6,40
a.1.2	1295,7	1238,7	4,40
a.1.3	1299,0	1238,3	4,67
b.1.1	1297,7	1220,2	5,97
b.1.2	1298,7	1206,5	7,10
b.1.3	1300,4	1230,2	5,40
c.1.1	1299,3	1197,3	7,85
c.1.2	1297,7	1203,7	7,24
c.1.3	1299,2	1191,3	8,31
d.1.1	1297,4	1226,6	5,46
d.1.2	1296,2	1195,5	7,77
d.1.3	1297,5	1221,6	5,85

## Appendix G – Indirect tensile strength outputs

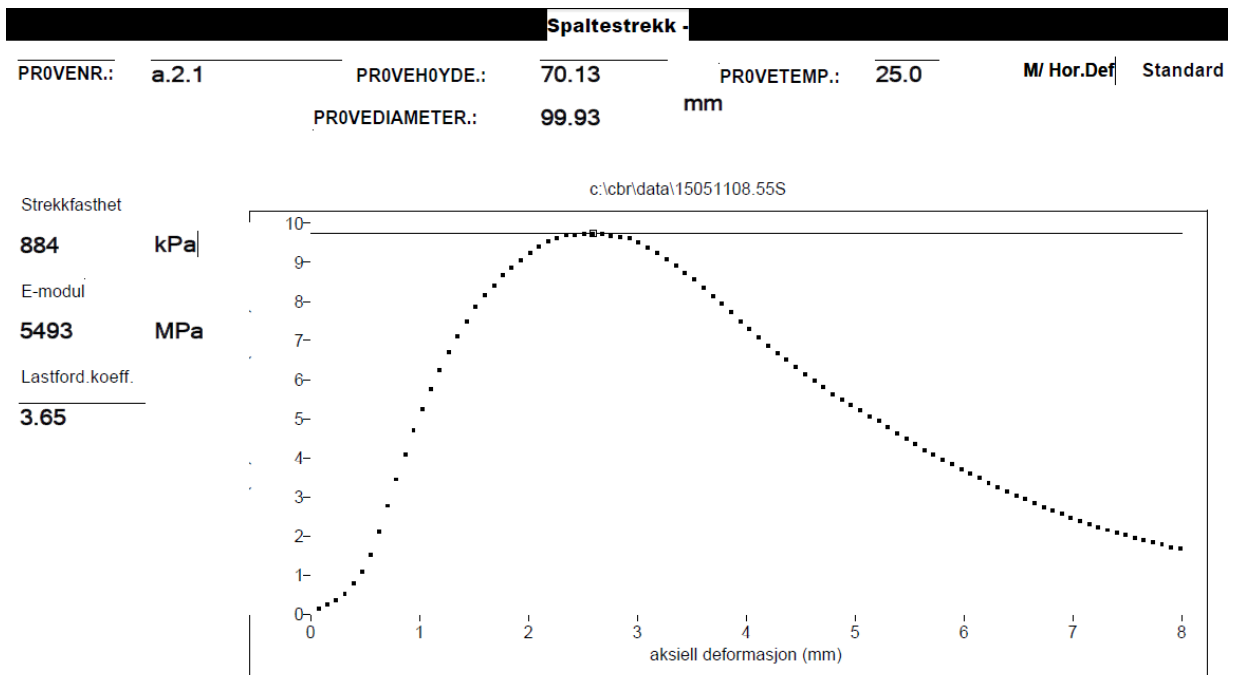


Figure G.1: Indirect tensile strength output for specimen a.2.1

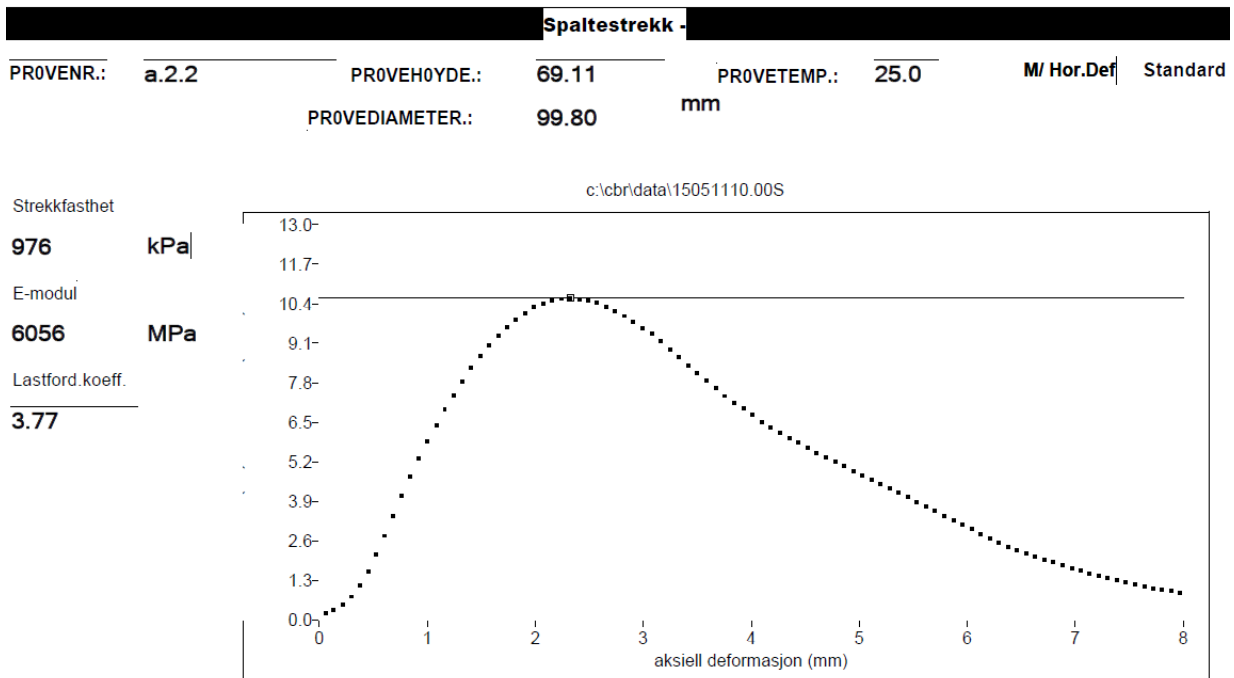


Figure G.2: Indirect tensile strength output for specimen a.2.2

Spaltestrekk					
PROVENR.:	a.2.3	PROVEHØYDE.:	69.14	PROVETEMP.:	25.0
		PROVEDIAMETER.:	99.81		M/ Hor.Def  Standard
					mm

Strekfasthet

**901** kPa

E-modul

**5598** MPa

Lastford.koeff.

**3.67**

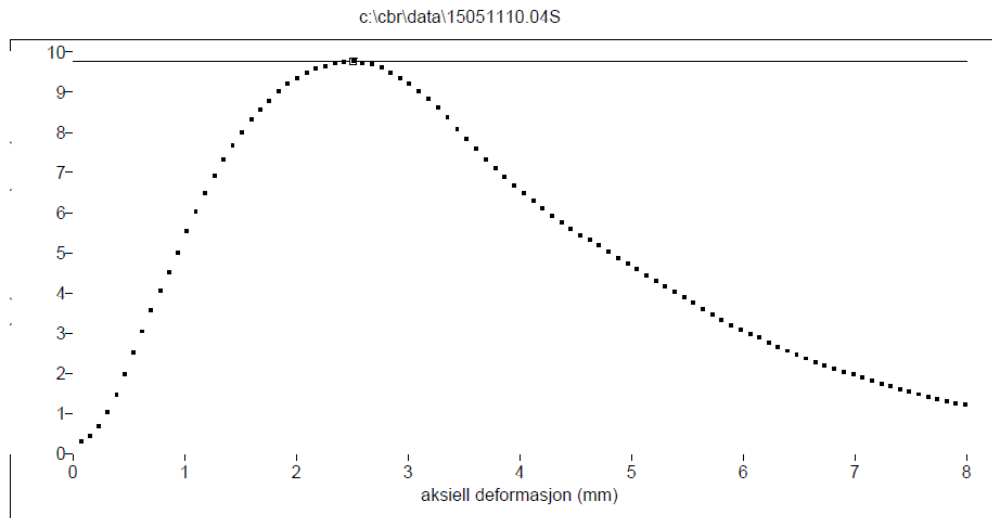


Figure G.3: Indirect tensile strength output for specimen a.2.3

Spaltestrekk					
PROVENR.:	b.2.1	PROVEHØYDE.:	68.21	PROVETEMP.:	25.0
		PROVEDIAMETER.:	99.68		M/ Hor.Def  Standard
					mm

Strekfasthet

**970** kPa

E-modul

**6017** MPa

Lastford.koeff.

**3.76**

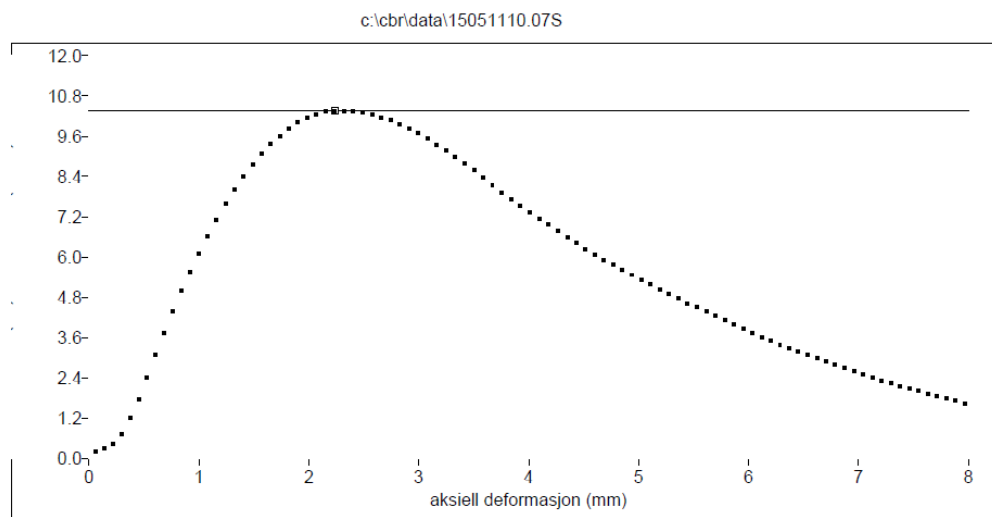


Figure G.4: Indirect tensile strength output for specimen b.2.1

Spaltestrekk					
PROVENR.:	b.2.2	PROVEHØYDE.:	67.78	PROVETEMP.:	25.0
		PROVEDIAMETER.:	99.91	mm	M/ Hor.Def   Standard

Strekfasthet  
**957** kPa  
 E-modul  
**5939** MPa  
 Lastford.koeff.  
**3.75**

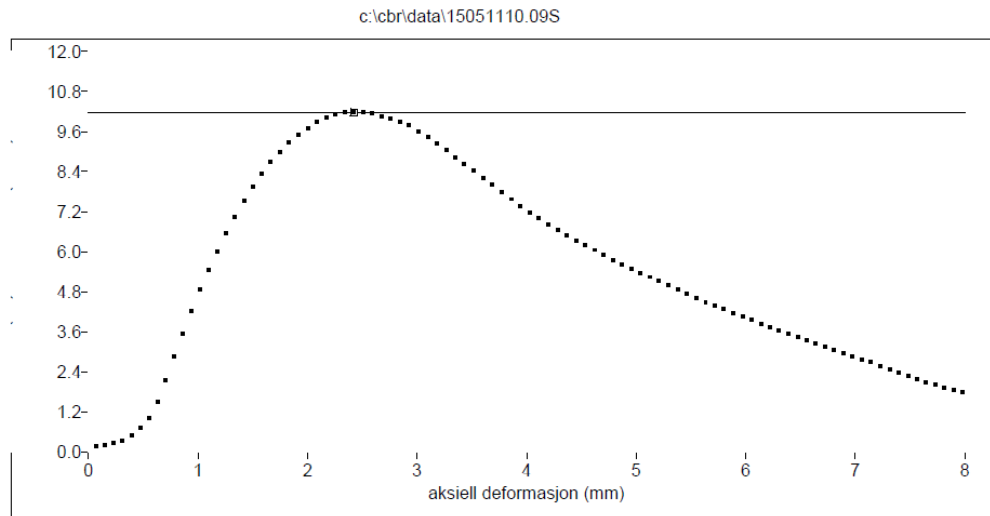


Figure G.5: Indirect tensile strength output for specimen b.2.3

Spaltestrekk					
PROVENR.:	b.2.3	PROVEHØYDE.:	67.25	PROVETEMP.:	25.0
		PROVEDIAMETER.:	99.87	mm	M/ Hor.Def   Standard

Strekfasthet  
**995** kPa  
 E-modul  
**6167** MPa  
 Lastford.koeff.  
**3.79**

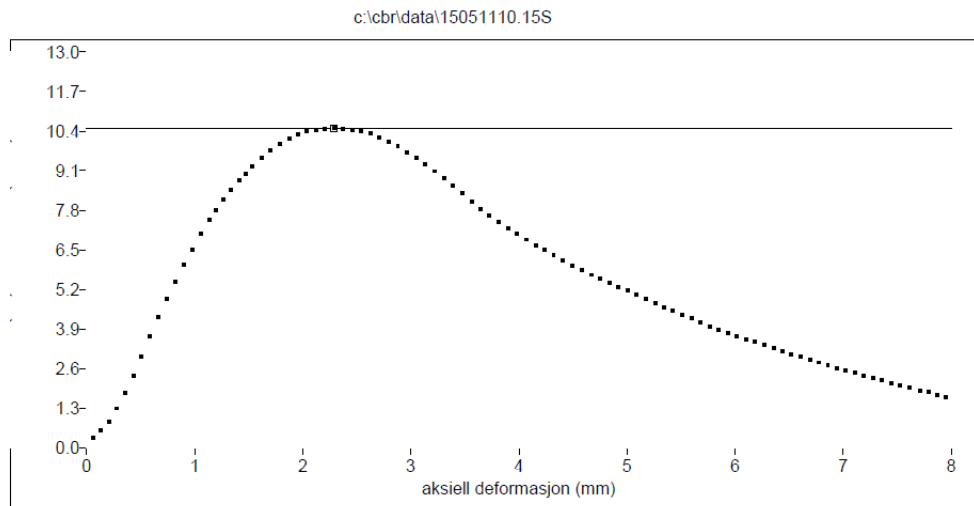
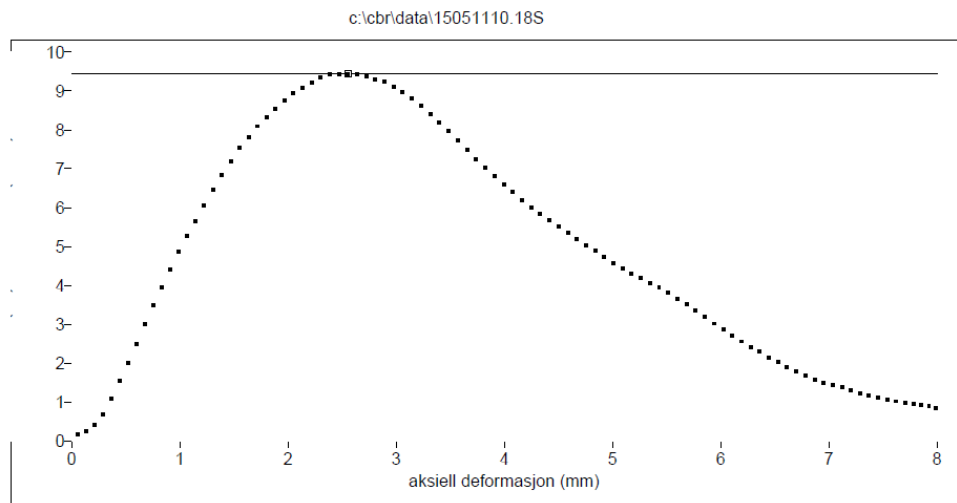


Figure G.6: Indirect tensile strength output for specimen b.2.3

Spaltestrekk					
PROVENR.:	c.2.1	PROVEHØYDE.:	69.75	PROVETEMP.:	25.0
		PROVEDIAMETER.:	99.89	mm	M/ Hor.Def   Standard

Strekfasthet  
**862** kPa  
 E-modul  
**5360** MPa  
 Lastford.koeff.  
**3.62**



**Figure G.7: Indirect tensile strength output for specimen c.2.1**

Spaltestrekk					
PROVENR.:	c.2.2	PROVEHØYDE.:	69.79	PROVETEMP.:	25.0
		PROVEDIAMETER.:	99.70	mm	M/ Hor.Def   Standard

Strekfasthet  
**917** kPa  
 E-modul  
**5691** MPa  
 Lastford.koeff.  
**3.69**

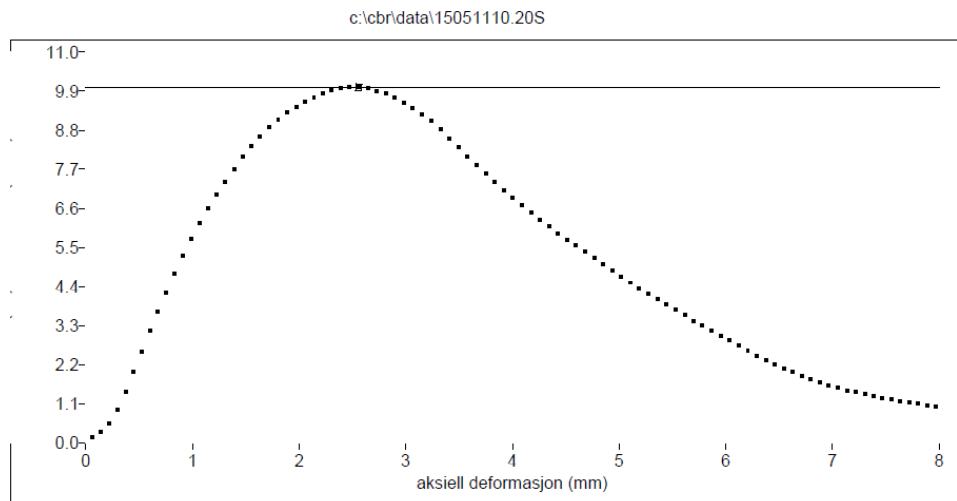


**Figure G.8: Indirect tensile strength output for specimen c.2.2**

**Spaltestrekk**

PROVENR.: c.2.3      PROVEHØYDE.: 70.54      PROVETEMP.: 25.0      M/ Hor.Def | Standard  
PROVEDIAMETER.: 99.71      mm

Strekfasthet  
**894**      kPa  
E-modul  
**5553**      MPa  
Lastford.koeff.  
**3.66**

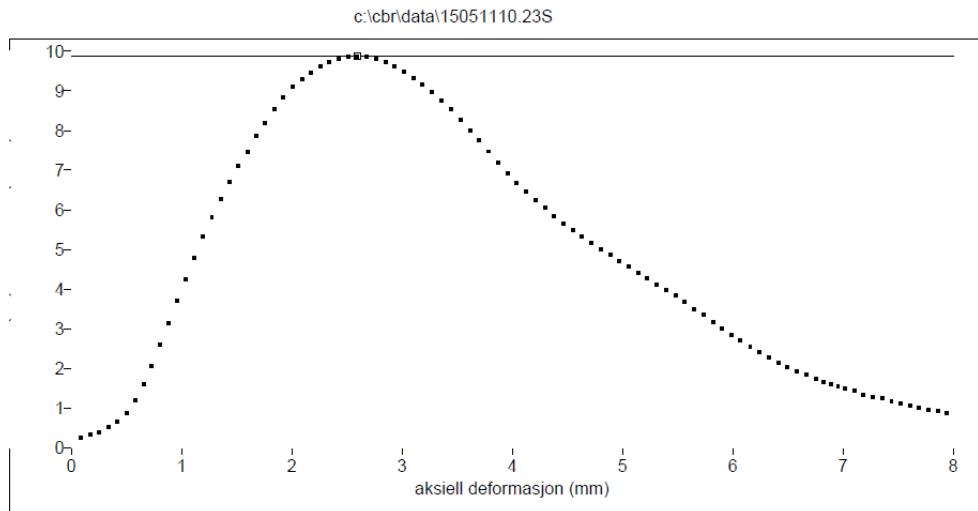


**Figure G.9: Indirect tensile strength output for specimen c.2.3**

**Spaltestrekk**

PROVENR.: d.2.1      PROVEHØYDE.: 71.70      PROVETEMP.: 25.0      M/ Hor.Def | Standard  
PROVEDIAMETER.: 99.83      mm

Strekfasthet  
**1023**      kPa  
E-modul  
**6339**      MPa  
Lastford.koeff.  
**3.83**

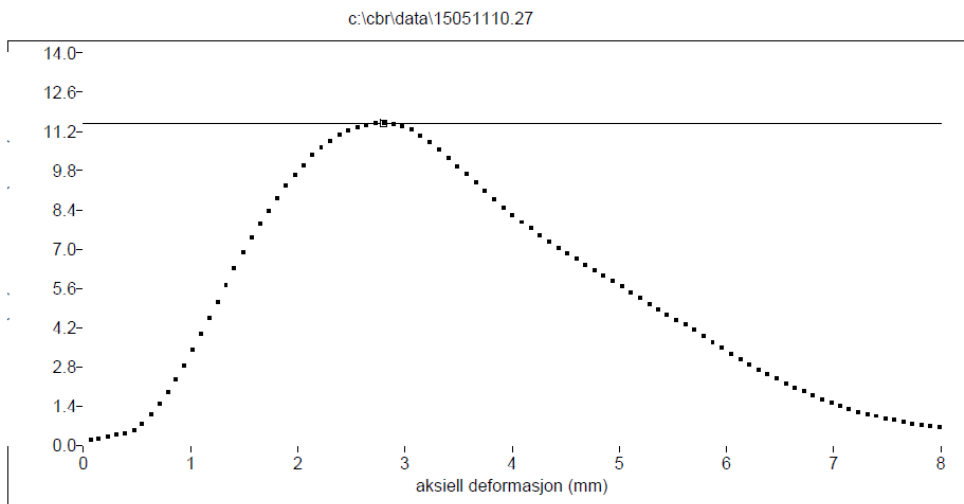


**Figure G.10: Indirect tensile strength output for specimen d.2.1**

Spaltestrekk					
PROVENR.:	d.2.2	PROVEHØYDE.:	72.58	PROVETEMP.:	25.0
		PROVEDIAMETER.:	99.89		M/ Hor.Def   Standard
				mm	

Strekfasthet  
**1028** kPa  
 E-modul  
**6373** MPa  
 Lastford.koeff.  
**3.84**

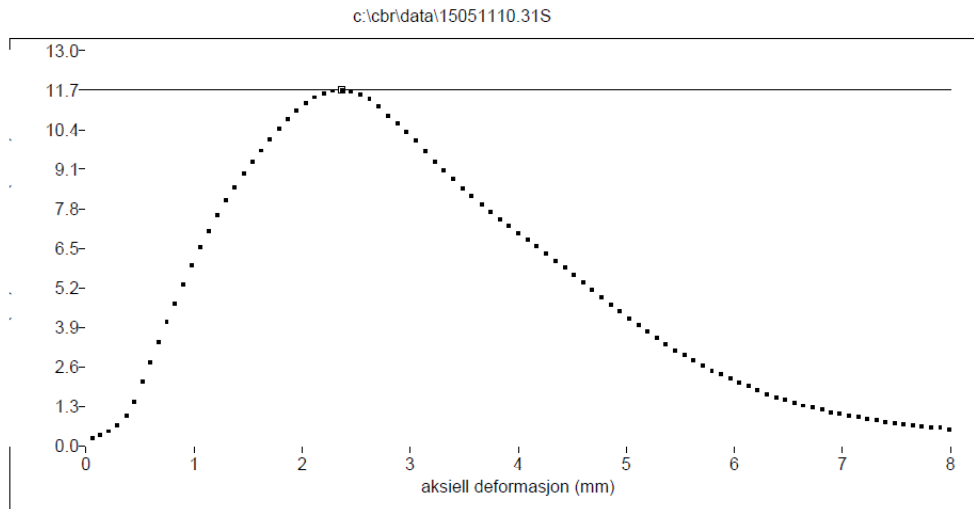


Figure G.11: Indirect tensile strength output for specimen d.2.2

Spaltestrekk					
PROVENR.:	d.2.3	PROVEHØYDE.:	71.70	PROVETEMP.:	25.0
		PROVEDIAMETER.:	99.84		M/ Hor.Def   Standard
				mm	

Strekfasthet  
**1069** kPa  
 E-modul  
**6624** MPa  
 Lastford.koeff.  
**3.89**

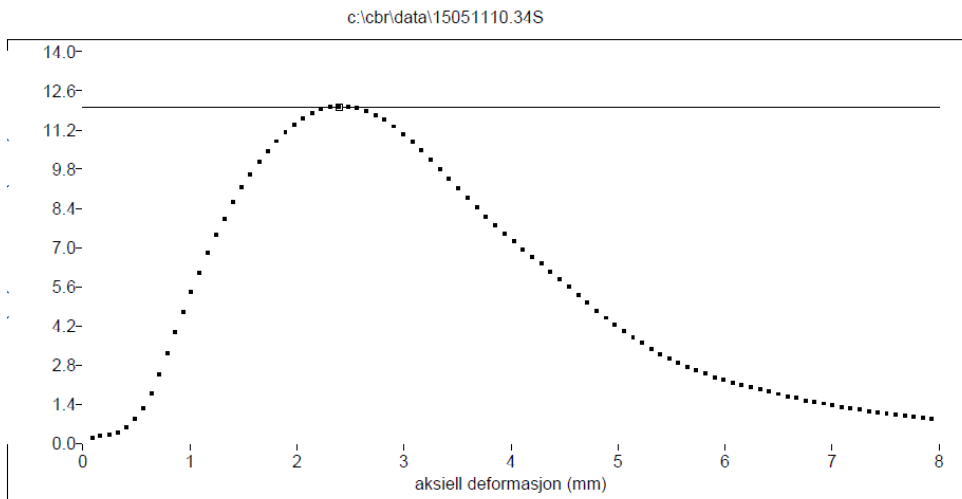


Figure G.12: Indirect tensile strength output for specimen d.2.3



## Appendix H – Data from the cyclic compression test

Table H.1: Data from the cyclic compression test

Specimen	Initial height (mm)	Load cycle at point, stage 1 and 2	Cumulative axial strain at point, stage 1 and 2 ( $\mu\epsilon$ )	Gradient of slope in stage 2 ( $\mu\epsilon/\text{load cycle}$ )	Cumulative axial strain at $n = 3600$ ( $\mu\epsilon$ )	Displ. at $n=3600$ (mm)	Pre-heating (h)
a.3.1	58,98	304	6438,946	0,643	8558,473	0,534	4
a.3.2	61,09	295	6373,182	0,720	8752,001	0,534	4
a.3.3	59,75	390	8269,376	0,972	11389,283	0,695	6
b.3.1	59,73	218	6110,402	0,636	8259,597	0,511	4
b.3.2	58,69	413	9963,971	0,694	12174,603	0,719	6
b.3.3	59,52	418	10201,013	0,622	12179,130	0,834	4
c.3.1	60,70	486	14342,342	2,599	22432,790	1,394	4
c.3.2	62,25	300	16903,433	2,139	23963,558	1,521	6
c.3.3	61,15	431	19590,468	3,452	30524,133	1,894	4
d.3.1	61,29	236	9698,431	1,609	15107,413	0,988	4
d.3.2	61,49	340	10523,199	1,929	16810,441	1,060	6
d.3.3	61,07	368	7656,488	0,957	10747,306	0,683	4

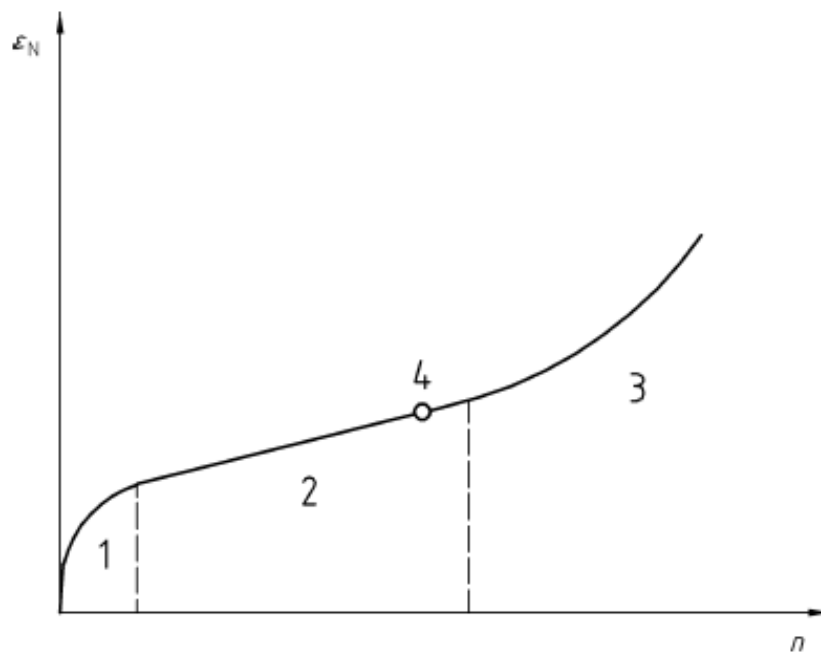


Figure H.1: Creep curve with different stages (NS-EN 12697-25:2005)

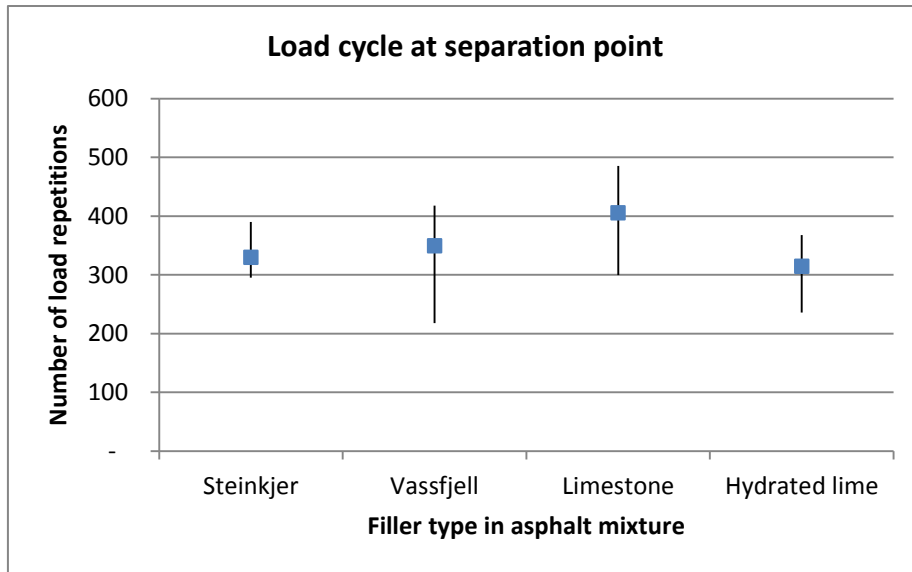


Figure H.2: Load cycle at separation point between stage 1 and 2

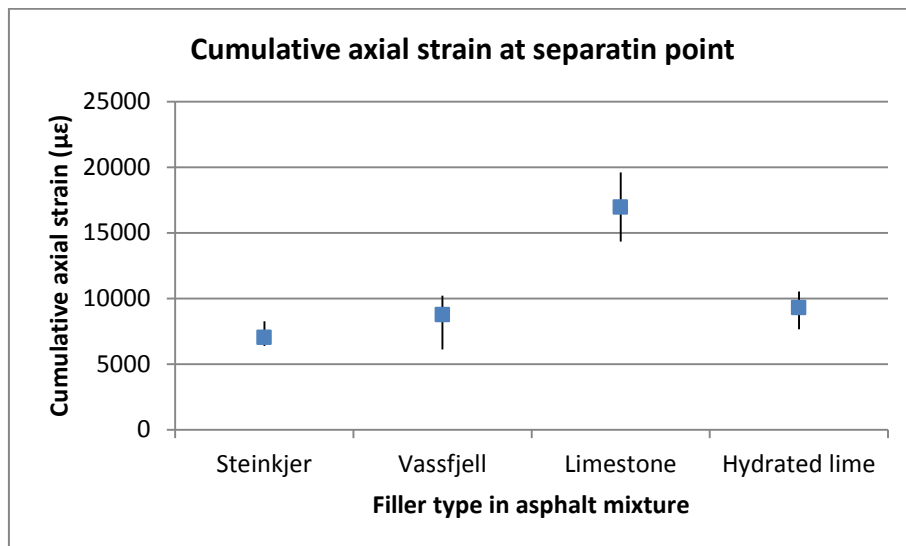


Figure H.3: Cumulative axial strain at separation point between stage 1 and 2

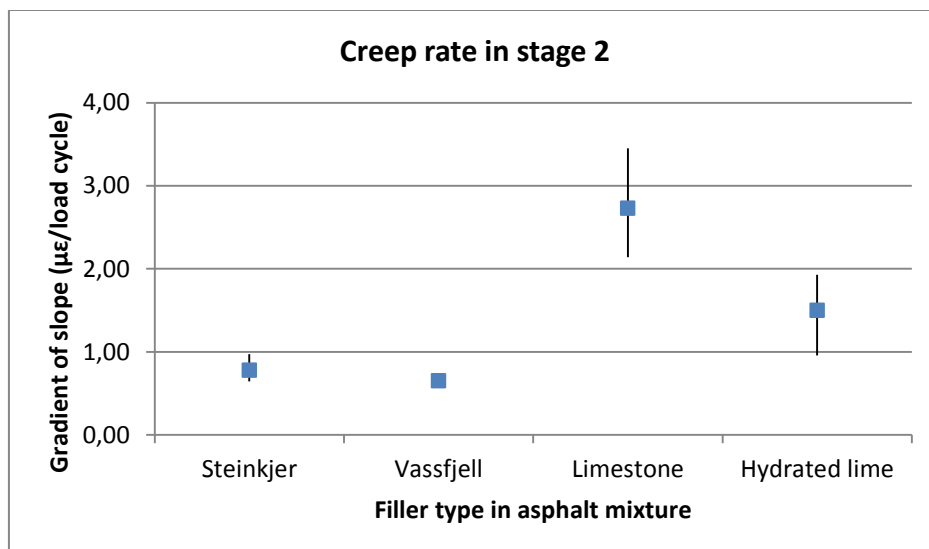


Figure H.4: Range of the values of gradient of slope in stage 2

## Appendix I – Two-sample t-test assuming unequal variances

Table I.1: *t*-test indirect tensile strength

	<i>Steinkjer</i>	<i>Vassfjell</i>
Gjennomsnitt	920,333333	974
Varians	2396,333333	373
Observasjoner	3	3
Antatt avvik mellom gjennomsnittene	0	
fg	3	
t-Stat	1,76635354	
P(T<=t) ensidig	0,08775465	
T-kritisk, ensidig	2,35336343	
P(T<=t) tosidig	0,1755093	
T-kritisk, tosidig	3,18244631	

	<i>Steinkjer</i>	<i>Limestone</i>
Gjennomsnitt	920,333333	891
Varians	2396,333333	763
Observasjoner	3	3
Antatt avvik mellom gjennomsnittene	0	
fg	3	
t-Stat	0,90390819	
P(T<=t) ensidig	0,21633655	
T-kritisk, ensidig	2,35336343	
P(T<=t) tosidig	0,4326731	
T-kritisk, tosidig	3,18244631	

	<i>Steinkjer</i>	<i>Hydrated lime</i>
Gjennomsnitt	920,333333	1040
Varians	2396,333333	637
Observasjoner	3	3
Antatt avvik mellom gjennomsnittene	0	
fg	3	
t-Stat	3,76334256	
P(T<=t) ensidig	0,01640743	
T-kritisk, ensidig	2,35336343	
P(T<=t) tosidig	0,03281486	
T-kritisk, tosidig	3,18244631	

	<i>Limestone</i>	<i>Hydrated lime</i>
Gjennomsnitt	891	1040
Varians	763	637
Observasjoner	3	3
Antatt avvik mellom gjennomsnittene	0	
fg	4	
t-Stat	6,89735974	
P(T<=t) ensidig	0,00115839	
T-kritisk, ensidig	2,13184679	
P(T<=t) tosidig	0,00231678	
T-kritisk, tosidig	2,77644511	

	<i>Vassfjell</i>	<i>Limestone</i>
Gjennomsnitt	974	891
Varians	373	763
Observasjoner	3	3
Antatt avvik mellom gjennomsnittene	0	
fg	4	
t-Stat	4,26529972	
P(T<=t) ensidig	0,00649932	
T-kritisk, ensidig	2,13184679	
P(T<=t) tosidig	0,01299864	
T-kritisk, tosidig	2,77644511	

	<i>Vassfjell</i>	<i>Hydrated lime</i>
Gjennomsnitt	974	1040
Varians	373	637
Observasjoner	3	3
Antatt avvik mellom gjennomsnittene	0	
fg	4	
t-Stat	3,59702848	
P(T<=t) ensidig	0,01140922	
T-kritisk, ensidig	2,13184679	
P(T<=t) tosidig	0,02281844	
T-kritisk, tosidig	2,77644511	

Table I.2: *t*-test Cantabro loss

	<i>Steinkjer</i>	<i>Vassfjell</i>
Gjennomsnitt	5,15702181	6,15661685
Varians	1,17574198	0,7489418
Observasjoner	3	3
Antatt avvik mellom		
gjennomsnittene	0	
fg	4	
t-Stat	-1,24797253	
P(T<=t) ensidig	0,1400536	
T-kritisk, ensidig	2,13184679	
P(T<=t) tosidig	0,28010719	
T-kritisk, tosidig	2,77644511	

	<i>Steinkjer</i>	<i>Limestone</i>
Gjennomsnitt	5,15702181	7,799692205
Varians	1,17574198	0,283636393
Observasjoner	3	3
Antatt avvik mellom		
gjennomsnittene	0	
fg	3	
t-Stat	-3,78895697	
P(T<=t) ensidig	0,01612298	
T-kritisk, ensidig	2,35336343	
P(T<=t) tosidig	0,03224596	
T-kritisk, tosidig	3,18244631	

	<i>Steinkjer</i>	<i>Hydrated lime</i>
Gjennomsnitt	5,15702181	6,35854726
Varians	1,17574198	1,53028463
Observasjoner	3	3
Antatt avvik mellom		
gjennomsnittene	0	
fg	4	
t-Stat	-1,26510791	
P(T<=t) ensidig	0,13725649	
T-kritisk, ensidig	2,13184679	
P(T<=t) tosidig	0,27451298	
T-kritisk, tosidig	2,77644511	

	<i>Limestone</i>	<i>Hydrated lime</i>
Gjennomsnitt	7,79969221	6,358547265
Varians	0,28363639	1,530284626
Observasjoner	3	3
Antatt avvik mellom		
gjennomsnittene	0	
fg	3	
t-Stat	1,85335708	
P(T<=t) ensidig	0,08044363	
T-kritisk, ensidig	2,35336343	
P(T<=t) tosidig	0,16088726	
T-kritisk, tosidig	3,18244631	

	<i>Vassfjell</i>	<i>Limestone</i>
Gjennomsnitt	6,15661685	7,79969221
Varians	0,7489418	0,28363639
Observasjoner	3	3
Antatt avvik mellom		
gjennomsnittene	0	
fg	3	
t-Stat	-2,80063578	
P(T<=t) ensidig	0,03390856	
T-kritisk, ensidig	2,35336343	
P(T<=t) tosidig	0,06781712	
T-kritisk, tosidig	3,18244631	

	<i>Vassfjell</i>	<i>Hydrated lime</i>
Gjennomsnitt	6,15661685	6,358547265
Varians	0,7489418	1,530284626
Observasjoner	3	3
Antatt avvik mellom		
gjennomsnittene	0	
fg	4	
t-Stat	-0,23166937	
P(T<=t) ensidig	0,41408189	
T-kritisk, ensidig	2,13184679	
P(T<=t) tosidig	0,82816378	
T-kritisk, tosidig	2,77644511	

Table I.3: *t*-test cumulative axial strain at 3600 load cycles

	<i>Steinkjer</i>	<i>Vassfjell</i>		<i>Steinkjer</i>	<i>Limestone</i>
Gjennomsnitt	9566,58576	10871,11007	Gjennomsnitt	9566,58576	25640,16024
Varians	2501033,12	5115005,13	Varians	2501033,12	18475703,3
Observasjoner	3	3	Observasjoner	3	3
Antatt avvik mellom gjennomsnittene fg	0		Antatt avvik mellom gjennomsnittene fg	0	
	4			3	
	-			-	
t-Stat	0,81874422		t-Stat	6,07860795	
P(T<=t) ensidig	0,22945263		P(T<=t) ensidig	0,00446945	
T-kritisk, ensidig	2,13184679		T-kritisk, ensidig	2,35336343	
P(T<=t) tosidig	0,45890526		P(T<=t) tosidig	0,0089389	
T-kritisk, tosidig	2,77644511		T-kritisk, tosidig	3,18244631	

	<i>Steinkjer</i>	<i>Hydrated lime</i>		<i>Limestone</i>	<i>Hydrated lime</i>
Gjennomsnitt	9566,58576	14221,71958	Gjennomsnitt	25640,1602	14221,71958
Varians	2501033,12	9778740,697	Varians	18475703,3	9778740,697
Observasjoner	3	3	Observasjoner	3	3
Antatt avvik mellom gjennomsnittene fg	0		Antatt avvik mellom gjennomsnittene fg	0	
	3			4	
	-			-	
t-Stat	2,30089931		t-Stat	3,72069477	
P(T<=t) ensidig	0,05245091		P(T<=t) ensidig	0,01023106	
T-kritisk, ensidig	2,35336343		T-kritisk, ensidig	2,13184679	
P(T<=t) tosidig	0,10490183		P(T<=t) tosidig	0,02046212	
T-kritisk, tosidig	3,18244631		T-kritisk, tosidig	2,77644511	

	<i>Vassfjell</i>	<i>Limestone</i>		<i>Vassfjell</i>	<i>Hydrated lime</i>
Gjennomsnitt	10871,1101	25640,16024	Gjennomsnitt	10871,1101	14221,71958
Varians	5115005,13	18475703,3	Varians	5115005,13	9778740,697
Observasjoner	3	3	Observasjoner	3	3
Antatt avvik mellom gjennomsnittene fg	0		Antatt avvik mellom gjennomsnittene fg	0	
	3			4	
	-			-	
t-Stat	5,26674997		t-Stat	1,50377367	
P(T<=t) ensidig	0,00667015		P(T<=t) ensidig	0,10353734	
T-kritisk, ensidig	2,35336343		T-kritisk, ensidig	2,13184679	
P(T<=t) tosidig	0,01334031		P(T<=t) tosidig	0,20707468	
T-kritisk, tosidig	3,18244631		T-kritisk, tosidig	2,77644511	

Table I.4: *t*-test gradient of slope in stage 2 of the creep curve

	<i>Steinkjer</i>	<i>Vassfjell</i>		<i>Steinkjer</i>	<i>Limestone</i>
Gjennomsnitt	0,77854757	0,6504531		0,77854757	2,72991329
Varians	0,02966935	0,00146387		0,02966935	0,44380208
Observasjoner	3	3		3	3
Antatt avvik mellom gjennomsnittene	0			0	
fg	2			2	
t-Stat	1,25741587			4,91193271	
P(T<=t) ensidig	0,16776832			0,01951819	
T-kritisk, ensidig	2,91998558			2,91998558	
P(T<=t) tosidig	0,33553664			0,03903638	
T-kritisk, tosidig	4,30265273			4,30265273	

	<i>Steinkjer</i>	<i>Hydrated lime</i>		<i>Limestone</i>	<i>Hydrated lime</i>
Gjennomsnitt	0,77854757	1,49838614		2,72991329	1,49838614
Varians	0,02966935	0,24586888		0,44380208	0,24586888
Observasjoner	3	3		3	3
Antatt avvik mellom gjennomsnittene	0			0	
fg	2			4	
t-Stat	-2,3752253			2,56852412	
P(T<=t) ensidig	0,07038448			0,03103779	
T-kritisk, ensidig	2,91998558			2,13184679	
P(T<=t) tosidig	0,14076897			0,06207559	
T-kritisk, tosidig	4,30265273			2,77644511	

	<i>Vassfjell</i>	<i>Limestone</i>		<i>Vassfjell</i>	<i>Hydrated lime</i>
Gjennomsnitt	0,6504531	2,72991329		0,6504531	1,49838614
Varians	0,00146387	0,44380208		0,00146387	0,24586888
Observasjoner	3	3		3	3
Antatt avvik mellom gjennomsnittene	0			0	
fg	2			2	
t-Stat	5,39760988			2,95312187	
P(T<=t) ensidig	0,01632605			0,04904296	
T-kritisk, ensidig	2,91998558			2,91998558	
P(T<=t) tosidig	0,03265211			0,09808592	
T-kritisk, tosidig	4,30265273			4,30265273	